





This is to certify that the  
dissertation entitled  
Studies on the Detection of  
Chemical and Biological Agents  
by Triple Quadrupole Mass Spectrometry

presented by

MARK RICHARD BAUER

has been accepted towards fulfillment  
of the requirements for

Ph. D. degree in Chemistry

A handwritten signature in cursive script, reading "Chris Enke", written over a horizontal line.

Major professor

Date Jan 5, 1987





RETURNING MATERIALS:  
Place in book drop to  
remove this checkout from  
your record. FINES will  
be charged if book is  
returned after the date  
stamped below.

--	--	--

STUDIES ON THE DETECTION OF CHEMICAL AND BIOLOGICAL AGENTS  
BY TRIPLE QUADRUPOLE MASS SPECTROMETRY

By

Mark Richard Bauer

A DISSERTATION

Submitted to  
Michigan State University  
in partial fulfillment of the requirements  
for the degree of

DOCTOR OF PHILOSOPHY

Department of Chemistry

1986

15-2-85

## ABSTRACT

### STUDIES ON THE DETECTION OF CHEMICAL AND BIOLOGICAL AGENTS BY TRIPLE QUADRUPOLE MASS SPECTROMETRY

By

Mark Richard Bauer

Two new applications for triple quadrupole mass spectrometry have been developed for the detection of chemical and biological agents in mixtures. These methods illustrate how MS/MS can, with appropriate ionization and compound class characterization, easily detect organophosphorus pesticides and whole bacteria in complex matrices with no sample work-up.

Research is presented on a new method to detect and identify whole bacteria in a mixture by combining pyrolysis and tandem quadrupole mass spectrometry. Pyrolyzing a sample produces a mixture of compounds all of which represent the species pyrolyzed, but only a few of which are characteristic of the species. MS/MS is used to discover parent/daughter ion-pairs representative of the unidentified characteristic compounds. Unique ion-pairs were identified that can be used for the differentiation of *B.cereus*, *B.subtilis*, and *E.coli*. The capacity of pyrolysis tandem mass spectrometry to detect the presence of bacteria in a complex mixture is also demonstrated.

Characteristic low-energy CAD fragmentation pathways of organophosphorus compounds have been used to quickly screen samples for pesticides, their metabolites, and decomposition products. An examination of CAD spectra of the  $(M+H)^+$  ions of the organophosphorus

pesticides revealed several ions and fragmentation mechanisms indicative of the parent compounds. A set of ten different neutral loss and parent scans can be used to detect the presence of over 45 organophosphorus pesticides and related compounds. The ion-pairs employed in the scans can also be used for targeted analysis by monitoring specific parent/daughter pairs continuously or sequentially. The method has been used to detect pesticides on fruit samples which were placed directly in the mass spectrometer without prior extraction or other clean-up.

The organophosphorus pesticide analysis is facilitated by a new ionization method that uses methanol cluster ions for chemical ionization. The use of methanol as a reagent gas for chemical ionization mass spectrometry is demonstrated. At the pressures required for chemical ionization, methanol forms cluster ions of the type  $(\text{MeOH})_n\text{H}^+$ , where  $n=1,2,3,4$ , which provide ionization, with limited fragmentation, for several compound classes. The ratio of the cluster ions formed is a function of the source temperature, the concentration of GC carrier gas, and the pressure of methanol. The degree of fragmentation can be varied by adjusting the cluster ion ratios without affecting ionization efficiency. The proton affinity of the cluster ions, collisional stabilization, and stable leaving groups provided by the clusters have a combined role in decreasing fragmentation. Methanol chemical ionization increases sensitivity over other chemical ionization reagents and increases selectivity in mixture analysis experiments on fuels, pesticides, and other samples because the clusters will ionize heteroatom species but ignore hydrocarbons and other common matrix compounds.

#### ACKNOWLEDGEMENTS

I would like to express my appreciation to Dr. Christie G. Enke for the time he was able to spend on my problems during this especially troubled time in his own life. His advice and assistance during my research and in the preparation of this dissertation helped tremendously. I would also like to thank Dr. J. Throck Watson for teaching me a little grammar while serving as second reader.

I would like to thank the Department of Chemistry at Michigan State University and the Office of Naval Research for the financial support that they provided.

Special thanks are in order to the other members of Dr. Enke's research group and fellow graduate students who work in the NIH Mass Spectrometry Facility, both past and present, for their help in developing and maintaining the instrumentation and computer systems that make projects like this one possible. Dr. Anne Giordanni, Adam Schubert, and Hugh Gregg were especially helpful and I thank them for sharing their time and knowledge with me.

I also need to acknowledge Milton Webber and the other Jokers who are regulars at the E.Beak & C.Dome Bar and Grill, for providing a pleasant family atmosphere and support group in the laboratory.

Finally, I offer my thanks and appreciation to those whom this is all for: my mother and father, who always believed, and the rest of my family, Susan and Barclay *et al.*, who are constantly understanding, supporting, and loving.

It is easy to be blinded to the essential uselessness of an  
instrument by the sense of achievement you get from getting  
it to work at all.

Douglas Adams

## Table of Contents

List of Figures	vi
List of Tables	ix
Chapter One: Dissertation Introduction	1
A. Introduction	1
B. Organization of the Dissertation	4
C. References	7
Chapter Two: Chemical Ionization by Methanol Cluster Ions	8
A. Introduction	8
B. Background	9
C. Experimental	14
D. Results and Discussion	16
1. Reagent Ion Characterization	16
a) Pressure Characterization	16
b) Temperature Characterization	18
c) Gas Chromatography Conditions	22
2. Decreased Fragmentation	22
3. Sensitivity Increase	24
4. Active Ion Determination	26
5. Factors Affecting Fragmentation	30
a) Proton Affinity	30
b) Collisional Stabilization	35
c) Leaving Groups	37
6. Adduct Ions	37
E. Conclusion	46
F. References	48
Chapter Three: Detection of Organophosphorus Pesticides	50
A. Introduction	50
B. Experimental	57
C. Results and Discussion	58
1. Daughter ion spectra	58
a) Phosphorodithioates	60
b) Phosphorothioates	65
c) Phosphorothiolates	66
d) Phosphates	66
e) Miscellaneous organophosphorus pesticides	67
2. Screening analysis	69
3. Targeted Analysis	76
4. Sensitivity	78
D. Conclusions	82
E. References	84



Chapter Four: Detection of Whole Bacteria	86
A. Introduction	86
B. Experimental	96
C. Results and Discussion	98
1. Ionization	98
2. The search for species specific ion-pairs	100
3. Mixed daughter scans	105
4. Mixture analysis by pyrolysis tandem mass spectrometry	114
D. Conclusions	118
E. References	121
Appendices	124
Appendix 2A: Methanol CI spectra of test mixture	125
Appendix 2B: Isobutane CI spectra of test mixture	130
Appendix 3A: CAD spectra of the $(M+H)^+$ ions of the organophosphorus pesticides	135

## LIST OF FIGURES

### Chapter Two

Figure 2.1	Abundance of methanol CI reagent ions as a function of pressure.	17
Figure 2.2	Total ion current of methanol CI reagent ions, variation with pressure.	19
Figure 2.3	Abundance of methanol CI reagent ions as a function of temperature.	21
Figure 2.4	Abundance of malathion ion formed by methanol CI as a function of pressure.	23
Figure 2.5	Ion current maxima as a function of pressure for methane, isobutane, and methanol CI.	27
Figure 2.6	Selected ion monitoring chronograms of methanol reagent ion clusters and the (M+H) <sup>+</sup> ions for dursban and phosmet.	29
Figure 2.7	Mass spectra of malathion ionized by four chemical ionization reagent gases: (A) methane, (B) isobutane, (C) Ammonia, (D) Methanol.	31
Figure 2.8	Acetic acid and acetophenone ions vs. methane pressure for a constant pressure of methanol.	36
Figure 2.9	Total ion current chromatogram for programed test mix-- Methanol CI	39
Figure 2.10	Methanol CI spectra of four adduct forming compounds.	43
Figure 2.11	Total ion current chromatograms for programed test mix--Isobutane CI.	44

### Chapter Three

Figure 3.1 Eight sub-groups of organophosphorus pesticides	55
Figure 3.2 Common fragmentation routes present in the daughter spectra of organophosphorus pesticides.	59
Figure 3.3 Structure of the miscellaneous organo-phosphorus compounds studied.	68
Figure 3.4 Pesticides detected by two of the scans used in a screening analysis of a mixture containing ten organophosphorus pesticides.	74
Figure 3.5 Apple analysis: Spectrum A) normal mass spectra of the volatile components of an apple; Spectrum B) pesticide present (phosmet), detected by one of the scans in the general screen.	75
Figure 3.6 Several of the pesticides detected during a targeted analysis of a mixture of pesticides.	79

#### Chapter Four

Figure 4.1 Cutaway view of a Curie point pyrolyzer	97
Figure 4.2 Comparison of 70 eV Electron Ionization and Methane Chemical Ionization PY/MS spectra of <i>B.subtilis</i>	101
Figure 4.3 CI PY/MS spectra of <i>B.cereus</i> , <i>B.subtilis</i> , and <i>E.coli</i>	102
Figure 4.4 Mixed daughter scans of <i>B.cereus</i> , <i>B.subtilis</i> , and <i>E.coli</i>	107
Figure 4.5 Parent ion spectra for m/z 58: PY/MS/MS spectra of <i>B.cereus</i> , <i>B.subtilis</i> , and <i>E.coli</i>	109
Figure 4.6 Parent ion spectra of m/z 71: PY/MS/MS spectra of <i>B.cereus</i> , <i>B.subtilis</i> , and <i>E.coli</i>	110
Figure 4.7 Parent ion spectra of m/z 127: PY/MS/MS spectra of <i>B.cereus</i> , <i>B.subtilis</i> , and <i>E.coli</i>	112
Figure 4.8 Parent ion spectra of m/z 84: PY/MS/MS spectra of <i>B.cereus</i> , <i>B.subtilis</i> , and <i>E.coli</i> .	113

Figure 4.9 Pyrolysis mass spectra of *B.cereus*, plain corn starch, and corn starch spiked with *B.cereus*. ( $m/z$  80 has been removed for clarity) 115

Figure 4.10 Parent ion spectra of  $m/z$  84: PY/MS/MS spectra of *B.cereus*, plain corn starch, and corn starch spiked with *B.cereus*. 117

## LIST OF TABLES

### Chapter Two

Table 2.1	Proton affinities of common reagent ions	11
Table 2.2	Intensity of TIC peaks in chromatograms of test mixture ionized with isobutane and methanol CI	25
Table 2.3	Proton affinity and ions formed for compounds used to determine the proton affinity of methanol clusters	34
Table 2.4	Ions found in the methanol CI spectra of the test mixture	40
Table 2.5	Ions found in the isobutane CI spectra of the test mixture	45

### Chapter Three

Table 3.1	Ions represented in the daughter spectra of the (M+H) <sup>+</sup> ions of the organophosphorus pesticides studied	61
Table 3.2	List of scans used to screen for organophosphorus pesticides	71
Table 3.3	Organophosphorus pesticides detected by each of the scans in the screening analysis list	72

### Chapter Four

Table 4.1	Daughter ions detected for selectice parent ions in PY/MS/MS spectra of <i>B.cereus</i> , <i>B.subtilis</i> , and <i>E.coli</i>	104
Table 4.2	Selected daughter ions used for parent scans	108

## CHAPTER ONE

### Dissertation Introduction

#### A. INTRODUCTION

Since its inception a decade ago, tandem mass spectrometry (MS/MS) has gained rapid acceptance in the analytical community. Although there have been reports of its use for structural evaluation of unknowns, its acceptance has largely been due to the ability of MS/MS technology to provide rapid, sensitive, and extremely selective analysis of complex mixtures. There is a wide variety of commercial tandem mass spectrometers available today, and their expanding range of analytical capabilities is attracting a wider audience to the power of MS/MS. The basic instrumentation and common techniques used with MS/MS have been described in detail in a recent book<sup>(1)</sup> and several recent reviews<sup>(2-6)</sup>. These also have outlined the historical development of MS/MS instrumentation, its theoretical foundation, and several important areas of successful application.

MS/MS spectrometers are grouped according to the type of mass analyzers they use. The most common analyzers used include magnetic (B) and electrostatic (E) analyzers or sectors, quadrupoles (Q), Fourier transform cells (FT), and time of flight tubes (TOF). Tandem spectrometers using virtually every possible combination of analyzers have been built<sup>(1)</sup>. Each instrument has its advantages and special capabilities. Several of the new designs are useful for general analytical analysis and are now commercially available. Other

configurations are more specialized, often used for fundamental physical chemistry experiments, and are only available as home-built models.

Tandem sector instruments are available in configurations that combine all possible variations of B and E. MS/MS spectrometers with BE, EBE, BEB, BEEB, and EBEB geometries may be purchased from several vendors<sup>(7)</sup>. These instruments offer high resolution, at least for the first analyzer, a high mass range of 10,000 daltons or more, and high collision energy. The major limitation of these, generally, very large instruments is their accompanying large price tag, above one half million dollars. The large sector instruments are, however, in demand. These instruments provide a means to determine the molecular structure of macromolecules, such as those found in biomedical samples, plant materials, and commercial polymers. This information is unobtainable by other means, and, therefore, as the bioengineering field and the pharmaceutical industries continue to grow, and continue to analyze large biomolecules, the use of tandem sector instruments will continue to increase.

The tandem mass spectrometer that has become the most widely used MS/MS instrument is the triple quadrupole mass spectrometer (QQQ or TQMS). These instruments, that use low collision energy, have only unit mass resolution and a mass range limited to 2000 daltons, but are available for about \$250,000. Triple quadrupole mass spectrometers are easily automated, and extremely versatile. As such, triple quadrupole mass spectrometers have found a place in many fields of research. Numerous papers, from many different disciplines, reporting the use of TQMS for analysis have appeared in the literature in recent years<sup>(8-9)</sup>.



Triple quadrupole mass spectrometers could be the only instrument used by a general analysis laboratory for all their mass spectral analyses. Even though a TQMS instrument is theoretically capable of performing the same analyses that a single quadrupole is, these instruments are rarely, if ever, the only mass spectrometer a laboratory owns. With the addition of a gas chromatograph, experiments needing GC/MS, MS, MS/MS, or GC/MS/MS could all be accomplished as needed with the same instrument. However, TQMS instruments are usually only found in laboratories that have suitable funds to buy one as a second or third spectrometer to compliment other instruments.

Recently a third general class of MS/MS instrument has been introduced. Hybrid instruments made from both sectors and quadrupoles, offer a compromise in mass range, resolution, and price between the other groups. Because they combine the advantages of both types of analyzers, the new BEQQ and EBQQ instruments could become the most powerful and generally useful MS/MS instruments.

It should also be noted that mass spectroscopists who did not want to miss the MS/MS revolution, but only had traditional double focusing sector instruments at their disposal, were able to develop ways to scan both sectors simultaneously to achieve information similar to that available from tandem instruments. Most new double focusing instruments available, now have the capability to perform "linked scan" MS/MS experiments.

Although most analytical chemists are, by now, familiar with tandem mass spectrometry, there are those who consider MS/MS instruments to be novelties, with limited usefulness and high price tags. Scientists in the mass spectrometry community, while realizing that there

are many applications particularly suited for MS/MS, also realize that MS/MS is not the answer to all problems. This belief is also held by analysts experienced with the analytical capabilities of GC/MS. They tend to view MS/MS as a feeble attempt to replace chromatographic methods. This view is most likely inspired by the repeated comparison between the two techniques that MS/MS operators (myself included) make to tout the advantages of their methods.

There is, however, no reason to abandon GC, for although many MS/MS applications emphasize complete elimination of sample cleanup and chromatographic separation, more recent applications have demonstrated the value of retaining some cleanup and separation<sup>(9,10)</sup>. Indeed it would not be wise to give up everything we have learned from years of research on sample extraction and chromatographic separation. The detection of endogenous analytes in biological fluids at trace levels exemplifies a situation where even the tremendous selectivity of MS/MS can be foiled. Due to the presence of numerous structurally similar compounds, some of which may be present in large excess, satisfactory results cannot be obtained without sample cleanup and the aid of capillary columns for sample introduction<sup>(11,12)</sup>. The ultimate usefulness of MS/MS, specially TQMS, will most likely be as an extremely selective detector for GC techniques, thereby again combining the advantages of both techniques.

## B. ORGANIZATION OF THE DISSERTATION

This dissertation presents research which highlights the power and unique capabilities of triple quadrupole mass spectrometry and how TQMS can be applied successfully in areas where other analytical

techniques cannot be used. The dissertation is divided into four chapters. This chapter discusses the current state of available MS/MS instrumentation in the realm of analytical technology and introduces the chapters to follow.

The research presented in chapter two is a further investigation into a novel ionization technique first reported in my masters dissertation (13). The characterization of chemical ionization by methanol clusters is described. Reasons for the observed behavior and the potential advantages that this technique offers to certain MS/MS analyses are discussed.

Chapter three describes the development of a new method to screen for organophosphorus pesticides. The work presented here, also begun as part of my masters research project, uses the neutral loss and parent scans available with MS/MS to detect and identify over 40 organophosphorus pesticides in one quick screen. The established techniques used for the determination of organophosphorus pesticides are limited to identifying only one pesticide or to detecting the presence of pesticides without being able to determine which specific compound has been found(14-17). Also discussed are the differences in strategy between a general screen and a targeted analysis using the MS/MS methods developed. The chapter does not portray the development of new MS/MS techniques, but instead describes how the already established technology can be used for an important new application.

In chapter four, research on a method to detect and identify whole bacteria in a mixture by combining pyrolysis and triple quadrupole mass spectrometry is presented. Pyrolysis of mixtures containing species as complex as whole bacteria provides mass

spectroscopy with what is perhaps the ultimate mixture for analysis. Pyrolysis produces a mixture of compounds all of which represent the species pyrolyzed, but only a few of which are characteristic of the species. Pyrolyzing a mixture produces a mixture of mixtures of compounds which must be sifted through to detect those few compounds which signal the presence of the species of interest. This complex sample pushes triple quadrupole mass spectrometry to its limits and, therefore, new technologies must be developed for this analysis. Chapter four discusses the nature of the problems faced in combining pyrolysis and MS/MS techniques and reports the results of initial attempts at overcoming them. The ability of the combined instruments to detect specific bacteria in a mixture is demonstrated. Suggestions for further study are also described.

### C. REFERENCES

1. McLafferty, F.W., Ed. *Tandem Mass Spectrometry*; John Wiley & Sons: New York, 1983.
2. Yost, R.A., Fetterolf, D.D.; *Mass Spec.Rev.*, 1983, 2, 1
3. Cooks, R.G., Glish, G.L.; *Chem.Eng.News*, 1981 (Nov 30), 40
4. McLafferty, F.W.; *Science*, 1981, 214, 280
5. Johnson, J.V., Yost, R.A.; *Anal.Chem.*, 1985, 57, 758A
6. Borman, S.A.; *Anal.Chem.*, 1986, 58, 406A
7. Burlingame, A.L., Whitney, J.O., Russell, D.H.; *Anal.Chem.*, 1984, 56, 417R
8. Burlingame, A.L., Baillie, T.A., Derrick, P.J.; *Anal.Chem.*, 1986, 58, 165R
9. Yost, R.A., Fetterolf, D.D., Hass, J.R., Harvan, D.J., Weston, A.F., Skotnicki, P.A., Simon, N.M.; *Anal.Chem.*, 1984, 56, 2223
10. Trehy, M.L., Yost, R.A., Dorsey, J.G.; *Anal.Chem.*, 1986, 58, 14
11. Gaskell, S.J., Porter, C.J., Green, B.N.; *Biomed.Mass Spectrom*, 1985, 12, 139.
12. Johnson, J.V., Yost, R.A., Faull, K.F.; *Anal.Chem.*, 1984, 56, 1655
13. Bauer, M.R.; M.S. Dissertation, Michigan State University, 1983
14. Horwitz, W. ed.; *Official Methods of Analysis of the Association of Official Analytical Chemists*, 12th ed. ,Association of Official Analytical Chemists: Washington D.C., 1975
15. Thompson, J.F., ed.; *Analysis of Pesticide Residues in Human and Environmental Samples, A Compilation of Methods Selected for Use in Pesticide Monitoring Programs*, U.S. Environmental Protection Agency, Washington D.C., 1972
16. Biros, F.J.; *Pesticide Identification at the Residue Level*, Advances in Chemistry Series #104; Am. Chem.Soc.: Washington D.C., 1971
17. Stan, H.J. et al. ; *Fresenius Z. Anal. Chem.*, 1977, 287, 1065

## CHAPTER TWO

### Chemical Ionization with Methanol Cluster Ions

#### A. INTRODUCTION

Recent advances in the use of tandem mass spectrometry (MS/MS) for the analysis of mixtures has created a resurgence of interest in new ionization methods. An important ionization criterion for the analysis of mixtures with MS/MS is the absence of fragment ions formed during ionization. The goals of ionization for traditional MS as well as MS/MS structure elucidation experiments are to produce ions indicative of the molecular weight of the compound as well as fragment ions. Fragments formed in the ionization source are needed to deduce the structure and thereby determine or confirm the identity of the compound under investigation. MS/MS mixture experiments, however, create the fragment ions necessary for identification in the collision cell and, therefore, ionization methods that produce fragment ions should be avoided. Fragmentation in the source has two major disadvantages: (1) sensitivity is decreased by splitting the available ion current into several peaks instead of concentrating all ions into one large peak, and (2) selectivity and reliability of analyses for unknowns is decreased when metabolites and/or decomposition products of the compound of interest are misidentified as fragment ions. Or worse, the fragment ions are misidentified as additional components.

In the present work, chemical ionization (CI) using methanol as a reagent gas is investigated in response to the new ionization goals

MS/MS applications have introduced. In earlier work methanol was chosen as the chemical ionization reagent gas for the MS/MS analysis of organophosphorus pesticides because we found that few fragment ions were produced in the ion source<sup>(1)</sup>. The aim of this research was to continue the investigation of methanol CI to determine the cause of the decreased fragmentation and to assess the applicability of the technique to samples other than pesticides.

## B. BACKGROUND

Since its introduction by Munson and Field in 1966, chemical ionization has become accepted as one of the standard mass spectral ionization techniques<sup>(2)</sup>. The primary advantage chemical ionization offers is the appearance of, or increased abundance of, ions indicative of the molecular weight of samples which, when ionized by traditional electron impact ionization, fragment to the point that no peak representing the molecular ions is detected. In chemical ionization techniques, the sample of interest is ionized by a gas-phase ion-molecule reaction. Interactions between an ionized reagent gas, which is present in great excess, and sample molecules produce sample ions characteristic of the original sample. As new demands were made on mass spectrometry to analyze new types of samples, new reagent gases for chemical ionization were introduced that complemented, and helped further advance, improvements in mass spectrometric instrumentation and techniques to meet those demands.

Many new specialized chemical ionization reagents have been investigated that extend the usefulness of chemical ionization. These include more selective reagents which ionize specific compounds or



classes of compounds, and/or "softer" reagents which cause less fragmentation and therefore increase the abundance of  $(M+H)^+$  ions.<sup>(3-10)</sup> Popular reagent gases introduced include both isobutane<sup>(5)</sup>, which causes considerably less fragmentation than methane, and ammonia, whose high proton affinity at first attracted Dzidic and McClosky for use as a selective reagent to ionize only nitrogen-containing molecules<sup>(6)</sup>. They also noticed, however, that the proton transfer reaction using ammonium ions results in little fragmentation for many compound types that have high proton affinities<sup>(7)</sup>. These reagent systems can produce abundant molecular adduct ions, but they often produce many sample fragment ions as well.

Methanol, too, has been used as a chemical ionization reagent gas, but early users were forced to dilute the methanol with a non-polar gas to prevent clusters from forming<sup>(8)</sup> or use tandem instruments that allowed only one reagent ion species to enter the ionization chamber<sup>(9)</sup>. More recently Stan tried methanol as a reagent gas for the analysis of organophosphorus pesticides, but rejected it because it did not provide the fragment ions needed for compound identification<sup>(10)</sup>. Deuterated methanol was used by Hawthorn and Miller for chemical ionization-proton exchange to identify alkylbenzene isomers in diesel exhaust<sup>(11)</sup>.

All the chemical ionization reactions investigated in this work are ion-molecule reactions in which protons are transferred from gaseous Bronsted acids to neutral molecules, as shown in reaction 1.



The rate constants for these reactions are in the range 1 to  $4 \times 10^9$  cm<sup>3</sup> molecules<sup>-1</sup> sec<sup>-1</sup> and it has been determined that the reactions are exothermic. Therefore these reactions are all highly efficient with the

reaction occurring on essentially every collision. The reactions are exothermic provided the proton affinity of M is greater than the proton affinity of B. Table 2.1 lists the proton affinities of several of the common reagent gases. Ions with low proton affinities will react by exothermic proton transfer with most organic molecules, but ions with higher proton affinities such as  $C_6H_9^+$  and  $NH_4^+$  are more specific protonating agents.

**Table 2.1 Proton affinities of common reagent ions**

Reagent Gas	Reagent Ion	Proton Affinity <sub>a</sub>
H <sub>2</sub>	H <sub>3</sub> <sup>+</sup>	100.7
CH <sub>4</sub>	CH <sub>5</sub> <sup>+</sup>	130.5
	C <sub>2</sub> H <sub>5</sub> <sup>+</sup>	163.5
H <sub>2</sub> O	H <sub>3</sub> O <sup>+</sup>	173.0
CH <sub>3</sub> OH	CH <sub>3</sub> OH <sub>2</sub> <sup>+</sup>	184.9
i-C <sub>4</sub> H <sub>10</sub>	C <sub>4</sub> H <sub>9</sub> <sup>+</sup>	196.9
NH <sub>3</sub>	NH <sub>4</sub> <sup>+</sup>	205.0

a. expressed in kcal/mole, from reference 8

The reagent ions themselves are formed by similar ion-molecule reactions in which reagent ions and radicals (created by electron-molecule reactions) combine with other reagent molecules. In practice a high pressure of the reagent gas is introduced into the ionization chamber and, as the ion-molecule reactions equilibrate, a reagent ion plasma is formed. The sample is then introduced at a pressure approximately a thousand times lower than the reagent gas pressure. This assures that sample ions are made through interactions with the reagent plasma and not by electron-molecule interactions.

The exothermicity of the proton transfer reaction is manifested as internal energy in the molecule and is lost through bond breaking, thereby fragmenting the newly formed  $(M+H)^+$  ions. The amount of energy deposited in the ion is given by the difference of proton

affinities between the conjugate base of the reagent ion and the sample molecule. To increase the abundance of  $(M+H)^+$  ions, in order to retain molecular weight information, the least possible exothermic protonation reaction should be used. Minimizing the difference in proton affinities is accomplished by choosing a "softer" reagent, one with a higher proton affinity. In mass spectrometry structural information is derived from fragment ions and therefore some excess exothermic energy is generally needed. The extent of fragmentation actually depends on both the exothermicity of the protonation reaction and the molecular structure. Because methane CI can ionize almost all organic compounds and produces adequate  $(M+H)^+$  ions as well as substantial fragment ions, methane is probably the most widely used reagent gas.

Interactions other than proton transfer reactions can occur between the reagent ions and sample molecules. Other adduct ions, often  $(M+BH)^+$  ions, can also be formed between electron-rich neutral molecules and the ions generated by the reagent gas. Condensation, clustering and displacement reactions are all found in certain situations. The adduct ions  $(M+C_2H_5)^+$  and  $(M+C_4H_9)^+$  are occasionally observed in low abundance in methane CI and isobutane CI, respectively. When polar samples or reagent gases are involved,  $(M+BH)^+$ ,  $(2M+H)^+$ ,  $(M+2B+H)^+$  and  $(MB-X)^+$  ions may be observed. These ions are often a nuisance, obscuring the identity of the protonated molecule.

In other cases, researchers have used the adduct ions advantageously to help identify the protonated molecule, functional groups and double bonds<sup>(6,12-18)</sup>. Much of the research concerning adduct ions involves the chemistry of ammonia CI. Ammonia will ionize compounds with proton affinities greater than 205 kcal/mole by proton



transfer, but for compounds with proton affinities less than 205 kcal/mole, ammonia CI spectra frequently show  $(M+NH_4)^+$  adduct ions. Keough and DeStafano showed that  $(M+NH_4)^+$  ions are not formed if the proton affinity of M is less than -188 kcal/mole<sup>(14)</sup>. It also appears that a lone pair of electrons at the basic site is a prerequisite for formation of the adduct ions. The structure of the ammonia adduct has also been investigated. Traditionally  $(M+NH_3+H)^+$  ions are thought to be either products of electrophilic attachment by  $(NH_4)^+$  or collision-stabilized complexes in which endothermic proton transfer is incomplete, as represented in equation 2.



It has been shown, however, that adduct ions formed through the reaction of amine ions with ketones, esters, and acids involve the formation of a new covalent bond<sup>(15)</sup>.



These adduct ions, of the general formula  $(AMH)^+$ , are highly stable in comparison to adducts formed by reaction 2. The difference in stability has been used to distinguish the compounds that react via reaction 3 from alcohols, ethers, and acetals which form adducts through reaction 2<sup>(16)</sup>. The selective reactivity of vinyl methyl ether reagent ions has also been used to determine the position of double bonds in unsaturated esters, acetates, and other olefins<sup>(12,17)</sup>. Adduct ions have also proven useful for mixtures and other cases where the ionization methods produce confusing spectra in which the ionized molecule is not

apparent<sup>(16,18)</sup>. In the same way that silver salts or other compounds are added to fast atom bombardment (FAB) samples to help identify ionic species containing the intact molecule<sup>(19)</sup>, mixtures of normal and deuterated reagent gases provide an isotope peak intensity pattern that is easily identified in the desorption CI spectrum of large biomolecules<sup>(16)</sup>.

### C. EXPERIMENTAL

All mass spectra were taken on a prototype Extrel ELTQ-400-3 triple quadrupole mass spectrometer and computerized control system. All data were collected with the triple quadrupole mass spectrometer configured as a single stage mass spectrometer. The first quadrupole was used as a mass filter, while the second and third quadrupoles were kept in RF only mode such that they would pass ions of all masses. No collision gas was present in the collision quadrupole.

The instrument is equipped with a CI/EI Simulscan™ ionizer which is fitted with interchangeable ion volumes. For this study it was important that the CI volume portion of the ionization source be as gas tight as possible to achieve the high pressures and long residence times needed to form clusters. Therefore, a modified CI volume was used with small 1.5 mm inlet holes for the direct insertion probe, gas chromatograph, and reagent gas. The electron entrance slit was enlarged slightly to allow a greater flux of electrons to enter the ionization region. Electron energy for CI was maintained at 300 eV. For pressure studies the GC interface was removed so that a thermocouple pressure gauge could be fitted through the GC port directly into the

source. The glass inlet tubes connecting the CI gas line and the gauge to the source were both wrapped with Teflon™ tape to make a tighter than normal fit with the source. Except during temperature studies and GC/MS experiments, the source temperature was kept at 100°C. This was the lowest steady temperature possible, since when the CI filament is on, it heats the source above 90°C, even if the heater is off. The concave repeller was maintained at the same voltage as the walls of the CI volume in order both to increase the ion residence times in the source so that the ion-molecule reactions could equilibrate and to help minimize source fragmentation. Changes in the repeller voltage affect the ratio of methanol clusters, with potentials more positive than the ion volume producing fewer cluster ions. Keeping the potentials equal did not adversely affect sample ion abundances and, in fact, gave the greatest abundance for all ions.

GC/MS was performed with the addition of a Hitachi 633-30 gas chromatograph. Separations were achieved using a 30-meter narrow-bore (0.25 mm ID) DB-1 fused silica capillary column with a 1 micron coating (J&W Scientific, Rancho Cordova, Ca.). The column was interfaced directly into the ion source by passing it through a heated transfer line maintained at 200°C. Helium carrier gas was used at a flow rate of 1 ml/min (a flow velocity of 40 cm/sec at 200°C). Sample sizes of 0.7 microliters were injected into a splitless injector maintained at 175°C. Temperature programs maintained the oven at 50°C for 2 min then ramped to 200°C at 10°C/min.

Methanol vapors for CI were generated by injecting 2-3 ml of methanol (anhydrous reagent grade) through a GC septum into an evacuated 500 ml expansion bulb maintained at room temperature. The



vapors were then transferred into the source through a variable leak needle valve. This system provides the wide range of pressures necessary for this study. Other chemical ionization reagents, methane, isobutane, ammonia were at least ultra-high purity grade. All chemical samples and pesticide standards used were from Chem Service Inc. and were used without further purification. Ortho Lawn Insect Spray™ was used as a source for the organophosphorus pesticide chlorpyrifos and was purchased at a local garden supply store. The programmed test mixture of 12 organic compounds in methylene chloride was purchased from Supelco.

Data were collected on the instrument's microcomputer and then uploaded to a PDP 11/23 minicomputer, running the RSX 11M operating system, for data interpretation. Scan data were interpreted with the aid of a multi-dimensional data base package<sup>(20)</sup> and other software developed inhouse.

## D. RESULTS and DISCUSSION

### 1. Reagent Ion Characterization

#### a) Pressure Characterization

At the pressure required for chemical ionization, the methanol ions formed by the impact of electrons are quickly converted by ion-molecule reactions to proton-bound cluster ions of the type  $(\text{MeOH})_n\text{H}^+$  where  $n=1,2,3,4$ . The relative abundance of the different cluster ions is dependent on the temperature of the ionization source and the methanol pressure within the source. Figure 2.1 shows a plot of the abundance of major methanol ions versus pressure in a cool, 100 °C, source. At



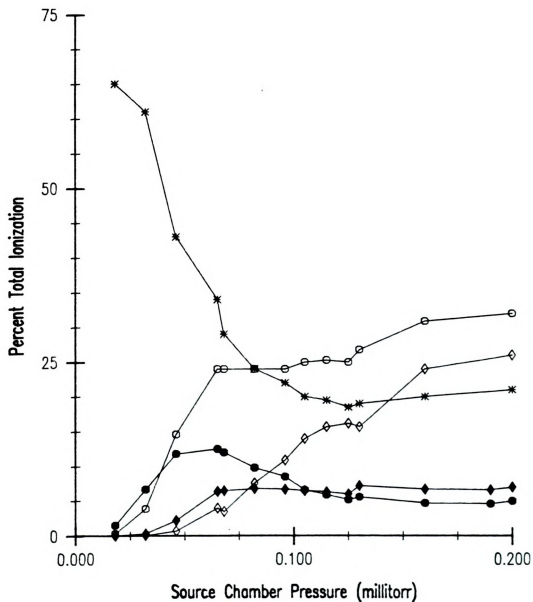


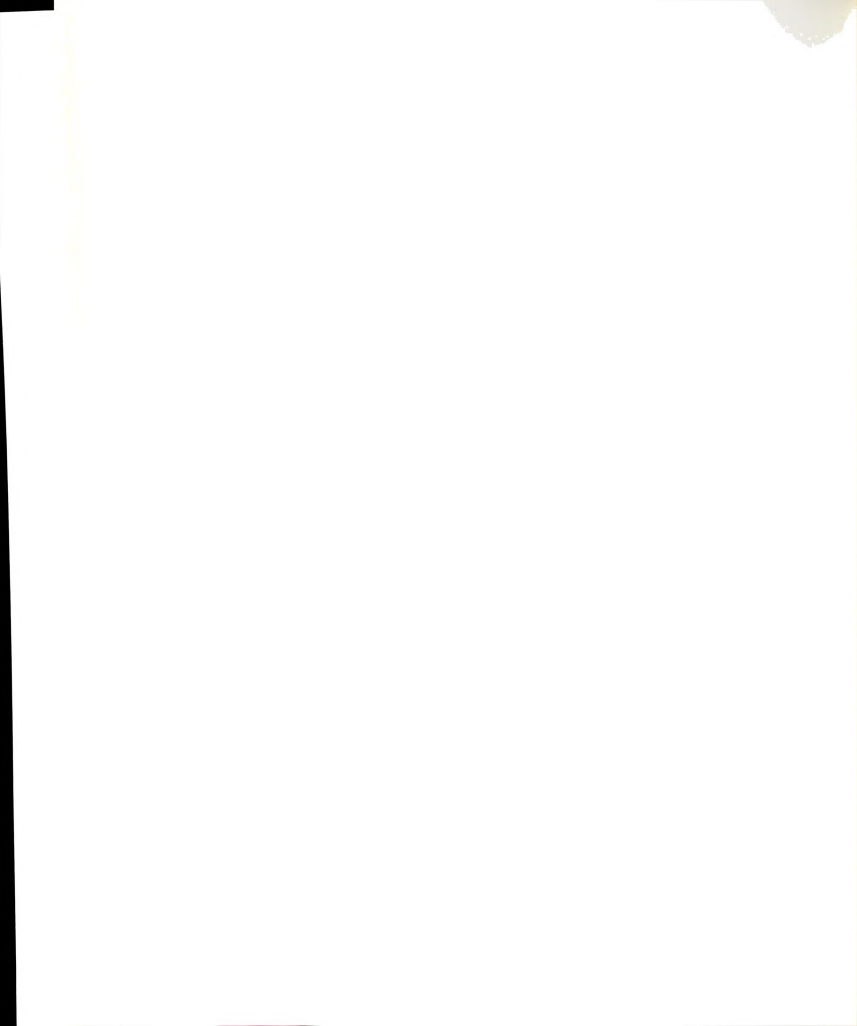
Figure 2.1 Abundance of methanol CI reagent ions as a function of pressure: (\*)  $\text{MeOH}+\text{H}^+$ , (O)  $(\text{MeOH})_2+\text{H}^+$ , ( $\diamond$ )  $(\text{MeOH})_2+\text{H}^+$ , ( $\bullet$ )  $(\text{MeOH})_2+\text{H}^+-\text{H}_2\text{O}$ , ( $\blacklozenge$ )  $(\text{MeOH})_2+\text{H}^+-\text{H}_2\text{O}$ .

low pressure, the methanol monomer is the predominant ion. As the pressure is increased the relative abundance of the monomer ion decreases as the dimer, and then the trimer ions, each with their associated water loss ions, increase in relative abundance. Only a small amount of the tetramer is formed and is not shown. This phenomenon is in general agreement with the spectra reported by both Katz *et al.*<sup>(21)</sup> and Kebabian *et al.*<sup>(22)</sup>, who have postulated that the dimer and trimer are favored over the larger clusters for energy reasons.

The clusters are an agglutination of neutral methanol molecules hydrogen bonded to a central protonated methanol ion. In the  $n=2$  and  $n=3$  clusters, the neutral molecules are bound directly to a central ion. Any additional molecules added must go to less favored outer positions. When the pressure gets too high the entire chemical ionization process is quenched and the abundance of all the ions decreases. Figure 2.2, a plot of the total ion current versus pressure, shows that there is a wide range of pressures where the current maximum remains constant, while the relative abundances of the cluster ions change under this plateau. This provides a relatively wide range of reagent gas compositions without sacrificing total ion current. It should be noted that in a single stage mass spectrometer, abundant reagent ions at masses up to  $m/z$  129 would restrict the mass range adversely. This is not a problem, however, with an MS/MS instrument which can filter out the reagent ions with the first mass spectrometer.

#### b) Temperature Characterization

At higher source temperatures, the same changes in relative ion abundance with pressure are observed but the contribution to the CI plasma from higher order clusters remains small, even at the higher



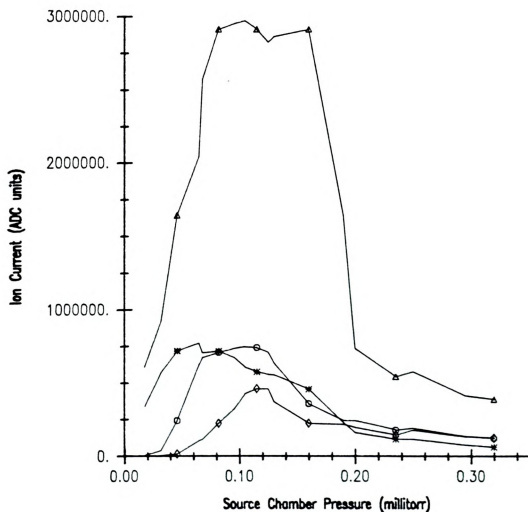
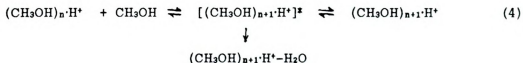


Figure 2.2 Total ion current of methanol CI reagent ions, variation with pressure: (▲) Total ion current, (★) MeOH+H<sup>+</sup>, (○) (MeOH)<sub>2</sub>+H<sup>+</sup>, (◇) (MeOH)<sub>3</sub>+H<sup>+</sup>.

pressures. Figure 2.3 shows the change in the reagent ion abundances at different temperatures and constant methanol pressure of 0.12 torr. As the temperature is raised, first the trimer ion falls in abundance while the  $((\text{MeOH})_3-18)^+$  ion at  $m/z$  79 and the dimer ion increase until, as the temperature continues to rise, these ions, too, decrease in abundance. The intensity of the monomer ion and the  $((\text{MeOH})_2-18)^+$  ion at  $m/z$  47 both increase steadily with temperature, as the bigger clusters decline. At low temperatures the dimer and the trimer ion abundances are much larger than the fragment ions formed by loss of neutral water from the cluster. However as the temperature increases the fragment ions become more abundant as the hydrogen bonded clusters expel water to form protonated dimethylether. In general, the amount of fragmentation occurring for a given compound increases as the temperature increases as a result of the larger amount of thermal energy contained in the compound. This is one factor responsible for the decrease in abundance of the large clusters at high temperatures, but there are several other factors that also apply. The cluster formation can be expressed by the equilibrium reaction represented below.



An excited  $n+1$  cluster formed by either a  $n$  cluster ion reacting with a neutral or an  $n+1$  cluster ion being activated by a third body collision, can either dissociate back to the  $n$  cluster, be stabilized by a third body collision to form the  $n+1$  cluster, or fragment by losing

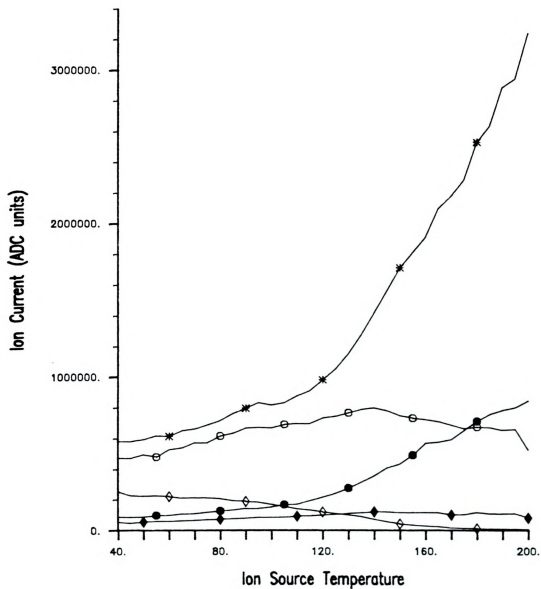
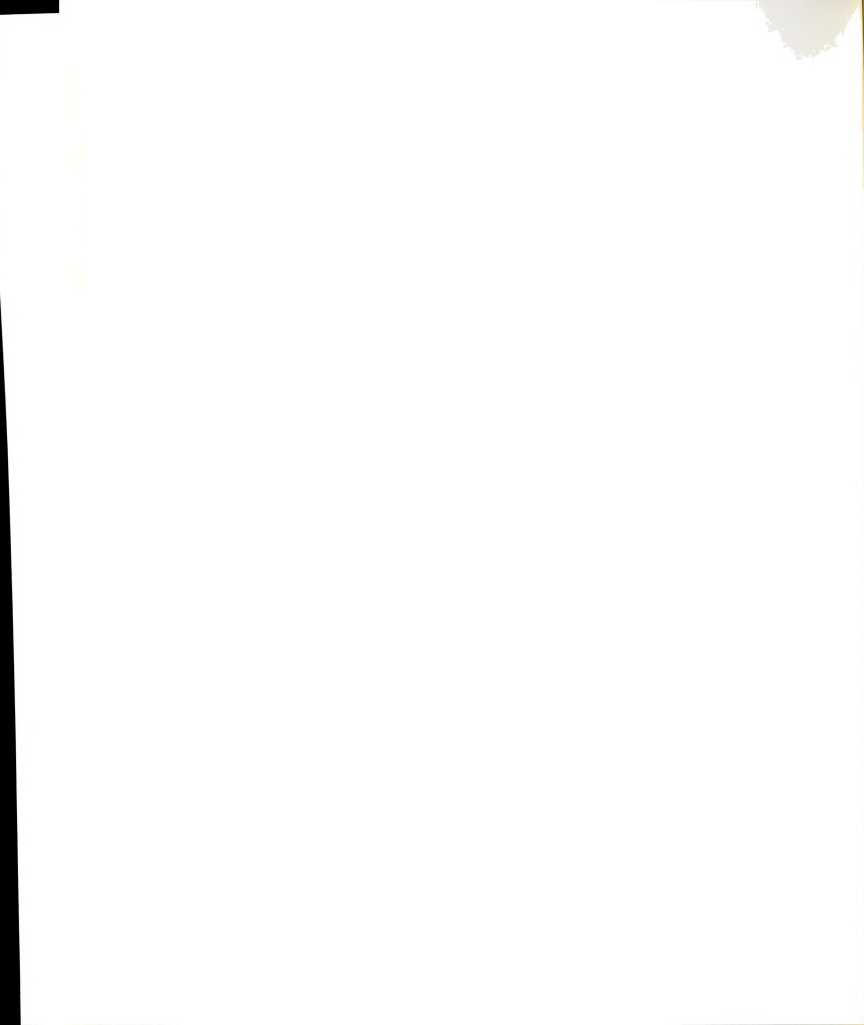


Figure 2.3 Abundance of methanol CI reagent ions as a function of temperature: (\*)  $\text{MeOH}+\text{H}^+$ , (O)  $(\text{MeOH})_2+\text{H}^+$ , (◇)  $(\text{MeOH})_3+\text{H}^+$ , (●)  $(\text{MeOH})_2+\text{H}^+-\text{H}_2\text{O}$ , (◆)  $(\text{MeOH})_3+\text{H}^+-\text{H}_2\text{O}$ .





water. At low temperatures the equilibrium is shifted towards stabilization and the higher order clusters are formed. As the temperature is raised, however, the kinetics are changed. The rate constants for clustering are lower and the rate for fragmentation and decomposition are raised, which shifts the equilibrium in favor of the smaller clusters.

### c) Gas Chromatography Conditions

The added gas load inherent with gas chromatography also affects the ratio of cluster ions. Under GC conditions, the He flowing from a capillary column reduces the abundance of the larger clusters because the methanol concentration becomes diluted by the carrier gas. With high temperatures and carrier gas present the ratio of the clusters is still dependent on the pressure, but the greatest variability occurs when lower temperatures and no excess gas are used.

## 2. Decreased Fragmentation

As the relative abundances of the methanol ions change, the ionization conditions and hence the amount of fragmentation also changes. Figure 2.4 shows the effect methanol pressure has on the ionization of malathion. At low pressures, when the monomer is the predominant ion, the malathion spectrum is dominated by fragment ions. As the concentration of the methanol clusters increases, the fragment ion relative abundances decrease while the  $(M+H)^+$  ion abundance increases. In the spectra of some compounds, the  $(M+H)^+$  ion becomes the only ion in the spectrum, while in other easily fragmented molecules a small number of fragments may still remain. The amount of fragmentation and the abundance of the  $(M+H)^+$  ion can be varied by



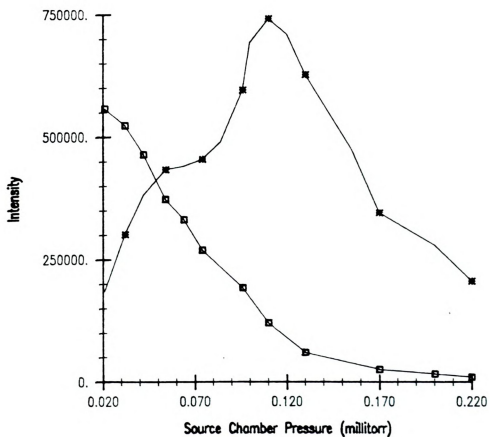


Figure 2.4 Abundance of malathion ions formed by methanol CI as a function of pressure: (\*) (M+H)<sup>+</sup>, (□) Σ fragment ions.



changing the methanol pressure. Often the pressure where the minimum amount of fragments are formed is not the same as that where the abundance of the  $(M+H)^+$  ion is greatest. Selected ion monitoring experiments can therefore be run at a pressure that maximizes the  $(M+H)^+$  ion, while mixture analysis can be run at higher pressures where the absence of fragments is most important.

Deciphering exactly what it is that causes the decrease in fragmentation is hindered by the many ion-molecule reactions possible in a high pressure chemical ionization source. It is generally considered that the extent of fragmentation of the  $(M+H)^+$  ion depends on the internal energy deposited in the sample molecule during an exothermic proton transfer reaction. However, proton affinity reasons alone cannot explain the decrease in fragmentation. The number of different reactive reagent ions present in methanol makes the situation more complex. The proton affinity of the clusters, collisional stabilization, and the availability of leaving groups all have a combined role in decreasing fragmentation.

### 3. Sensitivity Increase

In addition to decreased fragmentation, another advantage methanol chemical ionization offers is the increased sensitivity often found when molecules containing heteroatoms are ionized. Table 2.2 compares the peak intensities from two total ion current (TIC) chromatograms of a test mixture containing a variety of compound classes. The data were taken using the same GC and MS conditions, but one chromatogram was taken using methanol CI and the other using isobutane CI. The two resulting TIC chromatograms were identical except that, even though the same sample volumes were injected, the

Table 2.2 Intensity of TIC peaks in chromatograms of test mixture ionized with isobutane and methanol CI

COMPOUND	INTENSITY	
	Isobutane	Methanol
2,3 Butanediol	40462	66213
Decane	4949	0
1-Octanol	9001	27614
2,6 Dimethylphenol	18677	53800
Nonanol	5175	15211
Undecane	4647	0
2-Ethylhexanoic acid	5175	14774
2,6 Dimethylaniline	34563	64564
C <sub>10</sub> acid methyl ester	26464	41229
Dicyclohexylamine	10367	24528
C <sub>11</sub> acid methyl ester	14832	50372
C <sub>12</sub> acid methyl ester	17360	17212





peaks in the methanol run were on average 2.4 times more intense than the corresponding peaks in the isobutane chromatogram. Due to factors not yet understood, methanol CI enhances ion signals, and hence increases sensitivity, for most molecules containing heteroatoms. This is especially useful for the detection of trace components in mixtures, where the peaks representing the species of interest rise above the background matrix which is often not enhanced. Even greater sensitivity increases are observed in selected ion monitoring chromatograms, particularly when the  $(M+H)^+$  ions formed by methanol CI are compared to fragmenting ionization systems, such as methane CI. Sensitivity increases of up to two orders of magnitude can frequently be achieved in these experiments.

#### 4. Active Ion Determination

One of the first theorems that had to be tested was whether or not the cluster ions are involved in the actual proton transfer reaction. It is known that the molecular weight of the reagent gas is inversely related to the maximum in a plot of ion current versus pressure<sup>(23)</sup>. Figure 2.5 shows plots of sample ion current, as  $(M+H)^+$  ions from a constant amount of 2-pentanone, vs. pressure for methane, isobutane and methanol. Pressure plots similar to these are observed for all CI gases. The decrease at higher pressure results from a decreased penetration of the electrons into the source. The maximum sensitivity for methanol occurs at a lower pressure than the other gases. This indicates that the methanol ions involved in the ionization reaction have more mass than the other reagent ions. Methane has two reagent ions,  $CH_5^+$  and  $C_2H_5^+$ , at  $m/z$  17 and  $m/z$  29. Isobutane's reagent ion is the  $C_4H_9^+$  ion at  $m/z$  57. The pressure plot data, therefore, indicates that it

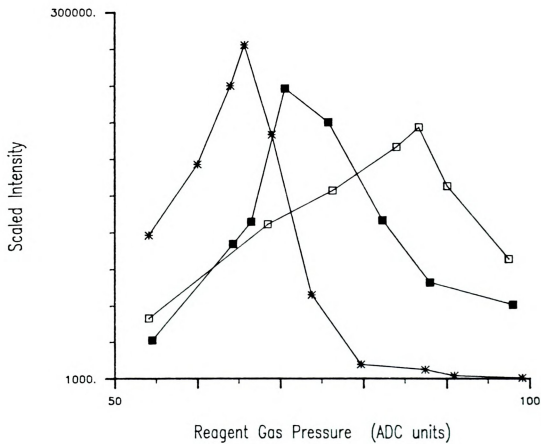


Figure 2.5 Ion current maxima as a function of pressure: (□) methane, (■) isobutane and (\*) methanol.



is the  $m/z$  65 methanol dimer, or larger cluster, that is involved in the proton transfer reaction, not the monomer. This is corroborated by the fact that at the pressure where the plot maximum occurs, the  $m/z$  65 ion is the most abundant ion in a spectrum of the methanol reagent gas.

A further indication that the cluster ions are responsible for the proton transfer can be discerned by monitoring the reagent ion abundances as a sample is introduced. Figure 2.6 shows the selected ion monitoring traces of the three cluster ions and the  $(M+H)^+$  ions of dursban and phosmet at  $m/z$  350 and 319. The samples were kept on a cooled probe for the first 250 seconds to allow the reagent gas pressure to equilibrate, after a pressure surge initiated by the probe insertion, and to establish good base line intensities. After the 250 seconds the probe cooling system was turned off and the probe was heated to volatilize both pesticides. As the intensity of the sample peaks increase, the abundances of the reagent ions decrease. The intensity decrease is observed because the equilibrium between the clusters is upset by the sample. The concentration of the clusters cannot be replenished fast enough after their charge is transferred, with the proton, to the sample to maintain equilibrium. The contour of the  $m/z$  65 ion trace especially mirrors the sample peak shape. The rise in the ion current at  $m/z$  97, which starts right after the temperature increase, as well as its overshooting of the base line after the sample is gone, is not understood. The behavior is very reproducible and is probably a temperature phenomenon, even though temperature increases should make the higher clusters decrease in intensity.

The decreased reagent ion abundance is not unusual or unique to cluster ions. Monitoring the intensity of a reagent ion peak is a

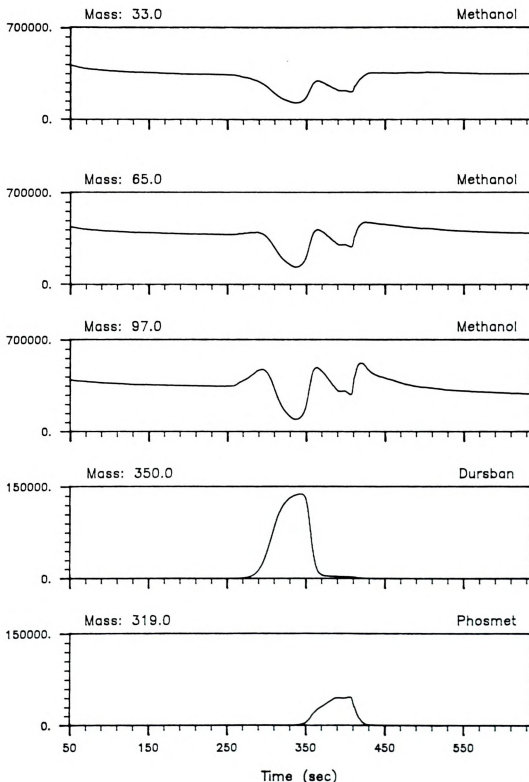


Figure 2.6 Selected ion monitoring chromatograms of methanol reagent ion clusters and the  $(M+H)^+$  ions for dursban and phosmet.



convenient way to collect a total ion chromatogram for a gas chromatographic analysis while using selected ion monitoring. The ion chromatogram collected in this manner resembles an inverted total ion chromatogram obtained by normal scanning methods.

## 5. Factors Affecting Fragmentation

### a) Proton Affinity

The proton affinity of methanol is reported as 184.9 kcal/mol, which places it above methane at 130.5 kcal/mol and below isobutane and ammonia, at 196.7 and 205.0 kcal/mol, respectively<sup>(8)</sup>. Figure 2.7 shows the mass spectra of malathion ionized with several different reagent gases. The methane and isobutane spectra both have  $(M+H)^+$  peaks at  $m/z$  331 as well as many fragment peaks at  $m/z$  285, 173, 129, 97, etc. The ammonia spectrum has a smaller  $(M+H)^+$  peak, a peak at  $m/z$  348 due to the  $(M+NH_4)^+$  ion and again many lower mass fragment ions. The total ion current of the ammonia spectrum is also much lower than that of the others, indicating that the ionization reaction is almost too soft or nearly thermoneutral. The methanol spectra contains only one peak at  $m/z$  331 due to the  $(M+H)^+$  ion. The lack of fragment ion peaks in the methanol spectrum indicates that methanol is a softer reagent gas than the other gases tested even though the reported proton affinity for methanol is lower than the proton affinity of both isobutane and ammonia. Therefore, reported proton affinity alone does not predict the observed results.

The reported values for the proton affinity of methanol are for the methanol monomer. The proton affinity of the methanol clusters is not known, but because increasing the solvation order of a cluster

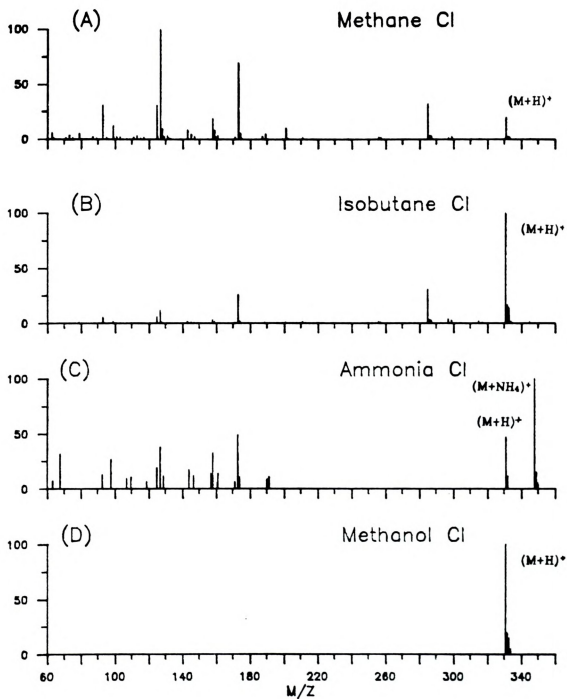


Figure 2.7 Mass spectra of malathion ionized by four chemical ionization reagent gases: (A) methane, (B) isobutane, (C) Ammonia, (D) Methanol.



raises proton affinity<sup>(8)</sup>, the cluster affinity is assumed to be higher than that for the monomer. Proton affinities can be estimated by bracketing the compound with unknown proton affinity between two compounds whose proton affinity is known. Since the unknown will transfer a proton during reactions with compounds that have a higher proton affinity and not react with species of lower proton affinity, testing for proton transfer with a series of compounds of increasing proton affinity will give upper and lower limits to the unknown's proton affinity.

We attempted to bracket the proton affinity of the methanol cluster reagent mixture. The initial information we had from ionization studies with the organophosphorus pesticides suggested that the proton affinity for the methanol clusters lay between isobutane at 196.7 kcal/mol and ammonia at 205.0 kcal/mol. Therefore, an initial set of five compounds was chosen with proton affinities between 180 kcal/mol and 231 kcal/mol. These compounds were introduced into the ion source so that they could react with the methanol ions. Unfortunately, instrument malfunctions made it appear as if none of these samples were ionized, indicating that the proton affinity was above 231 kcal/mol. Higher proton affinity compounds were found and added to the test mixture which was then analyzed again. This time all the compounds were ionized. Lower proton affinity compounds were added and analyzed. Again all were ionized. By this time, however, it became apparent that more was involved in these reactions than just proton transfer. There were numerous peaks in the spectra that represented the products of other ion-molecule reactions. Ions due to hydride abstraction, sample dimers, methanol adducts and fragmented adducts were all present.

The presence of adducts added an additional variable into the proton affinity determination. Since ammonia forms adduct ions with compounds that have a lower proton affinity than ammonia, but produce  $(M+H)^+$  ions with compounds of higher proton affinity, the formation of the methanol adduct ions was examined in terms of proton affinity to determine if the same trend applies to this situation. In order to minimize variables, new compounds with similar functional groups were used to quantify methanol's proton affinity. The results are summarized in table 2.3.

All compounds with proton affinity above 185 kcal/mol were ionized. Compounds with proton affinities below 185 kcal/mol were not ionized by proton transfer. The acknowledged value for the proton affinity of the methanol monomer is 185.0 kcal/mol, and our data agree with this value. No conclusions could be drawn from this data about the proton affinity of the clusters, since the methanol reagent gas mixture always contains a substantial concentration of the monomer. Even though the clusters seem to be responsible for the decreased fragmentation, and they should have proton affinities greater than 185 kcal/mol<sup>(8)</sup>, if compounds are introduced that will not react with the clusters, the monomers are still present to take over the reaction.

No conclusions were drawn on the role of proton affinity in the relative production of adducts vs.  $(M+H)^+$  ions. There was no relation found between adduct formation and proton affinity. Instead, the presence of, and abundance of, all the different adducts is determined

by the capacity of the samples to form stable hydrogen bonds or undergo reaction. Adducts are only formed with polarizable compounds capable of forming hydrogen bonds. Relative proton affinities have no



**Table 2.3** Proton Affinity and ions formed for compounds used to determine the proton affinity of methanol clusters

Compound	Proton Affinity <sup>a</sup>	Ions Formed <sup>b</sup>
Water	166.0	---
Chlorobenzene	181.6	M-H
Trichloacetic acid	183.0	---
Trifluoroacetic acid	185.0	---
Acetaldehyde	186.0	adducts
Propionaldehyde	191.4	adducts
o-Xylene	193.0	M+H
n-Valeraldehyde	193.3	adducts
Nitrobenzene	193.6	M+H
2-Pentanone	200.0	adducts
Anisole	200.6	M+H
Diethylether	206.0	adducts
Aniline	211.5	M+H

a. in kcal/mole, taken from reference 8

b. all compounds with adducts also produced M+H ions

relation to the production of adducts. Adduct formation is discussed in greater detail in section F.

These questions could be answered with different instrumentation. Ion cyclotron resonance (ICR) mass spectrometry or fourier transform mass spectrometry (FTMS) instruments are usually employed in this sort of research. These instruments could isolate the cluster ions and then react them individually with the test compounds thereby avoiding the complications that arise in our multiple-simultaneous-reaction system.

#### b) Collisional Stabilization

The role of collisional stabilization is also relevant at high source pressures. Excess energy can be transferred to other species an ion encounters while in the relatively high pressure source region, thus stabilizing the excited ions and preventing fragmentation. Fragmentation will be reduced if the rate of collisional stabilization exceeds the rate of fragmentation. We investigated the contribution of collisional stabilization to methanol cluster CI by using a mix of methanol and methane as a reagent gas. Because methanol has the higher proton affinity of the two gases, the mixed system equilibrates to form only methanol reagent ions. Changing the methane pressure does not change the ratio of the methanol clusters, but does change the ionization conditions and number of collisions. Experiments were run at a constant methanol pressure, one that produces predominantly  $(\text{MeOH}+\text{H})^+$  ions, and increasing amounts of methane. The results of two of these experiments are summarized in figure 2.8. Shown are plots of the abundance of several ions from acetic acid and acetophenone versus the pressure of methane. The ion intensities have been normalized to the intensity of the methanol ion. In the acetic acid plot, the fragment ion peak, at  $m/z$

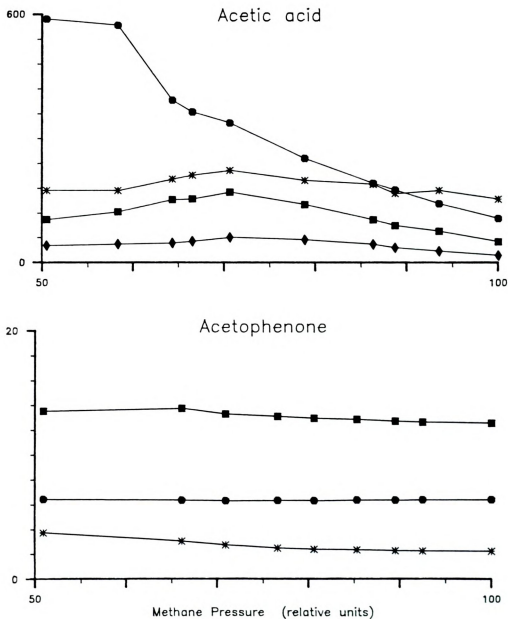


Figure 2.8 Acetic acid and acetophenone ions vs. methane pressure for a constant pressure of methanol. Acetic acid: (\*) (M+H)<sup>+</sup>, (●) fragment ion, (■) & (◆) adduct ions; Acetophenone: (\*) (M+H)<sup>+</sup>, (●) fragment ion, (◆) adduct ion

43 decreases with pressure as the abundance of both the  $(M+H)^+$  ion and the other adducts increase at first, but then fall back. The rise is due, in some cases, to an initial collision induced stabilization, and in other cases to a general increase in abundance for the species that require third body collisions. These ions fall in abundance because, after stabilization, additional collisions can re-energize and fragment these newly formed complexes. The data for acetophenone, however, show virtually no change in intensity with pressure for either fragment ions or adduct ions. These data indicate that collisional stabilization may be a factor when small molecules are ionized, but is much less important with larger molecules that are capable of effectively absorbing the excess energy themselves.

#### c) Leaving Groups

The third factor to consider is the availability of good leaving groups which can carry away some of the excess energy. The major fragmentation reactions of even-electron ions involve elimination of stable, even-electron neutral molecules which may be present in the ion. Methanol, unlike most reagent systems, provides its own leaving groups. The cluster ions contain an abundance of neutral methanol molecules which are excellent leaving groups. During the proton transfer reaction methanol molecules can be facilely expelled so that the sample ion remains intact.

#### 6. Adduct Ions

Methanol has become the ionization gas of choice in our laboratory, used in some instances to discriminate against hydrocarbons in mixtures, and in other cases, when pure species are used, because it

increases signal intensities. Most all the compounds run with methanol CI have produced predominantly  $(M+H)^+$  ions. These compounds, too numerous to list, are involved in all facets of our research. There are, however, several compound classes which react with methanol to form adducts other than  $(M+H)^+$  ions.

Figure 2.9 shows the total ion chromatogram formed when methanol is used to ionize compounds in a twelve-component chromatographic test mixture containing a variety of compound classes. The major ions in the individual mass spectra, which are presented in appendix 2A, are tabulated and listed in table 2.4. There are only 8 prominent peaks in the chromatogram besides the solvent peak. Because the chromatographic conditions used, including capillary column coating, were not those recommended for ideal separation, several of the peaks co-eluted. Nonanal and 2,6-dimethylphenol are both present in the peak centered at scan number 205. The peak at scan 350 is comprised of both dicyclohexylamine and the methyl ester of the  $C_{10}$  acid. The underivatized 2-ethylhexanoic acid is seen as a shoulder on the 2,6-dimethylaniline peak at scan 228 but actually has a broad profile and is present from scan 215 through scan 240. The last peak, at scan 510, is not part of the test mixture and was never identified.

Methanol ionization formed  $(M+H)^+$  ions for all the compounds except the straight chain hydrocarbons, which were not ionized. The  $(M+H)^+$  ions form the base peak in the spectra of seven of the compounds and are the only peaks found in the spectra of the two aromatic species. The base peak in the spectra of both alcohols is a fragment ion due to loss of water. The abundance of this fragment can be lowered, while at the same time increasing the  $(M+H)^+$  ion intensity,





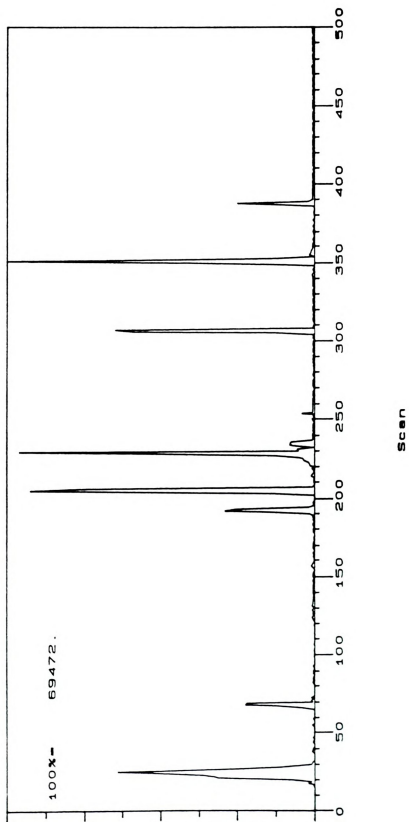


Figure 2.9 Total ion current chromatogram for programmed test mix--  
Methanol CI

Table 2.4 Ions found in the Methanol CI spectra of the Test Mixture

COMPOUND	BASE PEAK	OTHER MAJOR IONS	IONS >10%
2,3 Butanediol	M-17	M+H, M+33	M+15, 2M+H
Decane	---		
1-Octanol	M-17	M+33, C <sub>8</sub> H <sub>11</sub>	M+H
2,6 Dimethylphenol	M+H		
Nonanal	M+H	M+33	M+15
Undecane	---		
2-Ethylhexanoic acid	M+15	M+H, M-17	M+33
2,6 Dimethylalanine	M+H		
C <sub>10</sub> acid methyl ester	M+H		M+33
Dicyclohexylamine	M+H		M+33
C <sub>11</sub> acid methyl ester	M+H		M+33
C <sub>12</sub> acid methyl ester	M+H		M+33

by raising the methanol pressure. But this would also increase the amount of other adducts formed.

As noted above, reactions that form adducts can play a significant role in chemical ionization experiments when polar molecules capable of hydrogen bonding are involved. Since methanol itself is able to form hydrogen bonds, it is not surprising to find adducts, especially  $(M \cdots H \cdots MeOH)^+$  ions, in the spectra of many of the polar compounds. Adducts require third body collisions for stabilization and are, therefore, formed predominantly at high pressures. The rates for such reactions are considerably slower than bimolecular processes, but at high pressures ion residence times are increased and the probability of forming adducts is higher. Lowering the pressure, to rid the spectra of adduct ions, may, however, increase the number of fragment ions formed. So again, the goal of the experiment should be considered when adjusting the reagent gas pressure. The abundance of these ions can be controlled in the same way that fragmentation can be controlled, by changing the methanol pressure.

As expected, the small diol in the mix formed the most adducts. Ions due to addition of methanol, addition of methanol and subsequent loss of water, proton-bound diol dimers, and dimers minus water were all present in the spectrum. Eight of the ten compounds ionized formed  $(M+H+MeOH)^+$  adduct ions. The other adduct ion found in the test mixture was the  $(M+15)^+$  ion which is present in the spectrum of the underivatized acid. This ion is formed by a gas phase esterification reaction similar to acid-catalysed reactions prevalent in solution chemistry. No attempt was made to discern if these adducts are covalent or hydrogen bonded. As a class, the acids formed the most

adduct ions, but multiple adducts can also be found in the spectra of other small polarizable compounds. As typical examples, figure 2.10 shows the spectra of three other organic acids and a ketone. They all have prominent  $(M+15)^+$  peaks and many other adduct ions. The adducts are most prevalent with smaller molecules that are more easily assimilated into the proton-bound clusters. The larger acids, like docosanoic acid, tend to form adducts due to addition of only one methanol, creating the  $(M+15)^+$  and  $(M+MeOH)^+$  adducts.

In order to compare the observed methanol ionization traits with another reagent gas, the programed test mixture was also run with isobutane CI. The total ion chromatogram for this experiment is shown in figure 2.11. The chromatographic conditions were changed slightly in an attempt to resolve some of the unresolved peaks. The underivatized acid was resolved cleanly, but the others remained unchanged. The solvent also trailed badly, almost obscuring the diol peak. Retention times are all changed too, but the same trends are seen in the chromatogram.

The mass spectra, however, were different. The major ions found are given in Table 2.5, with the individual spectra shown in appendix 2B. Peaks due to  $(M+H)^+$  ions are present in the spectra of all the compounds except decane, undecane, and octanol. Isobutane CI ionized both of the straight chain hydrocarbons by hydride abstraction, producing  $(M-H)^+$  ions in the molecular ion region. These ions were not the base peak, however, as typical hydrocarbon fragment ions at  $m/z$  71, 85, and 99 dominated the spectra. Fragment ions are also present in the spectra of most compounds in the test mixture. The octanol spectrum contains peaks indicative of hydrocarbons at  $m/z$  71 and  $(M-$

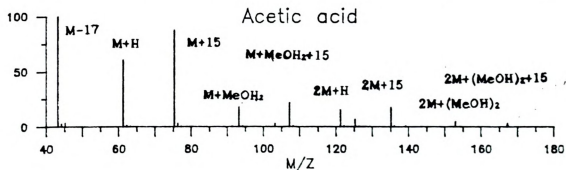
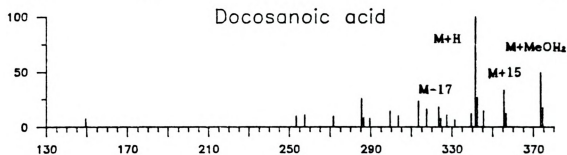
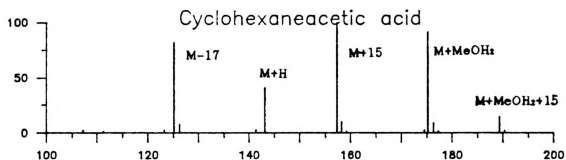
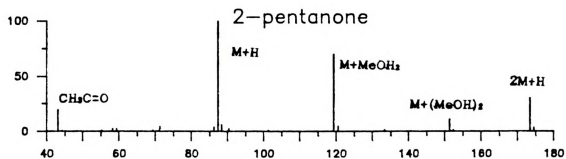


Figure 2.10 Methanol Ci spectra of four adduct forming compounds.



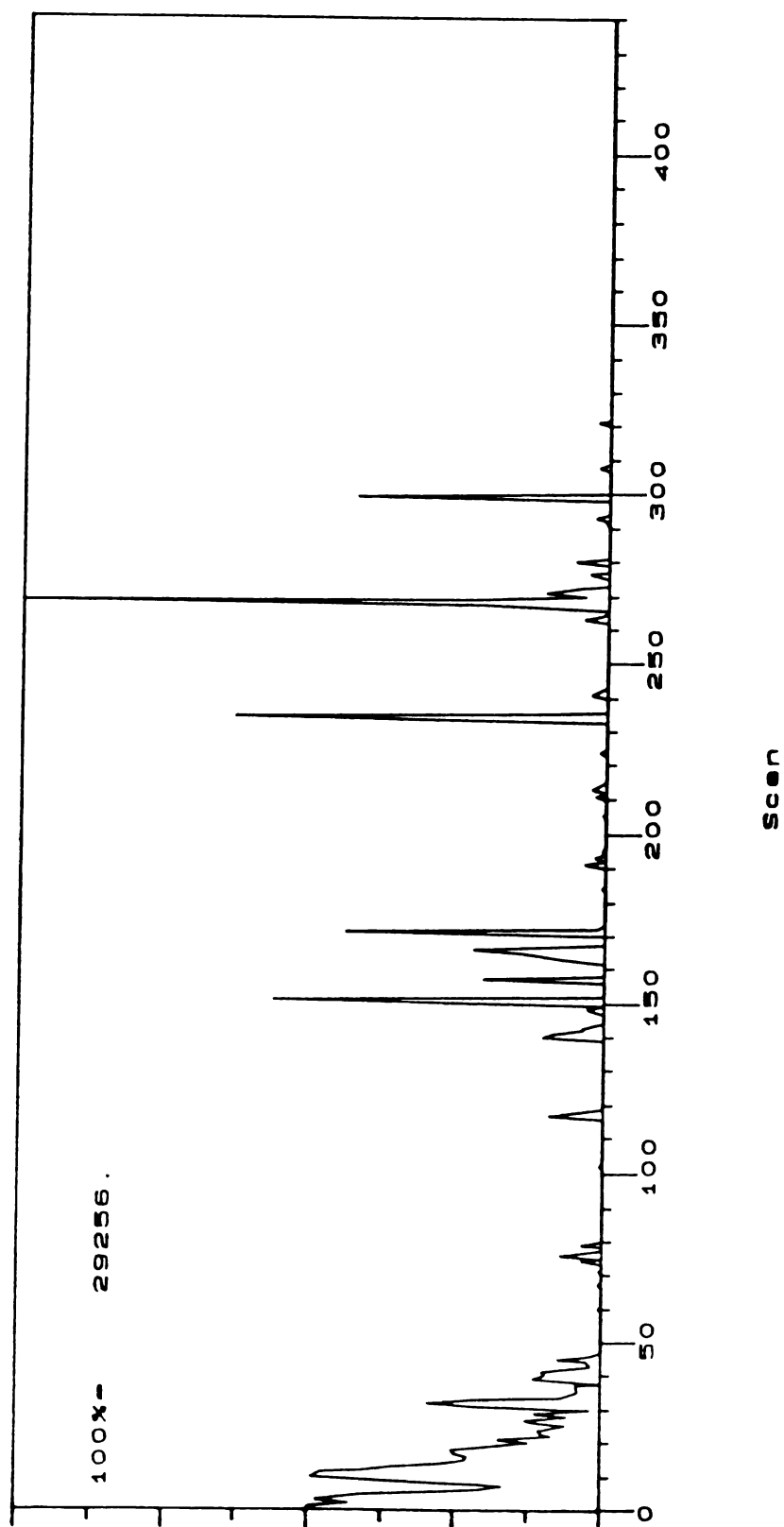


Figure 2.11 Total ion current chromatograms for programmed test mix--  
Isobutane CI.





**Table 2.5** Ions found in the isobutane CI spectra of the test mixture

COMPOUND	BASE PEAK	OTHER MAJOR IONS	IONS >10%
2,3 Butanediol	M-17	M+H,	
Decane	C <sub>5</sub> H <sub>11</sub>	C <sub>6</sub> H <sub>13</sub> , M-H	
1-Octanol	M-17	C <sub>5</sub> H <sub>11</sub>	M-H
2,6 Dimethylphenol	M+H		
Nonanal	M+H		C <sub>5</sub> H <sub>11</sub> , C <sub>6</sub> H <sub>13</sub>
Undecane	C <sub>5</sub> H <sub>11</sub>	M-H, C <sub>6</sub> H <sub>13</sub> , C <sub>7</sub> H <sub>15</sub>	
2-Ethylhexanoic acid	M+H		
2,6 Dimethylaniline	M+H		
C <sub>10</sub> acid methyl ester	M+H		C <sub>3</sub> H <sub>6</sub> O <sub>2</sub> , M-H
Dicyclohexylamine	M+H		M-44
C <sub>11</sub> acid methyl ester	M+H		C <sub>3</sub> H <sub>6</sub> O <sub>2</sub> , M-H
C <sub>12</sub> acid methyl ester	M+H		C <sub>3</sub> H <sub>6</sub> O <sub>2</sub> , M-H

H)<sup>+</sup>, but also retains the typical alcohol peak at (M-17)<sup>+</sup>. The spectrum of the other alcohol, 2,3-butanediol, had only two peaks, (M-17)<sup>+</sup> and (M+H)<sup>+</sup>. This exemplifies the other major difference in the spectra produced by isobutane. The non-polar reagent gas does not provide the best environment for adduct formation and, therefore, the isobutane CI spectra are marked by the absence of adduct ions.

#### E. CONCLUSION

Methanol CI is a very versatile ionization technique that can be tailored to meet the demands of many different mass spectrometric experiments. The methanol cluster ions formed under chemical ionization pressures provide increased sample ion currents and variable ionization conditions. The ratio of the reagent cluster ions is affected by the ion source temperature and amount of carrier gas present, but can be varied and controlled by changing the pressure of methanol introduced into the ion source. The change in reagent ion composition changes the ionization conditions and, hence, changes the sample ions formed. The methanol pressure can be set to favor increased (M+H)<sup>+</sup> ion current or adjusted to eliminate fragment ions. The decreased fragmentation is due to a combination of decreased exothermicity in the proton transfer reaction, collisional stabilization (especially for small molecules), and the presence of stable leaving groups. Methanol, being polar and capable of hydrogen bonding, forms adduct ion with several compound classes. Adduct formation is not dependent on proton affinity but instead is determined by the size of the sample molecule and the presence of chemical functional groups. The advantages offered by methanol chemical ionization, especially decreased fragmentation and enhanced



signal intensities, have found numerous uses in our lab, including the analysis of sulphur-containing compounds in jet fuels and in screening analyses for organophosphorus pesticides on fruit<sup>(24,25)</sup>.

## F. REFERENCES

1. Bauer, M.R.; M.S. Thesis, Michigan State University, 1983.
2. Munson, M.S.B., Field, F.H.; *J.Am.Chem.Soc.*, **1966**, *88*, 2621.
3. Clemens, D., Munson, B.; *Anal. Chem.*, **1985**, *57*, 2022.
4. Hunt, D.F.; *Prog. Anal. Chem.*, **1973**, *6*, 359.
5. Field, F.H.; *J.Am.Chem.Soc.*, **1969**, *91*, 2827.
6. Wilson, M.S., Dzidic, I., McClosky, J.A.; *Biochim. Biophys. Acta*, **1971**, *240*, 623.
7. Dzidic, I., McClosky, J.A.; *Org. Mass Spec.*, **1972**, *6*, 939.
8. Harrison, A.G.; *Chemical Ionization Mass Spectrometry*; CRC Press: Boca Raton, Fl., 1983; Chapters 2&4.
9. Sunner, J., Szabo, I.; *Adv. Mass Spectrom.*, **1978**, *7B*, 1383.
10. Stan, H.J.; *Fresenius Z. Anal. Chem.*, **1977**, *287*, 104.
11. Hawthorn, S.B., Miller, D.J.; *Anal. Chem.*, **1985**, *57*, 694.
12. Jennings, K.R.; in *Gas Phase Ion Chemistry*, Vol 2, edited by Bowers, M.T., Chapter 12, Academic Press: New York (1979).
13. Burlingame, A.L., Whitney, J.D., Russel, R.H.; *Anal. Chem.*, **1984**, *56*, 417R.
14. Keough, T., DeStafano, A.J., *Org. Mass Spectrom.*, **1981**, *16*, 527.
15. Maquestiau, A., Flannery, R., Nielsen, L.; *Org. Mass Spectrom.*, **1980**, *15*, 376.
16. Carroll, D.I., Nowlin, J.G., Stillwell, R.N., Horning, E.C.; *Anal. Chem.*, **1981**, *53*, 2007.
17. Ferrer-Correia, A.J.V., Jennings, K.R., Sen Sharma, D.K.; *Org. Mass Spectrom.*, **1976**, *11*, 867.
18. Stillwell, R.N., Carroll, D.I., Nowlin, J.G., Horning, E.C.; *Anal. Chem.*, **1983**, *55*, 1313.
19. Musselman, B.D., Allison, J., Watson, J.T.; *Anal. Chem.*, **1985**, *57*, 2425.
20. Crawford, R.W., et al.; *Anal. Chem.*, **1984**, *56*, 1121.

21. Katz, R.N., Chaudhary, T., Field, F.H.; *J.Am.Chem.Soc.*, **1986**, 108, 3897.
22. Kebarle, P., Grimwald, E.P.; *J.Am.Chem.Soc.*, **1973**, 95, 7939.
23. McGuire, J.M., Munson, B.; *Anal. Chem.*, **1985**, 57, 680.
24. Schubert, A.J., Enke, C.G.; Unpublished data.
25. Bauer, M.R., Enke, C.G.; Paper MOA10 presented at the 32<sup>nd</sup> Annual Conference on Mass Spectrometry and Allied Topics, San Antonio, **1984**.

## CHAPTER THREE

### Detection of Organophosphorus Pesticides

#### A. INTRODUCTION

Organophosphorus compounds are widely used as agricultural pesticides and herbicides. Despite their generally high toxicity to man, these compounds are increasingly attractive because organophosphorus pesticides are much less persistent than other available pesticides. They decompose and/or oxidize readily, making them harmless. Earlier chlorinated compounds have been banned due to their carcinogenic properties and extraordinary environmental persistence. Detection of organophosphorus pesticides is accordingly much more difficult because the presence of all the metabolites and decomposition products, as well as the pesticides themselves, must be monitored. The organophosphorus pesticides are also more toxic than other pesticides and, therefore, less of the organophosphorus pesticide has to be applied to achieve comparable levels of pest control. Decreased application also means that smaller quantities of all the residues must be detected on harvested crops and produced food stuffs.

Gas chromatography (GC) is the most widely used and accepted method to detect organophosphorus pesticides because of the highly sensitive and specific response of available phosphorus detectors. Most of the "standard methods" <sup>(1,2)</sup> for determination of organophosphorus pesticides in water <sup>(3)</sup> and air <sup>(4)</sup> as well as techniques for analyses on food <sup>(1,5,6)</sup> involve gas chromatography as the determination step.





Research is continuing in the area of optimization of conditions for the analysis of organophosphorus pesticides. Incorporation of all the latest advances in chromatography research has lowered detection limits of organophosphorus pesticides below 1ppb. (7,8).

High performance liquid chromatography (HPLC) is rapidly gaining recognition in the field of pesticide analysis as a valuable chromatographic tool(8,9). Its major advantage is the ability to analyze heat-labile poorly volatile, and/or very polar compounds without resorting to chemical derivatization. Furthermore, HPLC is nondestructive and allows larger sample volumes to be injected than in gas chromatography. HPLC can be used as either a clean-up procedure for subsequent confirmation of compound identity or as a stand-alone technique. One of the shortcomings of this technique is the lack of specific detectors, although progress is being made on this front, especially with mass spectrometer interfaces. Due to the solubility of most organophosphorus pesticide metabolites, HPLC continues to be an important method for the analysis of these compounds in body fluids, including blood and urine.

There are, however, several inherent limitations for analyses utilizing chromatographic methods, the most obvious of which is time. Due to lengthy sample collection times, long multiple extractions and tedious clean-up steps prior to a time consuming chromatographic separation, a complete analysis can take days to complete. The potential for error is also introduced with each additional step in the analysis. Unequivocal identification of pesticides and their metabolites in most cases requires the use of at least two analytical techniques(9). GC and HPLC data need supporting or confirming evidence for a complete



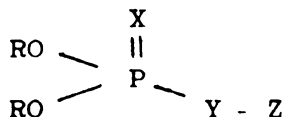
determination because retention time alone does not provide enough information <sup>(10)</sup>. Often it is mass spectrometry that provides this additional data. Triple quadrupole mass spectrometry offers an alternative detection method that is extremely rapid and needs no sample preparation. Yost has shown that triple quadrupole mass spectrometry can run 25 samples in a trace level drug screen 30 times faster than high resolution GC/MS <sup>(11)</sup>. Organophosphorus pesticides can be detected from food directly, with no extraction or chromatography steps needed. The complete analysis of a sample, therefore, takes only a minute or two.

To date, mass spectral analysis of organophosphorus pesticides has been largely limited to characterizations of ionization behavior and fragmentation mechanisms. In 1966 Domico<sup>(12)</sup> studied fragmentation and rearrangement mechanisms of 23 organophosphorus pesticides. Basing his findings on earlier work done by Quale<sup>(13)</sup>, Domico published the first spectra of organophosphorus pesticides and explained many of their prominent peaks. Holmstead and Cassida<sup>(14)</sup> published the first chemical ionization spectra of organophosphorus pesticides in 1974. They used methane as a reagent gas, but found that the spectra contained fewer  $(M+H)^+$  ions than the  $M^+$  ions in the electron impact (EI) spectra. Busch *et al.* <sup>(15)</sup> compared organophosphorus pesticide spectra derived from five ionization methods. They compared EI, methane CI, and three negative ion reagent gases and concluded that none of the techniques produced a satisfactory abundance of  $(M+H)^+$  ions. Negative CI of organophosphorus pesticides was also studied by both Daugherty *et al.* <sup>(16)</sup>, who used dichloromethane for the reagent gas, and Rankin <sup>(17)</sup>, who used electron capture reagents. Both studies reported spectra

of organophosphorus pesticides that were dominated by phosphorus ester anion fragments and little or no molecular ions. The bulk of the research on the development of an analytical method for organophosphorus pesticide detection using mass spectrometry has been done by Stan and co-workers (18-20). Using EI, isobutane CI, as well as methane negative CI, Stan has developed analytical methods based on straight MS and GC/MS to determine pesticides in biological, food, and environmental samples.

Recently a promising new technique for organophosphorus pesticide analysis was reported by Morelli and Hercules (21) that offers many of the same advantages that MS/MS has. Ambient pressure laser microprobe mass analysis (LAMMA) was used to obtain mass spectra of organophosphorus pesticides directly from the surface of plant tissues. The pesticides can be identified by the combination of positive and negative ion spectra each of which contains ions relevant to the structural features of the analyte. The authors also state that their technique enhances  $(M+H)^+$  species while reducing fragmentation. This claim is not supported by their data and in fact the reverse is more readily apparent as their spectra contain new ions not observed in other MS techniques.

A general formula for the organophosphorus pesticides under investigation can be represented by the structure



where R is an ethyl or methyl group, X and Y can be either oxygen or sulphur and Z is an organic moiety such as a substituted heterocyclic or aromatic ring, an aliphatic chain, or an amine. The main groups of



organophosphorus pesticides are distinguished by the four different possible combinations of oxygen and sulphur. Each group can be subdivided further into groups that have methyl or ethyl R groups. These eight basic structures are drawn in figure 3.1.

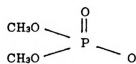
The biological activity of the various organophosphorus pesticide species is controlled by the type of Z group present. Z is generally a good leaving group and the Y-Z bond is very labile. Biological persistence and potency is altered by the addition to Z of electron withdrawing- or donating-substituents which change the strength of the Y-Z bond.

The mass spectra of the organophosphorus pesticides are also affected by the lability of the Y-Z bond as fragmentation often centers around this link. The spectra show that when Z is a good leaving group, it generally accepts the charge and the Z ions and their associated fragments dominate the spectrum. Important information of interest, namely the possibility of phosphorus esters being present, is lost because the phosphorus atom leaves as part of a neutral and is not seen in the spectrum. With other organophosphorus agents, especially those in which Z is electron withdrawing, the R groups help to support the positive charge. Mass spectra of these species are generally dominated by multiple peaks representing the phosphorus end of the molecule. Identification of the specific pesticide present in these cases cannot be determined from the spectra because the unique part of the molecule, the Z function, is lost as a neutral.

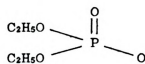
This is not to imply that neutral loss information is not available in normal mass spectra of pure compounds, for the above neutral losses certainly can be calculated in spectra that contain obvious molecular



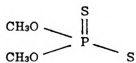




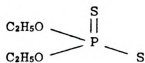
dimethoxyphosphate



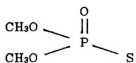
diethoxyphosphate



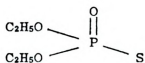
dimethoxy-  
phosphorodithioate



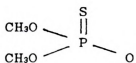
diethoxy-  
phosphorodithioate



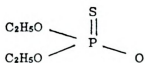
dimethoxyphosphorothiolate



diethoxyphosphorothiolate



dimethoxyphosphorothioate



diethoxyphosphorothioate

Figure 3.1 Eight sub-groups of organophosphorus pesticides



ions. This is how the above conclusions were reached. But in mixture analysis the spectrum represents all the compounds in the matrix and therefore, molecular-ion-fragment-ion relationships are not apparent. For this reason, only the ions present, not the neutral losses, can be used for detection in normal mass spectrometry.

Because the normal mass spectrum of an organophosphorus pesticide does not provide complete information about the identity of the specific agent, the potential for MS/MS to provide important additional information should be considered. Those compounds in which the charge remains on the Z group can be detected by neutral loss scans. The mass of the molecular ion along with the mass of the neutral lost can confirm the identity of these ions. Parent scans can be used to detect and identify those compounds for which the ions formed after fragmentation retain the phosphorous atom. Because the organophosphorus pesticides fragment through a limited number of mechanisms, MS/MS techniques can screen for a large number of compounds by using just a few scans.

In this work the collisionally activated dissociation (CAD) spectra of 47 organophosphorus pesticides have been collected and analyzed. Common ionic and neutral losses have been identified which can be used to screen for the general class of organophosphorus compounds. Many of the same parent/daughter ion-pairs identified also may be used for targeted analysis although in some cases the use of other daughter ions is recommended in order to lower detection limits. The technique thus developed has been used to detect trace levels of pesticides on fruit.

## B. EXPERIMENTAL

All mass spectra were taken on the Extrel ELTQ-400-3 triple quadrupole mass spectrometer and computerized control system described in chapter two. Normal mass spectra were collected by using the triple quadrupole mass spectrometer as a single stage mass spectrometer. The first quadrupole was set up as the mass filter, while the second and third quadrupoles were kept in RF-only mode such that they would pass ions of all masses. No collision gas was present in the collision quadrupole. Daughter ion spectra were collected using the instrument in the usual manner. Argon collision gas was maintained at  $\sim 4 \times 10^{-3}$  torr; collision energy, unless otherwise stated, was 25 eV.

Methanol vapors for CI were generated by injecting 2-3 ml of methanol (anhydrous reagent grade) through a GC septum into an evacuated 500 ml expansion bulb maintained at room temperature. The vapors were then let into the source through a variable leak needle valve. All chemical samples and pesticide standards used were purchased from Chem Service Inc., or provided free by the EPA, and were used without further purification. The malathion used was a commercial pesticide formula, ORTHO Malathion 50™, and was obtained from a local garden supply store.

For the mixture studies, approximately equal quantities of ten pesticides were mixed together and diluted with the ORTHO preparation and xylene to a final concentration of about two micrograms per microliter. The sample was introduced into the mass spectrometer with a solids probe into which was fitted a capillary tube containing one to two microliters of the mixture. The solids probe was slowly heated to 150°C, allowing the pesticides to volatilize.

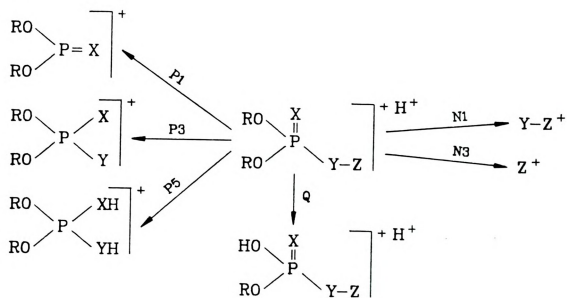
Data were collected on the instrument's microcomputer and then uploaded to a PDP 11/23 minicomputer, running the RSX 11M operating system, for data interpretation. Reaction monitoring and scan data were interpreted with the aid of a multi-dimensional data base package <sup>(22)</sup> and other software developed inhouse.

## C. RESULTS AND DISCUSSION

### 1. Daughter ion spectra

The collisionally activated dissociation spectra of the  $(M+H)^+$  ions of the organophosphorus pesticides have many of the same peaks that are present in the EI spectra reported earlier by others<sup>(12,20,23)</sup>. The daughter spectra tend to be simpler, often with only a few peaks present. Because the parent ions are formed by proton transfer chemical ionization and are therefore even-electron species, the common odd-electron, radical initiated, fragmentation mechanisms are not applicable. The peak intensities in the daughter ion spectra are a function of collision energy and the concentration of collision gas present. Increasing either, or both, in order to increase internal energy and/or number of collisions may form additional daughter ions in a few cases, but for the spectra of most compounds, the relative intensity of the peaks present is all that changes.

As in the EI spectra, the fragmentation pathways found in the daughter spectra of the  $(M+H)^+$  ions generally involve breaking the Y-Z bond. A general schematic of the common fragmentation routes is shown in figure 3.2. Fragmentation routes labeled P1, P3, P5 produce ions that will be used in parent ion scans and those labeled N1 and N3 represent ions in which the phosphorus atom has been lost as part of a neutral.



3.2 Common fragmentation routes present in the daughter spectra of organophosphorus pesticides.

The loss of alkenes due to rearrangement and fragmentation of the R group named after Quale has been labeled Q<sup>(12,13)</sup>. The additional proton provided by chemical ionization changes the mass of some of the fragments and neutral losses observed in the CAD spectra by one mass unit from those recorded in EI spectra depending on whether the extra hydrogen stays attached to the daughter ion or is lost with the neutral. The major peaks in the daughter spectra of the (M+H)<sup>+</sup> ions of organophosphorus pesticides are presented in table 3.1. Appendix 3A contains the full spectra of all compounds in table 3.1

a) Phosphorodithioates

The base peak in the daughter spectra of all the dithioates, except two, is due to a Z<sup>+</sup> ion. In many cases it is the only daughter ion present in the spectrum. These Z<sup>+</sup> ions are formed by a loss of 186 u. from the diethoxy (M+H)<sup>+</sup> ions and a neutral loss of 158 u. from the dimethoxydithioates. The base peak for malathion, one of the exceptions, is also essentially a Z<sup>+</sup> ion. The m/z 127<sup>+</sup> peak observed is a stable cyclic ion formed by loss of C<sub>2</sub>H<sub>6</sub>O from the Z<sup>+</sup> ion and/or loss of C<sub>2</sub>H<sub>6</sub>O from the (M+H)<sup>+</sup> ion followed by a Y-Z bond fragmentation. The other exception is dimethoate, which forms a P1 daughter ion and an ion at m/z 88. The origin of this ion is not readily apparent and has not yet been established, but it is most likely the protonated version of the m/z 87 ion seen in the EI spectrum of dimethoate, to which Domico has assigned the formula S-CH<sub>2</sub>-C=N-CH<sub>3</sub> by using high resolution MS techniques<sup>(12)</sup>. Coincidentally, the m/z 88 ion arises from a neutral loss of 142 u. which is the same mass lost when dimethoxy-thioates and thiolates form Z<sup>+</sup> ions.

Table 3.1: Ions in the daughter spectra of the (M+H)<sup>+</sup> ions of the organophosphorus pesticides studied.  
Mass in bold type, fragmentation mechanism<sup>a</sup>, normalized intensity in parentheses.

	Base Peak	(M+H) <sup>+</sup>	Z <sup>+</sup>	Pl <sup>+</sup>	Other Ions
<b>Ethoxyphosphates</b>					
<b>Chlorfenphos</b>	155 P5	359 (50)	205 (35)	--	137 P5-Q (30)
<b>Dursban O Analog</b>	278 M-2Q	334 (45)	--	--	306 M-Q (30), 198 N1o (70)
<b>Paraoxon</b>	220 M-2Q	276 (55)	--	--	248 M-Q (20), 174 (30), 109 (10)
<b>Methoxyphosphates</b>					
<b>Dicrotophos</b>	112 Z <sup>+</sup>	238 (80)	(100)	--	193 (30), 127 P5 (40), 72 (50)
<b>Heptanophos</b>	127 P5	251 (30)	125 (60)	--	
<b>Mevinphos</b>	127 P5	225 (10)	99 (20)	109 (10)	193 M-33 (10), 67 (40)
<b>Naled</b>	127 P5	381 (40)	--	--	
<b>Phosphamidon</b>	174 Z <sup>+</sup>	300 (50)	(100)	--	227 (35), 132 (20), 127 P5 (65), 100 (35)
<b>Tetrachlor</b>	127 P5	367 (35)	241 (30)		
<b>Ethoxydithioates</b>					
<b>Azinphos ethyl</b>	160 Z <sup>+</sup>	346 (40)	(100)	--	132 Z-Q (70)
<b>Dialifor</b>	208 Z <sup>+</sup>	394 (25)	(100)	--	187 P5 (80)
<b>Disulfoton</b>	89 Z <sup>+</sup>	275 (15)	(100)	--	
<b>Ethion</b>	199 Z <sup>+</sup>	385 (25)	(100)	153 (20)	171 (20), 143 (10)



Table 3.1 continued

	Base Peak	(M+H) <sup>+</sup>	Z <sup>+</sup>	Pl <sup>+</sup>	Other Ions
Phorate	75 Z <sup>+</sup>	261 (10)	(100)	--	
Phorate sulfoxide	99 Z <sup>+</sup>	277 (20)	(100)	153 (40)	171 (55), 143 (60)
Phosalone	182 Z <sup>+</sup>	368 (20)	(100)	153 (10)	322 (10)
Methoxydithionates					
Azinphos	160 Z <sup>+</sup>	318 (25)	(100)	125 (20)	132 (50)
Dimethoate	125 Pl	230 (70)	--	(100)	199 (75), 171 (35), 157 (10), 88 (60)
Malathion	127	331 (15)	--	125 (15)	285 (25), 256 (10) 99 (35)
Phosmet	160 Z <sup>+</sup>	318 (30)	(100)	--	
Thiometon	89 Z <sup>+</sup>	247 (10)	(100)	--	
Ethoxythioates					
Demeton-O	89 Z <sup>+</sup>	259 (15)	(100)	--	
Diazinon	169 Nls	305 (65)	--	153 (95)	277 M-Q (10), 249 M-2Q(30) 125 Pl-Q(45), 97 Pl-2Q(30)
Dursban	198 Nlo	350 (40)	--	153 (90)	322 M-Q (20), 299 M-2Q(20) 125 Pl-Q(45), 97 Pl-2Q(30)
Parathion	236 M-2Q	292 (25)	--	--	269 M-Q (18), 156 Nls (10) 140 Nlo (10)
Pirimiphos	(M+H) <sup>+</sup>	334 (100)	--	--	198 Nls (95), 182 Nlo (98) 125 Pl-Q(45), 97 Pl-2Q(30)
Quinalphos	97 Pl-2Q	299 (35)	129 (30)	153 (35)	243 M-2Q (50), 163 Nls(80) 147 Nlo (95), 125 Pl-Q(60)

Table 3.1 continued

	Base Peak	(M+H) <sup>+</sup>	Z <sup>+</sup>	Pl <sup>+</sup>	Other Ions
<u>Methoxythiolates</u>					
Etrimphos	(M+H) <sup>+</sup>	293 (100)	--	125 (85)	245 (25), 217(40), 149(20)
Fentrothion	125 Pl	278 (30)	--	125 (100)	246 M-32(40), 79 (15)
				109 (85)	
Methyl dursban	125 Pl	322 (12)	--	125 (100)	246 M-32(20), 79 (10)
				109 (75)	
Methyl parathion	125 Pl	264 (15)	122 (40)	125 (100)	232 M-32 (45), 154 Nls(10)
				109 (45)	138 Nlo(10)
Pirimiphos methyl	164 Z <sup>+</sup>	306 (50)	(100)	125 (30)	274 M-32(10), 108 Z-2Q(55)
				109 (10)	
Terphos	(M+H) <sup>+</sup>	467 (100)	--	125 (70)	419 M-48(80), 249 1/2M(55)
<u>Ethoxythiolates</u>					
Demeton-S	89 Z <sup>+</sup>	259 (10)	(100)	--	
Phorate O Analog	75 Z <sup>+</sup>	245 (15)	(100)	--	
<u>Methoxythiolates</u>					
Dimethoate O Analog	(M+H) <sup>+</sup>	214 (100)	72 (10)	125 (20)	183 (50), 155 (45)
				109 (20)	
Malathion O Analog	127	315 (25)	173 (15)	--	143 P3 (15), 99(40)
Oxydemeton	169	247 (60)	105 (30)	125 (10)	
				109 (25)	
Phosmet O Analog	160 Z <sup>+</sup>	302 (20)	(100)	--	

Table 3.1 continued

	Base Peak	(M+H) <sup>+</sup>	Z <sup>+</sup>	Pl <sup>+</sup>	Other Ions
Miscellaneous organophosphorus compounds					
Edifenphos	111 N1	311 (30)	--	--	283 M-Q(35), 201 (15), 173(50), 141(20), 109(60)
Ethoprop	131 M-Q-2Q'	243(10)	--	--	215 M-Q(10), 201 M-Q'(10), 173 M-Q-Q'(40), 77(50)
Profenophos	305 M-Q-Q'	375 (85)	--	--	139 M-Q-N1(20), 97(80) 125 M-Q'-N1(15)
Sulprofos	(M+H) <sup>+</sup>	323 (100)	--	--	347 M-Q(45) 247(50), 219(75), 125(25) 155 N1s(25), 139 N1o(30)

a) Q = Quale fragmentation, loss of ethene from ethoxy group

Q' = loss of any alkene from an R group, leaving OH or SH

N1s = N1 fragment containing sulphur

N1o = N1 fragment containing oxygen

Pls = Pl fragment containing sulphur

Pl o = Pl fragment containing oxygen

There were several other less intense daughter ions in the dithioate spectra that are also found in the CAD spectra of the other organophosphorus pesticides classes. Most of the diethoxy compounds had daughter ions due to a single loss or successive losses of 28 u. from the  $(M+H)^+$  ion or P type ions. This rearrangement and fragmentation is named after Quale who first observed the loss of stable ethene from trialkylphosphates<sup>(13)</sup>. This loss of ethylene is, of course, only possible with the ethoxy compounds, the corresponding loss of  $CH_2$  from the methoxy compounds is not observed. Instead methoxy compounds tend to form stable P1 type ions. P1 ions can be present in the daughter spectra of ethoxy compounds but are usually more abundant and more common in methoxy species.

#### b) Phosphorothioates

P1 type ions are perhaps most important in the dimethoxythioate spectra where they are represented by a major peak if not the base peak. Another important peak in the CAD spectra of both the methoxy and ethoxy thioates represents another P1 ion formed after an isomerization of the X and Y atoms. The results of the interchanging of the sulphur and oxygen has also been seen in the EI spectra of some of the thioates and thiolates<sup>(12,23)</sup>. When P1 ions are present, both types are usually present and in all cases the peak representing a sulphur containing ion is larger than the peak representing an oxygen containing ion.

Another ion formed in all the daughter ion spectra of the dimethoxythioates is an  $(M-32)^+$  species due to loss of methanol. This neutral loss is only observed in this class of organophosphorus pesticides. Only the methyl analog of pirimiphos forms an appreciable

amount of  $Z'$  ions, it is in fact the base peak in the daughter ion spectrum. This is somewhat unusual because pirimiphos, an ethoxythiolate, forms no  $Z'$  ions during fragmentation. The CAD spectrum of pirimiphos contains peaks representing ions due to loss of ethylene and both P1 ions which are very small peaks in the methyl pirimiphos daughter spectrum. These spectra are unusual because for most compounds in which the major peaks in the CAD spectrum are representative of  $Z'$  ions,  $Z'$  ion peaks are also present in the spectrum of the related analog compounds.

The other important peaks in the spectra of the diethoxythioate class are due to ions formed by breaking the P-Y bond, creating (M-P1)<sup>+</sup> ions. Again both sulphur and oxygen P1 ions are involved, but in these cases, as neutrals lost.

#### c) Phosphorothiolates

The phosphorothiolates, many of which are oxygen analogs of the dithioates, have spectra containing many of the same peaks observed in the mass spectra of dithioates. Most of the thiolate daughter spectra are dominated by peaks due to  $Z'$  ions created by neutral losses of 170 u. for the ethoxy and 142 u. for the methoxy compounds. The oxygen analog of dimethoate is the exception again; its spectrum only has peaks for the two P1 ions and the unusual  $m/z$  88 ion.

#### d) Phosphates

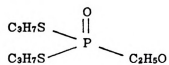
The CAD spectra of the two phosphate groups are perhaps the least similar. The daughter spectra of two of the dimethoxy species, dicrotophos and phosphamidon, have base peaks representing  $Z'$  ions formed by neutral losses of 126 u. The CAD spectra of other dimethoxy

compounds have base peaks from P3 ions at  $m/z$  127 and smaller peaks representing Z<sup>+</sup> ions. The spectra of the diethoxyphosphates are dominated by peaks representing the typical Quale ethylene losses from the (M+H)<sup>+</sup> ion. There are, however, some P3 ions, P3 minus ethylene ions, as well as a low abundance Z<sup>+</sup> ion represented in the daughter spectrum of chlorfenphos.

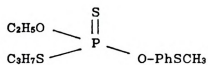
e) Miscellaneous organophosphorus pesticides

Daughter spectra of four other organophosphorus compounds that do not fit the general structure of the pesticides above were also collected. These four compounds are similar to the other phosphorus esters in that there are three R groups bonded to the phosphorus through a sulphur or oxygen atom. They are different though because the R groups are not the same in two species and there is no real Z group in the other two. The structure of these four species is shown in figure 3.3.

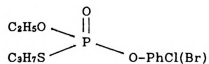
The CAD spectra of the (M+H)<sup>+</sup> ions for these compounds are characterized by peaks due to daughter ions from fragmentations similar to P1, N1 and Quale-type reactions as the different appendages are lost one after another with and without hydrogen transfer. Sulprofos, a compound with an identifiable aromatic Z group, has fragmentation behavior similar to that of other compounds with aromatic Z groups. The daughter spectrum has a few very small peaks representing Z group ions and large peaks from phosphorus containing ions. The daughter ions at  $M/z$  125, 150 and 155 all have the same general structure, ROP=X(OH), with different combinations of sulphur, oxygen and R groups. The high mass ions at  $m/z$  247 and 219 are due to successive losses of C<sub>2</sub>H<sub>5</sub>SH and ethylene from the (M+H)<sup>+</sup> ion.



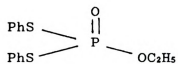
Ethoprop



Sulprofos



Profenophos



Edifenphos

Figure 3.3 Structure of the miscellaneous organophosphorus compounds studied.

Profenphos, because it has an aromatic Z group with two electronegative halogen substituents, has just two daughter ions due to successive Quale-type losses of ethylene from the ethoxy group and loss of propene from the propylthio group. There are no Z group ions.

Ethoprop and edifenphos have the general structure  $(RS)_2P=O(C_2H_5)$  with R representing propyl and phenyl, respectively. The CAD spectra of both compounds have peaks representing Quale ions, Ethoprop, with three alkyl R groups, has many Quale-type losses of propene and ethene represented in its daughter spectrum. The base peak in the CAD spectrum of ethoprop represents the stable ion,  $[(SH)_2P(OH)_2]^+$  at  $m/z$  331. Other peaks at  $m/z$  125 and 139 represent the same ions as those above in which several side chains are lost from the  $(M+H)^+$  ion. The base peak in the daughter spectrum of edifenphos represents a pseudo Z type ion,  $(phSH_2)^+$ , at  $m/z$  111. There are also ions at  $m/z$  109, from the same bond cleavage but without hydrogen rearrangement, and the complementary ions at  $m/z$  201 and 141, due to successive losses of this neutral from the  $(M+H)^+$  ion, present in the daughter spectrum.

## 2. Screening analysis

By studying all the ions and neutral losses represented in the daughter scans, a list can be compiled that contains ten scans: seven neutral loss and three parent ion scans. These scans can detect all the organophosphorus pesticides. The instrument control and data collection software can be programed such that the mass spectrometer repetitively loops through the list of scans one at a time. In this way, any organophosphorus pesticides, metabolites and other related residues of organophosphorus pesticides can be detected in one automated screening



experiment. A complete pass through all the scans takes less than 3 seconds using typical scanning conditions. The actual time is dependent on the mass range scanned, the scan speed, and the number of data points averaged per mass.

The list of ten scans, given in table 3.2, contains only scans which involve the presence of, or loss of, the phosphorus group. Other losses, such as 28 u. for ethylene or 32 u. for methanol, are not included even though these losses may represent the base peak in some spectra, because these ions are not specific for the organophosphorus pesticides and might give false positives. Many of the compounds can be detected by more than one of the scans, providing additional confirmation of compound identity. Table 3.3 lists the compounds detected by each of the scans in the list used for screening. Peaks detected during a run provide two pieces of information: the molecular weight of the compound and which neutral loss or parent ion was detected. This information is usually sufficient to confirm the identity of species previously identified. The structure of newly discovered metabolites can be deduced from complete daughter scans.

It was originally thought that the miscellaneous group of organophosphorus compounds would not be detectable with the general screen because they do not have the generic structures, but that they could be detected with a targeted analysis. However, because they have many of the same substructures as the rest of the organophosphorus pesticides, they do have some of the same daughter ion masses and neutral losses. Three of the miscellaneous compounds, edifenphos, ethoprop, and sulphophos, do fit into the general screen and should be detectable.

Table 3.2 List of scans used to screen for organophosphorus pesticides

<u>Neutral Loss Scans</u>	<u>Parent Ion Scans</u>
-126	+109
-136	+125
-142	+127
-152	
-158	
-170	
-186	

---

Table 3.3 organophosphorus pesticides detected by each of the scans in the screening analysis list

-126	-136	-142
temphos	quinalphos	pirimiphos methyl
tetrachlorvinphos	pirimiphos	methyl parathion
mevinphos	parathion	phosmet oxygen
phosphamidon	diazinon	analog
heptenophos	dursban oxygen	oxydemeton
dicrotophos	analog	malathion oxygen
		analog
		dimethoate oxygen
		analog
		dimethoate
-152	-158	-170
quinalphos	mevinphos	quinalphos
pirimiphos	azinphos	demeton-0
parathion	phosmet	pirimiphos methyl
dursban	thiometon	phorate oxygen
diazinon		analog
phorate sulfoxide		demeton-S
		ethion
		edifenphos
-186	+109	+127
phorate	temphos	chlorfenphos
ethion	pirimiphos methyl	malathion oxygen
disulfoton	methyl parathion	analog
phosalone	fentrothion	mevinphos
dialifor	methyl dursban	tetrachlorvinphos
azinphos ethyl	oxydemeton	phosphamidon
azinphos	dimethoate oxygen	naled
	analog	malathion
	edifenphos	dicrotophos
	mevinphos	heptenophos
	paraoxon	
	+125	
azinphos	fentrothion	pirimiphos
diazinon	heptenophos	pirimiphos methyl
dimethoate	malathion	quinalphos
dimethoate oxygen	methyl dursban	sulprofos
analog	methyl parathion	temphos
ethoprop	oxydemeton	
etrimfos	phorate sulfoxide	

To test this list of scans, two samples were made: one with 1-2 mg. of ten different pesticides mixed in a commercial pesticide matrix, and the other, an apple with pesticide applied. Both samples were introduced into the ion source on a direct insertion probe while the data system was looping through the scan list.

In the first sample all ten compounds were detected. Because the pesticides have different boiling points, they did not all come off the probe at the same time, although most of them do overlap each other considerably. Figure 3.4 shows an example of two scans which detected several pesticides. The peak intensities in these scans are meaningless because, for example, the peak representing thiometon is just beginning to appear and will get larger in later scans, while the peak at  $m/z$  318 for phosmet is near its maximum.

After the bugs had been worked out of the detection scheme, an artificially made "real" sample was tried. An apple chunk, the approximate size of the end of the 1/2" diameter direct insertion probe, was cut out of a raw apple with a scalpel, weighed, and spiked, to a concentration of 3 ppm, with phosmet pesticide. The sample was placed in the probe, skin side out, and held in place with the spring clip normally used to hold small sample vials. The probe was then placed directly into the source as the data collection commenced. An additional scan, a normal mass spectrum, was added to the list of scans to monitor the volatile matrix compounds leaving the apple. Figure 3.5 shows a normal mass spectrum of the apple and a scan from the screening run that detected phosmet. There are hundreds of peaks in the normal scan, but nothing is visible at  $m/z$  318 where the  $(M+H)^+$  ion for

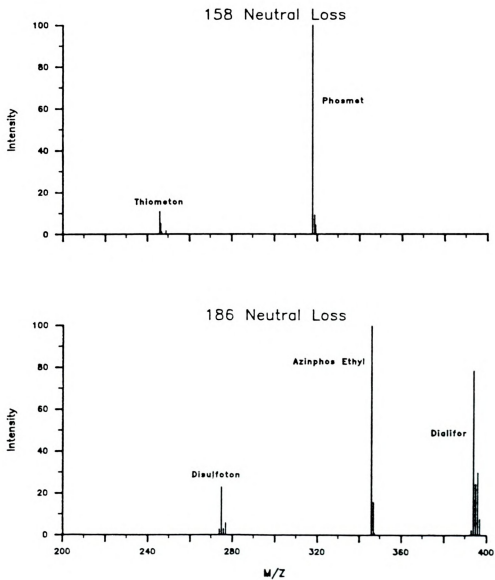


Figure 3.4 Pesticides detected by two of the scans used in a screening analysis of a mixture containing ten organophosphorus pesticides.

## SPIKED APPLE

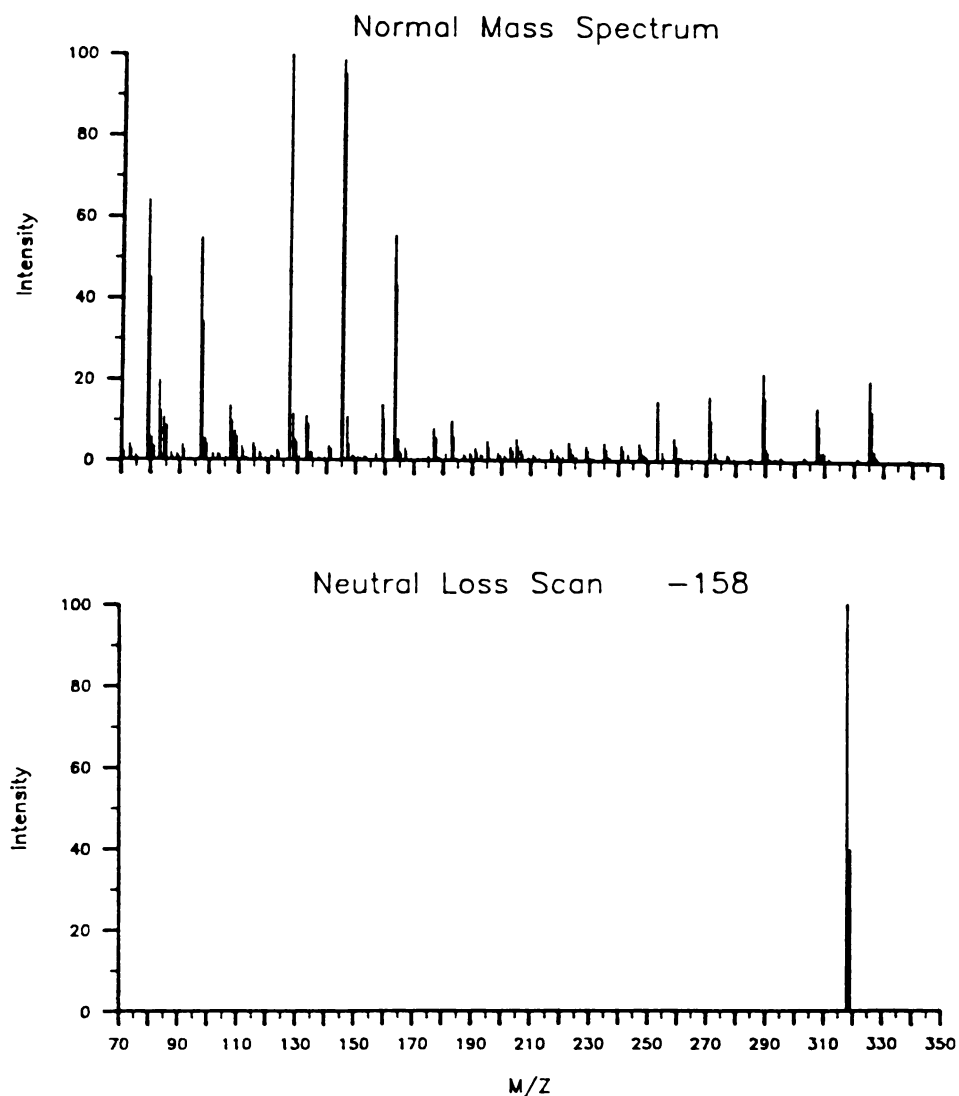


Figure 3.5 Apple analysis: Spectrum A) normal mass spectra of the volatile components of an apple; Spectrum B) pesticide present (phosmet), detected by one of the scans in the general pesticide screen.

phosmet would be seen. However, the 158 neutral loss scan did find the phosmet.

### 3. Targeted Analysis

When an analyst knows exactly what species is to be detected and does not care if there are other species also present, the analysis can be geared toward that specific compound and often lower detection limits may be realized. Triple quadrupole mass spectrometry is an ideal technique for targeted analysis because of its tremendous selectivity. The technique of multiple reaction monitoring (MRM), which is similar to the selected ion monitoring technique used in normal mass spectrometry, is used to monitor parent/daughter ion pairs specific to the species of interest. For each compound to be determined a unique reaction of a parent ion fragmenting to a daughter ion is chosen for monitoring. The chosen ion pairs are then programed into the instrument control and data collection system which continuously loops through the desired reactions, every 0.1 sec., as the sample comes off a chromatographic column or sample probe. Because the mass analyzers are not scanned, they are able to sit on the masses for longer times, increasing signal averaging, providing a better signal-to-noise ratio and, therefore, lower detection limits.

For targeted analysis of organophosphorus pesticides, many of the same parent/daughter ion pairs that are used in the screening scans can be used for multiple reaction monitoring. The best ions to use for multiple reaction monitoring are ions that are both intense and specific or unique for the species to be determined. Because only one ion is allowed to pass through each mass analyzer, sensitivity is improved by adjusting conditions so that that one ion is as intense as

possible. The ideal sensitivity situation is one in which there is only parent ion in the parent mass spectrum and all these ions fragment to form only one daughter ion. In this way 100% of the available ion current is used in the determination. Phosmet represents an ideal situation. Methanol ionization provides only the  $(M+H)^+$  ion as the parent ion, and fragmentation conditions can be adjusted so that no parent ions remain and the  $Z^+$  ion is the only daughter ion.

Most compounds, however, do not produce spectra ideal for this purpose. Even when using methanol CI, some species still have small fragment ions at pressures adjusted for maximum peak intensity and many species have their available ion current split into various isotope peaks. In fact, it is the increased sensitivity provided by methanol, not the lack of fragmentation, that is helpful in targeted analysis. Because only one parent ion is monitored it is actually the intensity of that one ion that is important. Other fragment ions, if present, will not be detected and will only interfere when they decrease the abundance of the ion of interest.

Daughter ion spectra generally contain more than one ion. Depending on the mass of the parent ion, it is generally advantageous to use the largest peak in the daughter spectrum as the peak for the second analyzer to monitor. However, this peak may be due to the loss of a common neutral, such as methanol, ethylene or carbon monoxide, and therefore other compounds as well as the species of interest may be detected. A trade off between sensitivity and selectivity must then be made by choosing a daughter ion formed by a more compound-specific neutral loss.



Fortunately, the biggest daughter ions from the  $(M+H)^+$  ions of organophosphorus pesticides are, for the most part, formed by uncommon neutral losses. It should also be noted that all the species detectable with the screening scans whether they are detected by parent or neutral loss scans can also be detected with multiple reaction monitoring. It is the final mass of the daughter ion that is monitored, regardless of how the ion is formed. For this reason, organophosphorus pesticides that are not detected in the screening analysis may be detected using multiple reaction monitoring. An example of multiple reaction monitoring data, taken from the mixture of ten pesticides, is given in figure 3.6. Multiple reaction monitoring was also the technique used in the sensitivity studies discussed below.

#### 4. Sensitivity

Any analytical detection scheme, whether a targeted or a general screen, is only as good as the sensitivity available. A screening method is no good if it always gives negative results only because it is not sensitive enough to detect pesticides actually there. Mass spectrometric methods are generally very sensitive and often used for trace analysis. Triple quadrupole mass spectrometry, because of the better signal-to-noise ratio produced by adding a second analyzer to the ion path, is capable of even lower detection limits than normal mass spectrometry. Yost and co-workers have reported femtogram detection levels using triple quadrupole mass spectrometry and a short six-inch GC column<sup>(24)</sup>.

It is the actual amount of analyte present that is important for mass spectrometric analysis, not the concentration of the analyte in the sample. Better sounding "part per" numbers can be achieved in artificial samples simply by increasing the quantity of matrix.

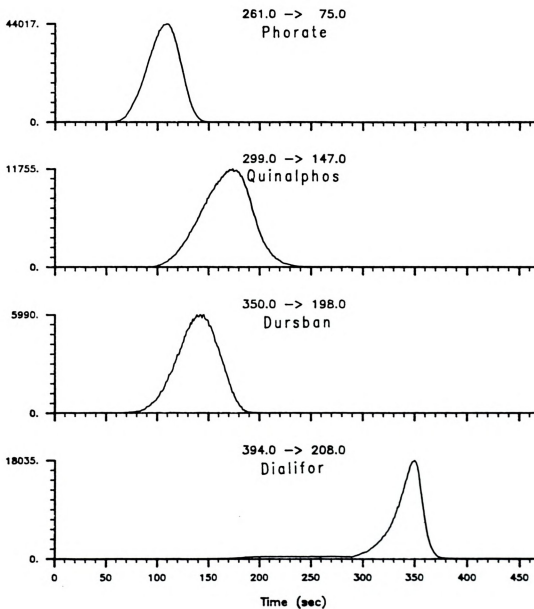


Figure 3.6 Several of the pesticides detected during a targeted analysis of a mixture of pesticides.

Increasing the sample size of actual field samples does not change concentration numbers but increases the amount of analyte present. This is a common method used to lower detection limits for some samples. Using more sample is limited only by the amount that will fit on the end of the sample probe. Reported detection sensitivity may sound impressive but the actual amount of analyte detected has not changed. Therefore, the actual weight of sample detected will be used in the discussion here.

The sensitivity of our instrument has never been very good and hence our detection limits are higher than those reported by others in the literature. It is a routine matter to detect the ~400 nanograms of pesticide present in the apple analysis. This weight of sample gave single digit part per million sensitivities, which is a reasonable number, similar to quantities actually found on field samples <sup>(25)</sup>. Since the work with apples was just for a pesticide screen, no attempt was made to establish detection limits.

Studies were conducted to find the sensitivity limits of our instrument. Initial attempts using the direct insertion probe to introduce samples were foiled by contamination in the vacuum interlock. No matter how little pesticide was inserted, including none, a small quantity was always detected. It was, however, possible to distinguish between the very broad and low background peak from the superimposed sharp taller peak representing the fresh sample. Sample sizes of 100ng were clearly distinguishable with signal-to-noise ratios of ~9:1. The peak shapes of 5ng samples resembled those of blanks. Using a GC for sample introduction overcame the contamination problem and gave more reproducible results. It was assumed that if the ion

current present in the broad peaks, detected as the sample volatilized off the sample probe, could be condensed and sharpened by using a chromatographic column, detection limits would be lowered because the sharp peaks would be taller. However, the He flow into the CI volume dilutes the CI plasma and adversely affects ionization efficiency. The smallest quantity of phosmet that could reproducibly detected was only 250ng at a signal-to-noise ratio of 32:1. This ratio was high enough that smaller sample sizes should have been detectable, but this was not the case. These results are three orders of magnitude above the instrument manufacturers quoted sensitivity of 100pg of benzophenone, measured using methane CI and monitoring the CAD reaction for the  $(M+H)^+$  ion at  $m/z$  183 fragmenting to a daughter ion at  $m/z$  105.

There are many factors which may be causing low sensitivity including: gas chromatographic conditions and interfacing, ion source ionization efficiency, alignment and tuning parameters, the transmission of each quadrupole and multiplier efficiency. These factors are present in any quadrupole mass spectrometer and those that are under user control must be optimized to the best of the operators ability.

Tandem instruments have the added performance standard of ion transmission through all the mass analyses. The sensitivity of our instrument is so low, in part, because it has very low transmission. Transmission is defined as the ion current measured for a particular mass after passing through two mass analyzers (without collision gas) divided by the ion current for the same mass passing through only one mass filter. Transmission values between 10-15% are considered normal. The transmission measured on our instrument consistently falls around 1%. This can be raised to approximately 4% with careful adjustment of

the quadrupole controllers, tuning of the ion path and luck. This is also the maximum that even the manufacturer's field service engineer was able to obtain. Dawson has published numerous papers and a book on his detailed studies of ion motion in quadrupoles and tandem quadrupoles<sup>(26-29)</sup>. Transmission is affected by a complex combination of RF field acceptance apertures, ion trajectories through the quadrupole and other factors dictated by ion physics. Increasing the transmission of our instrument would require substantial modification of the ion path after ion trajectory modeling studies. Rotating the quadrupoles with respect to each other, removing the lenses between the quadrupoles so that the quadrupoles can be placed closer together, and changing the collision gas containment cell so that the gas would not enter the first and third quadrupoles, could all be tried.

These changes might improve our instrument and therefore allow detection of smaller amounts of analyte during both targeted and screening analyses. Until such time that transmission is improved however, all is not lost. Methods may still be developed, similar to the pesticide screen, by using large samples and knowing that the technique is applicable in other labs with more efficient instruments.

#### D. CONCLUSIONS

Triple quadrupole mass spectrometry is a very powerful method for screening raw samples for organophosphorus pesticides. The list of ten scans discovered can be used to detect many different organophosphorus pesticides, metabolites, degradation products and related compounds in just a few seconds. The screen is specific enough to detect the presence of and specifically identify organophosphorus



pesticides in samples with out using any sample clean-up, extraction or chromatographic steps. The same parent-daughter ion pairs that are used to differentiate the organophosphorus pesticides in the screening method, can also be used as very specific detectors during targeted analyses for organophosphorus pesticides.

## E. REFERENCES

1. Horwitz. W. ed.; *Official Methods of Analysis of the Association of Official Analytical Chemists*, 12th ed. ,Association of Official Analytical Chemists: Washington D.C., 1975
2. Food and Drug Administration (U.S.); *Pesticide Analytical Manual*, FDA: Washington D.C., 1982, Vol. 2
3. Chau, A.S.Y., Afgau, B.K.; *Analysis of pesticides in Water*, CRC Press: Boca Raton, Fla., 1982, Vol.2, chapter 2
4. Thompson, J.F., ed.;*Analysis of Pesticide Residues in Human and Environmental Samples, A Compilation of Methods Selected for Use in Pesticide MONitoring Programs*, U.S. Environmental Protection Agency, Washington D.C., 1972
5. Smart, N.A. and Enos,H.F.; *J. Agri. Food Chem.* 1964, 17, 1186
6. Ministry of Agriculture, Fisheries and Food; *Analyst*, 1977, 102, 858
7. Lee, Y.W. and Westcott, N.D.; *J. Assoc. Off. Anal. Chem.*, 1979, 62(4), 782
8. Sherma,J., Zweig, G.; *Anal. Chem.*, 1985, 57(5), 1-15R
9. Biros, F.J.; *Pesticide Identification at the Residue Level*, Advances in Chemistry Series #104; Am. Chem.Soc.: Washington D.C., 1971
10. Faust, S.D.; *Fate of Organic Pesticides in the Aquatic Environment*, Advances in Chemistry Series #104; Am. Chem.Soc.: Washington D.C., 1972
11. Yost, R.A., et al.; *Anal.Chem.*, 1984, 56, 2223
12. Domico, J.N.; *J. Assoc. Off. Anal. Chem.*, 1966, 49, 1027
13. Quale, A. In *Advances in Mass Spectrometry*, Waldron, J.D. ed., Pergamon Press: London, 1959, Vol. 1, 365
14. Holmstead and Cassida; *J. Assoc. Off. Anal. Chem.*, 1974, 57, 1050
15. Busch, K.L. et al. ; *Applied Spectroscopy*, 1978, 32(4), 388
16. Daugherty, R.C., Wander, J.D.; *Biomed.Mass Spec.*, 1980, 7(9), 401
17. Rankin, P.C.; *J. Assoc. Off. Anal. Chem.*, 1974, 54(6), 1340
18. Stan, H.J. and Kellner, G. ; *Biomed Mass Spec.*, 1982, 9(11), 483



19. Stan, H.J. et al. ; *Fresenius Z. Anal. Chem.*, 1977,287, 1065
20. Stan, H.J.; *Fresenius Z. Anal. Chem.*, 1974, 287, 104
21. Morelli, J.J., Hercules, D.M.; *Anal. Chem.*, 1986, 58, 1294
22. Crawford, R.W., et al.; *Anal.Chem.*, 1984, 56, 1121
23. Safe, S. and Hutzinger, O.; *Mass Spectrometry of Pesticides and Pollutants*, CRC Press: Cleveland, Ohio, 1973
24. Yost, R.A., Johnson J.V.; *Anal.Chem.*, 1985, 57, 759A
25. Zabic, M., Michigan State University, personal communication, 1983
26. Dawson, P.H., *Quadrupole Mass Spectrometry and its Applications*, Elsevier Scientific Pub.: New York, 1976
27. Dawson, P.H., Bingqi, Y.; *Int.J.Mass Spec.Ion Phys.* 1983, 54, 159
28. Dawson, P.H., French J.B., et al.; *Org.Mass Spec.*, 1982, 17(5), 205
29. Dawson, P.H.; *Mass Spec. Rev*, 1986, 5, 1

## CHAPTER FOUR

### Detection of Whole Bacteria

#### A. INTRODUCTION

Modern microbiology employs highly developed routines which utilize a wide range of sophisticated morphological, serological and biochemical procedures for the identification of microorganisms. These methods, which have taken years to develop, can be used to differentiate, classify and identify thousands of microbial strains<sup>(1)</sup>. Identifying microbial strains is important in clinical medicine, ecological studies, industrial processes, military situations and in many other fields where infectious disease must be prevented. Classical physical methods of identification include size and shape differences detected by microscopy and enhanced by staining techniques. Biochemical methods used for identification are based on the ability of organisms to ferment sugars, produce toxins, or on other characteristic chemical reactions. These methods, although potentially very specific, can take several days for the reaction to produce enough substance for satisfactory identification. Newer faster chemical techniques that are also commonly used to identify bacteria at the strain level are immunofluorescence, radio-immuno assay, and serology. These methods are so specific that they have no general applicability and can only be used when the identification is nearly complete.

The demand for identifying microorganisms is increasing and can only be met by increasing levels of mechanization and automation. The

ideal means of identifying bacterial species would be a "black box" which would separate genes and instantly compare the nucleic acid sequences against standards<sup>(1)</sup>. Over the years analytical chemists have moved towards the ultimate "black box" by developing automated detection methods. Microbiologists, however, have concentrated their research on mechanization, providing labor saving devices but without removing the need for the analyst to make subjective decisions about species identity<sup>(2)</sup>.

The problem is that available automated analytical instruments cannot analyze samples as large and as complex as whole cells. Microorganisms must first be broken down into smaller pieces before gas chromatography, nuclear magnetic resonance, or mass spectrometers can divulge useful information. The two methods that are commonly used for this purpose are hydrolysis, in which the organisms are chemically decomposed into smaller components, and pyrolysis, wherein heat is used to fragment large complex samples.

The reason mass spectrometry cannot analyze whole cells is that mass spectrometry is limited to samples which are volatile. However, recent advances in mass spectral instrumentation have stretched the definition of volatile, allowing the analysis of many new types of samples including microorganisms.

Interfacing a gas chromatograph or a liquid chromatograph to a mass spectrometer permits the analysis of any compound that can be injected into either type of chromatograph. Fast atom bombardment (FAB) ionization has extended the mass range of compounds that may be ionized to over 1500 u. Proteins and other large biomolecules extracted from hydrolyzed cells are often analyzed by GC/MS or FAB MS<sup>(2-4)</sup>.



Secondary ion mass spectrometers (SIMS) and laser microprobe mass analysis (LAMMA) can analyze samples that are not at all volatile<sup>(4-7)</sup>. Metal surfaces, silicon semiconductors, and synthetic polymers are analyzed by bombarding the sample with high energy ions or photons which then explode volatile ionized pieces of the sample from surface craters.

These new instruments work well on samples with uniform or pure composition, but a representative mass spectrum will not be collected by ionizing a small portion of a large sample containing a variety of molecules. To analyze an entire microorganism by mass spectrometry an indiscriminating method of fragmentation must be used. Pyrolysis (PY), the chemical transformation through the energy of heat alone, meets these demands by producing a series of more volatile fragment molecules (pyrolysate) which may then be introduced into a gas chromatograph and/or mass spectrometer to record its "fingerprint". The resulting pyrograms which often have over 100 peaks, or mass spectra which have peaks at every mass, are extremely complex, and consist of contributions from all chemical components in the sample. The large amount of data obtained usually requires computerized pattern recognition techniques to extract the pertinent information from the data<sup>(8)</sup>. Generally, unknown samples only can be identified by comparison of their mass pyrograms to those of known compounds. Characterization is based on empiricism rather than the identity of specific fragments, as the profile of the entire gas chromatogram or mass spectrum is used to characterize the data.

Analysis via fragmentation is limited only by the ability to generate species that still retain some of the character of the material

of interest. This limitation is mastered by compromising between large characteristic nonvolatile fragments and small uncharacteristic volatile fragments. Pyrolysis tends to fragment molecules at specific points and, therefore, the final mixture of low molecular weight products can be expected to contain characteristic information<sup>(9)</sup>. Pyrolysis techniques have been used for the analysis of synthetic polymers, geochemical materials, and, more recently, for bacterial identification<sup>(2,9-14)</sup>.

To date, the use of PY/MS has been restricted to the identification of pure bacteria that have been isolated and cultured. Because existing PY/MS differentiation methods depend solely on the relative abundance of a few ions in the mass spectra; any foreign matter, other organisms, or a different growth media will throw off the pattern recognition and hence, foil the identification. Recently, we began using the added dimensionality available in MS/MS methods to investigate the detection and identification of bacteria in a mixture without prior workup. The goal of detecting a particular microorganism by PY/MS/MS is based on the assumption that the microorganism has some unique combination of chemical substructures and that these are distinguishable from those of all other species in the pyrolysate by its MS/MS spectra.

All bacteria are composed of the same basic structural units including proteins, carbohydrates, lipids, and nucleic acids. There are, however, fundamental differences in the structural composition of the different structural groups which, when degraded by pyrolysis, produce species that are unique in their absolute structure or in the distribution of components relative to the background against which the biological agent is to be discriminated. The advantage of MS/MS in detecting the chemical signs of toxic bacteria in a background of other



organic material, is the far greater chemical selectivity provided by the ability to monitor the presence of specific parent daughter combinations and neutral losses. The aim of this research is to find that small part of the MS/MS data set that can be used to take advantage of this selectivity for the detection and identification of bacteria in mixtures.

## 1. Background - Pyrolysis of Bacteria and Biopolymers

### a) Pyrolysis Gas Chromatography

As early as 1948 pyrolysis mass spectrometry was introduced as a promising technique for the study of polymers<sup>(15)</sup>. Pyrolysis was first applied to mass spectrometry of biopolymers by Zemay<sup>(16)</sup>, who showed that complex materials decompose in a reproducible fashion provided the pyrolysis parameters are carefully standardized. The first report of pyrolysis gas chromatography (PY/GC) was that of Davison *et al.*<sup>(17)</sup> who pyrolyzed chemical polymers and produced characteristic patterns. Since these first reports were published on the applicability of analytical pyrolysis, the subject has been addressed by hundreds of articles. For a number of years both techniques were applied mainly to synthetic polymers which tend to degrade in simple reproducible manners to form identifiable monomers<sup>(9)</sup>. The first application of analytical pyrolysis to biodetection was the work of Wilson and Oyama<sup>(18)</sup> who studied pyrolysis of biomaterials and microorganisms as part of the Viking mission to mars. This triggered an extensive series of studies by Reiner *et al.*<sup>(19,20)</sup> on the differentiation of microorganisms by PY/GC. Detailed accounts on the development of



pyrolysis techniques up to 1967 have been compiled by Levy<sup>(21)</sup>, up to 1979 by Irwin and Slack<sup>(22)</sup>, and more recently by Meuzelaar *et al.*<sup>(9)</sup>.

Most early use of pyrolysis employed the fingerprinting techniques for classification and identification of biomaterials, with reference library fingerprints for comparison. In these methods no chemical interpretation of the data is attempted or required. Computer evaluation of the data opened up new areas of application and scientists from many disciplines became interested in biochemical exploration of the observed differences. Pyrolysis GC/MS was introduced to decipher the identity of the peaks in the pyrograms. Soon biochemists and microbiologists began to see PY/GC/MS as a way to probe cells for structural information that is unattainable by other means<sup>(23-25)</sup>. Pyrolysis is also commonly used to gain information about specific structures within the cell. Different components can be separated from digested cells by standard biochemical methods before pyrolysis, thus eliminating many interferences and also somewhat simplifying the pyrograms.<sup>(9,26-28)</sup>.

Bacteria as well as fungi have been subject to PY/GC and PY/MS investigations, but most of the microbe studies have involved the differentiation and classification of bacterial strains. Most often, evaluation of results is restricted to fitting the data into already existing taxonomic schemes, thereby providing additional proof for the feasibility of analytical pyrolysis in bacteriology.

#### b) Pyrolysis Mass Spectrometry

Despite enormous strides in the development of PY/GC made by Morgan<sup>(29)</sup> and recently reviewed by Bayer<sup>(30)</sup> and Fox<sup>(31)</sup>, its use for characterizing organic solids remains limited due to poor standardization

and lack of inter-laboratory reproducibility<sup>(32)</sup>. This is not due to the pyrolysis but to several practical gas chromatography problems which hinder the establishment of a library of standard chromatograms, and thereby restrict this technique to a single laboratory. In an effort to overcome these problems, several researchers including Meuzelaar and Kistemaker developed fast techniques for obtaining reproducible mass spectra of bacteria by pyrolysis mass spectrometry (PY/MS)<sup>(33)</sup>. Their efforts have shown that it is possible to differentiate bacterial strains at either the genus, species, or subspecies level without using gas chromatography. Thus far, the analysis of over 35 bacterial strains has been reported<sup>(10)</sup>.

In the same way that mass spectrometry was able to identify molecular structures in pyrograms, tandem mass spectrometry has been used to examine the structures of the ions represented in PY/MS spectra<sup>(34-37)</sup>. Custom PY/MS/MS instruments and mass-analyzed ion kinetic energy spectrometers (MIKES) have been used with limited success to aid in the identification of peaks present in pyrolysis mass spectra. To date no one has used PY/MS/MS as a tool for mixture analysis.

#### c) Pyrolysis Technology

Originally, samples were pyrolyzed in separate inert containers or "bombs" and then the residues of gases were collected and analyzed. Due to problems in transferring the sample, direct pyrolysis, in which the sample is pyrolyzed directly at the head of a GC column or in a mass spectrometer have become more popular. Direct analysis of the fragments is usually desirable since the analysis will not be fouled by transport contamination, condensation or other side reactions.

There are three common pyrolysis methods used for direct analysis, the least common of which is laser pyrolysis. This is due to the high cost of laser equipment and because the laser beam breaks bonds by electronic excitation (photolysis) instead of vibrational excitation (thermolysis). Laser pyrolysis technology has been developed into LAMMA instrumentation by Kaufman *et al.*<sup>(5)</sup> and Wechsing *et al.*<sup>(6)</sup>. LAMMA, though very similar to pyrolysis, is no longer considered a pyrolysis technique.

The method used most often for pyrolysis is the heated filament, or "pyroprobe", method. The design basis for the heated-filament was developed in the mid 1960s<sup>(21)</sup>. These pyrolyzers are heated by passing a large current through the filament with the resulting dissipation of power causing the heating of the filament. The most successful of the heated-filament devices is the CDS Pyroprobe offered by several mass spectrometer manufacturers as a direct insertion probe. The probe may also be interfaced to gas chromatographs. The pyrolyzer controls the heating rate and final temperature by using a feedback circuit. The platinum filament is used as both the heating element and resistance sensor, which serves as one leg of a wheatstone bridge circuit. By changing the resistance of the opposite leg of the bridge, different final temperatures may be selected. This pyrolyzer design enables controlled heating rates of from 0.1 to 20°C/msec, and a temperature range of 20 to 1000°C can be achieved. A coiled filament that is designed to accommodate small quartz tubes can also be used with the CDS system. This allows solids and samples difficult to coat on the filament to be pyrolyzed directly, but due to the mass of the quartz tubes, the maximum heating rate is reduced to about 300°C/sec.

The last type of pyrolysis routinely used is Curie point pyrolysis. As first described by Giacobbo and Simon <sup>(38)</sup>, Curie point differs from other pyrolysis methods in that the wire coated with sample is inductively heated by a high frequency coil rather than heated by current. The final temperature of the wire is determined by the Curie point of the ferromagnetic filament rather than by a servo-controlled power supply. Small quantities of sample, typically 5-20 ng, are deposited directly on the wire surface, and the wire is placed in a high voltage RF field. As the temperature of the wire reaches its Curie point, the wire changes from ferromagnetic to paramagnetic. No energy is absorbed in the paramagnetic state, resulting in a temperature decrease. Below the Curie point temperature, the wire becomes ferromagnetic again and heating occurs. The final, or Curie, temperature is determined by the composition of the metal alloy used for the sample wire. A range of discrete temperatures between 350-970°C is available from different alloys made of Fe, Ni, and Co. The Curie temperatures are reached in less than 100 msec. and are extremely reproducible. In contrast, Wells *et al.*<sup>(39)</sup> have shown that pyroprobe pyrolyzers have neither reproducible temperature rise times nor constant final temperatures. Curie point also uses new wires and clean reaction tubes for each sample which eliminates the possibility of contamination from earlier experiments. Recently, Whitehouse *et al.*<sup>(40)</sup> compared the different pyrolysis technologies and found that they produced different spectra. Their results show that pyrolysis conditions are the most important factors for obtaining good reproducibility. Curie point pyrolysis has the best reproducibility because it has the steadiest pyrolysis conditions.

In the past, the literature has used the terms thermal degradation and pyrolysis interchangeably even though they are different processes. Both terms refer to the break-down of molecules into smaller molecules, but thermal degradation is a slow process and pyrolysis uses a rapid temperature jump and may also include subsequent recombination of fragments<sup>(21)</sup>. While the information obtained by either process is likely to be the same, thermal degradation offers the added dimension of time and controlled fragmentation. Risby and Yergey have taken advantage of these added features in studies of natural and synthetic polymers and geological samples<sup>(41)</sup>. They were able to use temperature-dependent profiles of specific ion intensities to create a taxonomical flow chart to differentiate bacteria<sup>(42)</sup>. The ion intensity profiles are different enough that the profile of ion current at a single mass to charge value can be used to distinguish between species. Their results are important because they prove that thermal decomposition of bacteria does produce unique compounds and that they can be detected by monitoring one mass-to-charge ratio.

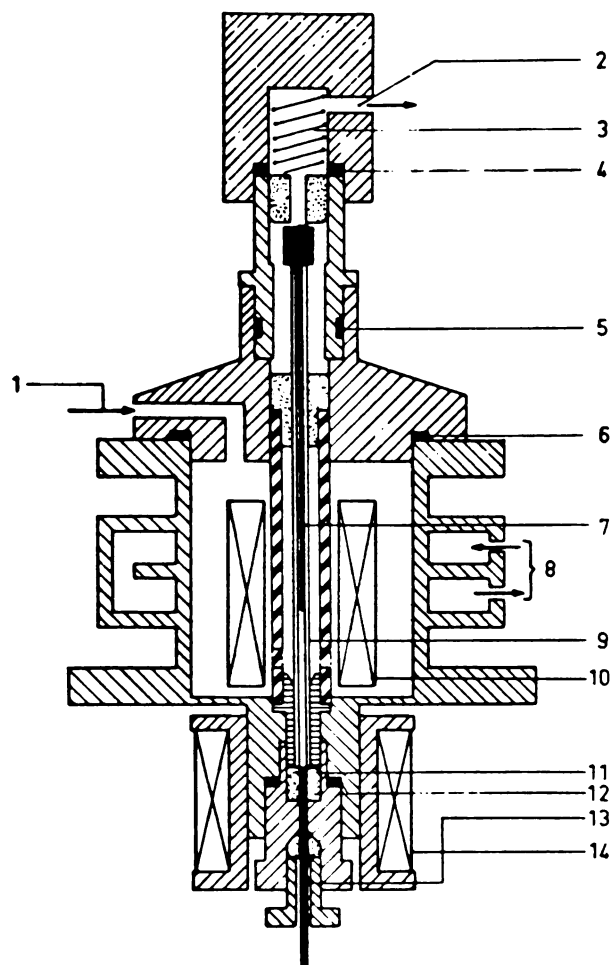
They also found that their results followed the established taxonomy of bacteria, as organisms known to be related to each other also had similar ion intensity profiles. Similar statements are made in many other pyrolysis papers as other authors used this relationship to lend validity to pyrolysis techniques. The situation is now changing as the technology has become established. There is no *a priori* reason why a pyrolysis based taxonomy should coincide, or even closely resemble, the taxonomy derived from traditional measurements, but the two could work together. However, as the pyrolysis techniques that the biochemists and microbiologists have developed are adapted by analytical

chemists, the emphasis of pyrolysis research is changing. The value of pyrolysis techniques is being realized in the field of rapid identification rather than in the provision of new or improved taxonomies.

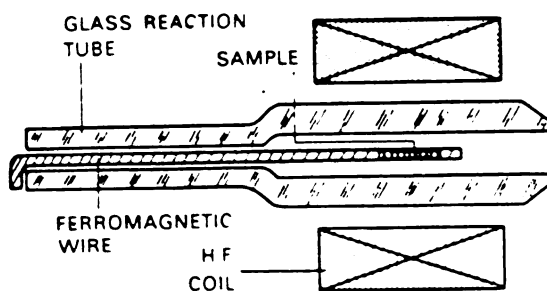
## B. EXPERIMENTAL

Pyrolysis experiments were run on the Extrel triple quadrupole mass spectrometer described in chapters two and three to which the following changes were made. The packed column injection port was removed from the gas chromatograph and replaced with a pyrolyzer unit similar to the one described in reference 10 (supplied by Dr. Voorhees, Colorado School of Mines). Figure 4.1 illustrates a typical Curie point pyrolyzer for use with a gas chromatograph. An uncoated 250 micron capillary column connected the pyrolyzer directly to the ion source via the heated gas chromatograph oven and mass spectrometer interface. The sample wire is held in a quartz reaction tube which is then placed in the RF coil. The pyrolyzer was powered by 1.5 kW, 1.1 MHz RF power supply (Fisher Labortechnik GmbH). Samples were pyrolyzed for 9.9 seconds in an ~1.5 ml/min flow of carrier gas.

Since no chromatographic separation was desired, the four meter uncoated capillary column used was the shortest possible that could still keep the large pressure drop necessary between the vacuum pressures in the ion source and the positive, above one atmosphere, pressure in the pyrolyzer. The pyrolysis chamber was kept at 300°C while the GC injector, oven, and mass spectrometer interface were maintained at 250°C, 230°C, and 250°C, respectively. The ionization source was kept at 200°C.



Schematic representation of a Curie-point pyrolysis reactor for Py-GC systems. (1) carrier gas inlet, (2) purge gas outlet to needle valve, (3) pressure spring, (4, 5, 6) O-ring (Viton), (7) pyrolysis wire, (8) cooling water, (9) glass reaction tube, (10) rf coil, (11) reaction tube-column seal (glass-filled PTFE), (12) washer (gold), (13) GC column (glass), (14) heating element (from Van de Meent, 1980).



Scheme of the Curie-point wire/reaction tube system located within the high-frequency induction coil

Figure 4.1 Cut away view of a Curie point pyrolyzer





Bacteria cultures of *B.subtilis*, *B.cereus*, and *E.coli* were grown on trypticase soy agar in a 35°C incubator for 24 hours, then kept refrigerated before use. New cultures were grown every week to insure that spores had not formed. For analysis, the bacteria were scraped off the agar plates and coated onto 510°C Curie wires. To increase sensitivity, two coats of bacteria were applied, allowing the bacteria to dry between applications.

Mass spectral data were collected with the instrument data system in "SWEEP" mode. In this mode, all the raw data points are collected and stored while the real-time peak finding routines are ignored. Sweeps were used because past experiments had shown that the peak finding software had trouble finding some peaks when there are ions present at every mass, which is the case with pyrolysis spectra. Post processing programs were written to average and identify the peaks in the data (using a peak jumping algorithm) after the raw data were uploaded to a Digital PDP 11/73 minicomputer. Computer tapes of the data were then sent to Dr. Voorhees' laboratory where factor analysis routines were applied to the data. Results of their data processing were then used for additional experiments as discussed in the following sections.

## C. RESULTS AND DISCUSSION

### 1. Ionization

Since no one had ever used a tandem quadrupole instrument to analyze bacterial pyrolysates for mixture analysis and PY/MS interface equipment that others have developed was not available, many of the experiments reported here are of an exploratory nature. Some of the

experiments worked and some did not, but there is important information to be gained from all of them.

Once mechanical problems with the flow of pyrolysate into the vacuum were overcome, initial studies centered on finding an ionization method that would provide adequate ion abundance for MS/MS experiments. Most PY/MS experiments use low voltage, 13-16 eV, electron impact ionization so that the fragments formed by pyrolysis are not fragmented further into smaller, less characteristic, pieces by the ionization process<sup>(36)</sup>. Spectra of the pyrolyzed bacteria obtained using low voltage EI ionization on our instrument highlighted the adverse side of low voltage EI, namely, low ionization efficiency. This ionization method did not produce adequate ion intensities. Consequently, spectra were obtained using 70 eV EI. This resulted in a sensitivity increase of more than a factor of ten. However, the most intense peaks in the spectra, those with enough intensity to fragment with CAD, were clustered at the low mass end of the spectra and no useful information would be gained by obtaining daughter spectra of these ions. The most satisfactory spectra were obtained using methane CI. Normal problems associated with He carrier gas diluting the reagent gas ion plasma were eliminated by using methane as the carrier gas as well as for the reagent gas. Spectra obtained in this manner exhibited another ten fold improvement in sensitivity, relative to the 70 eV spectra, and showed many higher mass ions with high intensity that were suitable for CAD. A comparison of the 70 eV EI and the methane CI pyrolysis mass spectra of *B.subtilis* is shown in figure 4.2.

## 2. The search for species specific ion-pairs

Once a functional ionization method was found, the search for unique ion pairs began. There are no obvious chemical flags to look for that would signal the presence of bacteria. It has not yet been determined what compound(s), if any, are in the bacterium that make certain microbes harmful and others perfectly safe. Some bacteria do produce identifiable toxins for which a mixture could be searched, but in other cases it is the bacterium itself which must be detected. Absolute information for verifying the presence of and identity of bacteria is encoded in their DNA and out of easy reach. The genetic information present in cells is expressed at different levels: in the molecular structure of the DNA itself, in the structures of the proteins whose synthesis is controlled by the DNA, and in the cell's morphology and behavior. Traditional detection and identification methods concern the outside level, but pyrolysis techniques open the inner levels for information gathering. Using pyrolysis, however, encodes the information using a cipher that is just beginning to be decoded. Because the chemical markers are not known, data are collected from different bacteria and then impartial computers look for differences. Once the differences have been discovered, then tandem mass spectrometry can be used to selectively monitor for the ions related to the specific differences.

Normal spectra were collected for the pyrolysate of *B.cereus*, *B.subtilis*, and *E.coli*. Figure 4.3 shows the pyrolysis mass spectra of the three bacteria. The scans were examined visually for peaks that seemed promising for discriminating among bacteria, namely peaks that are large in one spectrum and small in both of the others. Daughter

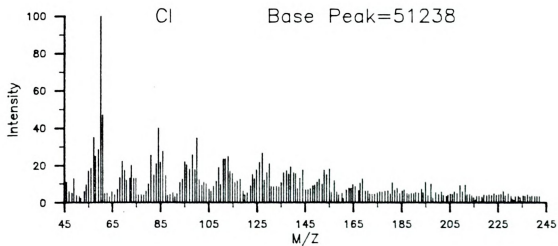
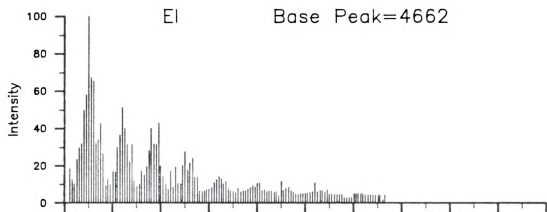
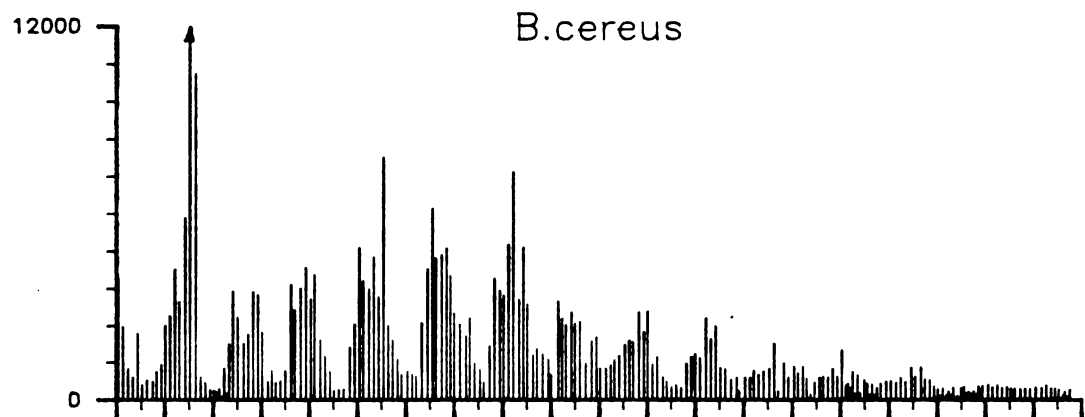


Figure 4.2 Comparison of 70 eV Electron Ionization and Methane Chemical Ionization PY/MS spectra of *B. subtilis*





spectra of these ions were then collected. The ions found are listed in table 4.1. For the daughter ions abundant enough to be detected, the daughter spectra were virtually identical in all of the bacteria for each parent ion selected. This indicates that the differences observed in the normal mass spectra were not from a unique parent ion found in one bacterium only, but were instead due to the same compound, with species dependent abundance.

This makes some sense considering the method used to select the ions to fragment. It is easy to distinguish between the three pure bacteria simply on the profile of their normal PY/MS spectra alone. Choosing the same ions that provide enough information for differentiation in normal mass spectrometry as parent ions, does not insure that any additional information will be obtained in the daughter spectra of these ions. There is no way to judge, or predict, the behavior of siblings by looking only at the parents. In fact in this case, the daughter spectra of these ions only reinforced what was already known. Since abundant daughter ions were present in the cases with intense parent ions, and daughter ions just above the detection limits were seen in the spectra of the less intense parents, all that could be learned was that the parent ions were more abundant in certain bacteria.

There are also only a few daughter ions present in the daughter spectra and in many cases only a single major peak. This is in contrast to the findings of Haverkamp et al.<sup>(37)</sup> who used a PY/MS/MS instrument in order to determine the identity of peaks in pyrolysate spectra but found that daughter spectra are actually composite spectra of several isobaric parent ions. No major conclusions were drawn from this

Table 4.2 Daughter ions detected for selected parent ions in PY/MS/MS spectra of *B.cereus*, *B.subtilis*, *E.coli*

Parent ion	Major Daughter Ions		E.coli	Minor Daughter ions	
	<u>B.cereus</u>	<u>B.subtilis</u>		<u>B.cereus</u>	<u>B.subtilis</u>
75	57	57	57	45,29	
81	53	53	53		
93	91	91	91	77,57	
100	72	72	72	82,55,44	82,55,44
104	58	58	58		
113	95,85	95,85	95,85	96,72,43	96,72,43
118	91	91	91		
136	94	94	94	108	108
164	98,84	98,84	98,84	116,44	44



ference however because the ion intensities recorded and lack of reproducibility in the data prevented much insight into actual chemical structures.

#### 4. Mixed daughter scans

Due to the large amount of information generated in a PY/MS spectrum, and the additional complexity that occurs when daughter ion spectra are considered in a PY/MS/MS experiment, a systematic approach for selecting characteristic parent/daughter ion combinations must be employed. The best method to use would be to collect daughter spectra for each of the parent ions present in the normal mass spectrum for all bacteria. This long arduous task, while providing all the parent-daughter relationships, would still not insure that the best ion pairs could be chosen for monitoring, because the amount of data generated could be overwhelming. In order to speedup the task and take advantage of computer tools available, a new method was developed, utilizing "mixed daughter" scans coupled with principal component analysis and pattern recognition, to find areas of MS/MS data space that could be used to detect and identify pyrolyzed bacteria.

Mixed daughter scans are taken by filling the second quadrupole with collision gas and scanning the third quadrupole as in normal daughter scans, but instead of selecting only one parent mass with the first quadrupole, it is put in RF mode so that ions of any mass will pass through into the collision region. The resulting spectrum is a two dimensional MS/MS map of all the daughters of all the parents in the pyrolysate. The software that has been developed to find small differences in normal PY/MS spectra can then be applied to the mixed

daughter spectra in an attempt to extract information from these compressed MS/MS maps.

Mixed daughter spectra were collected for the three different bacteria and the resulting data, which are displayed in figure 4.4, were sent to Dr. Durfee, at the Colorado School of Mines, for analysis. Several daughter ions from each of the spectra were identified by the computer as diagnostic ions for differentiating the bacteria. These ions, which are listed in table 4.2, were then used as the selected daughter ion for parent scans of the three bacteria. The three parent spectra taken for each daughter were then compared to identify any potentially useful parent-daughter ion pairs that could be monitored for mixture analysis.

In many cases, the parent spectra of the three bacteria again contained the same ions. This indicated that the difference in the daughter ion's abundance in the mixed daughter spectrum was probably not due to a different compound but instead a greater concentration of the same compounds that are in all the bacteria. This can be seen in the spectra of the parents of  $m/z$  58, shown in figure 4.5. All three spectra contain a peak at  $m/z$  104, but the peak is much larger in the *S. subtilis* spectrum. This difference is easy to discern, and the increased intensity of the 104 peak may be due to a different compound, but because the peak is found in all three spectra this difference in intensity is not useful for ion monitoring during mixture analysis.

However, in several instances, comparisons of parent spectra did reveal ions unique to one of the bacteria. Figure 4.6 shows the  $m/z$  71 parent spectrum of each bacterium. The spectra of *E. coli* has peaks at  $m/z$  202 and 229, while these peaks are absent in the spectra of the

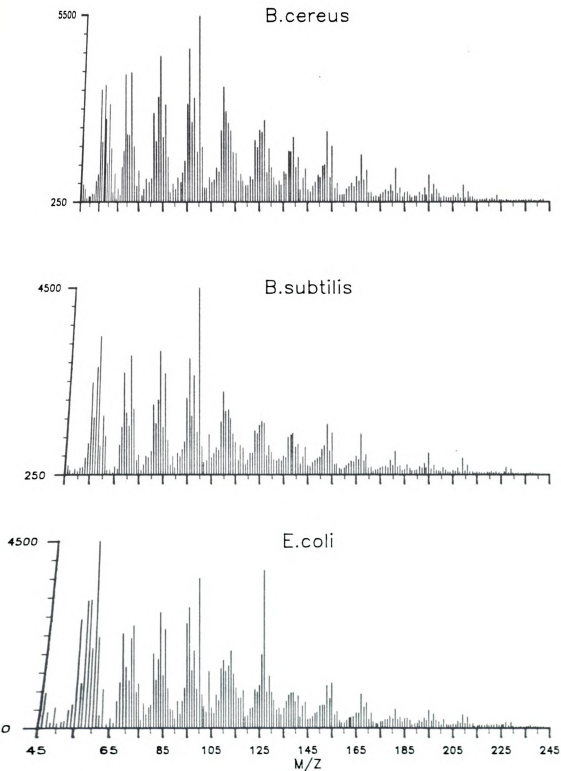


Figure 4.4 Mixed daughter scans of *B.cereus*, *B.subtilis* and *E.coli*

4.2      Selected daughter ions used for parent scans

<u>B.cereus</u>	<u>B.subtilis</u>	<u>E.coli</u>
60	58	70
63	84	77
81	104	84
96	117	95
110	118	113
136	144	127
	155	130

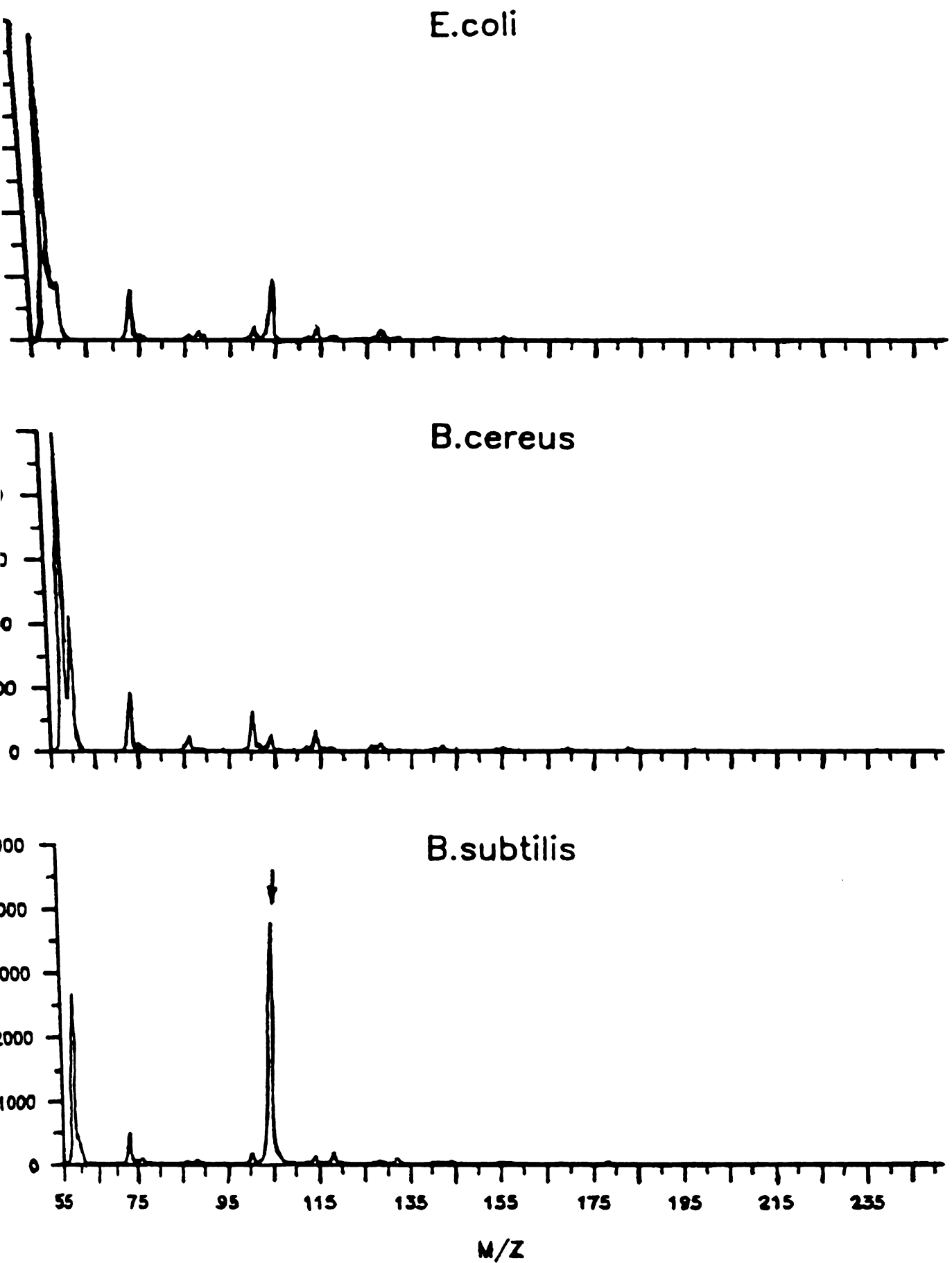


Figure 4.5 Parent ion spectra for m/z 58: PY/MS/MS spectra of *B.cereus*, *B.subtilis* and *E.coli*

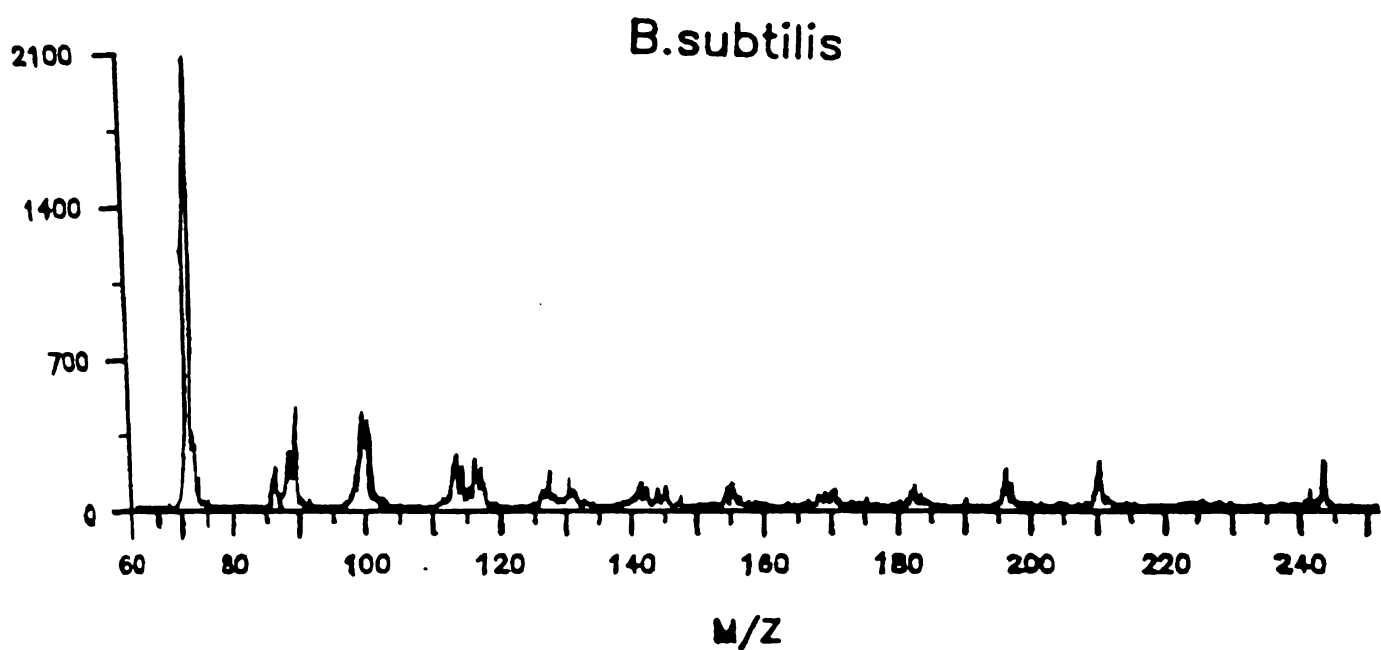
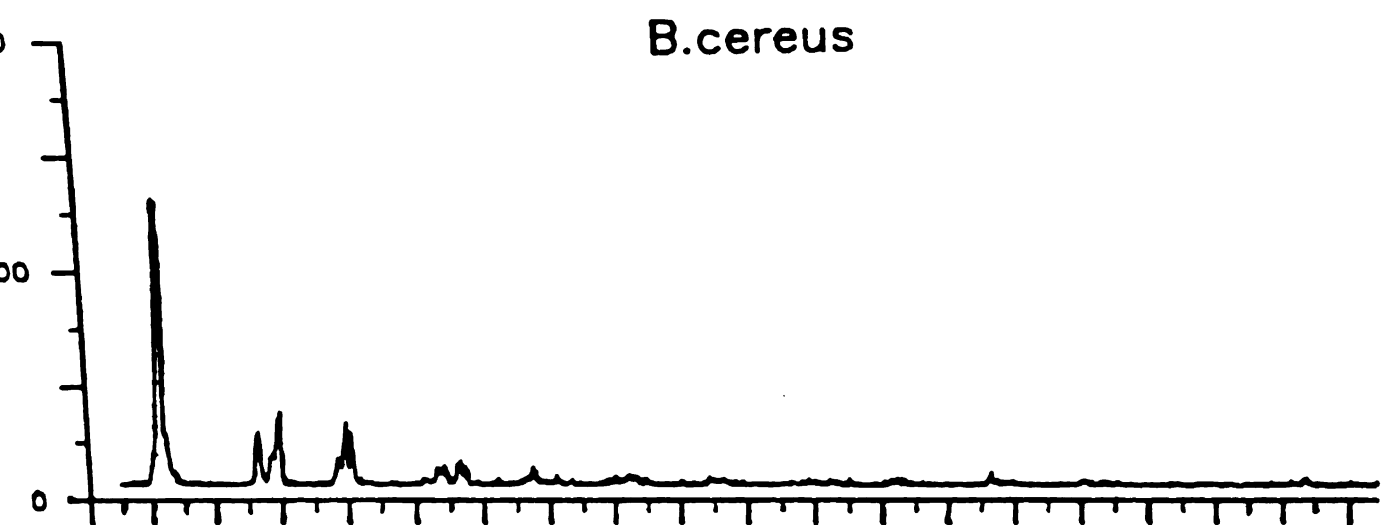
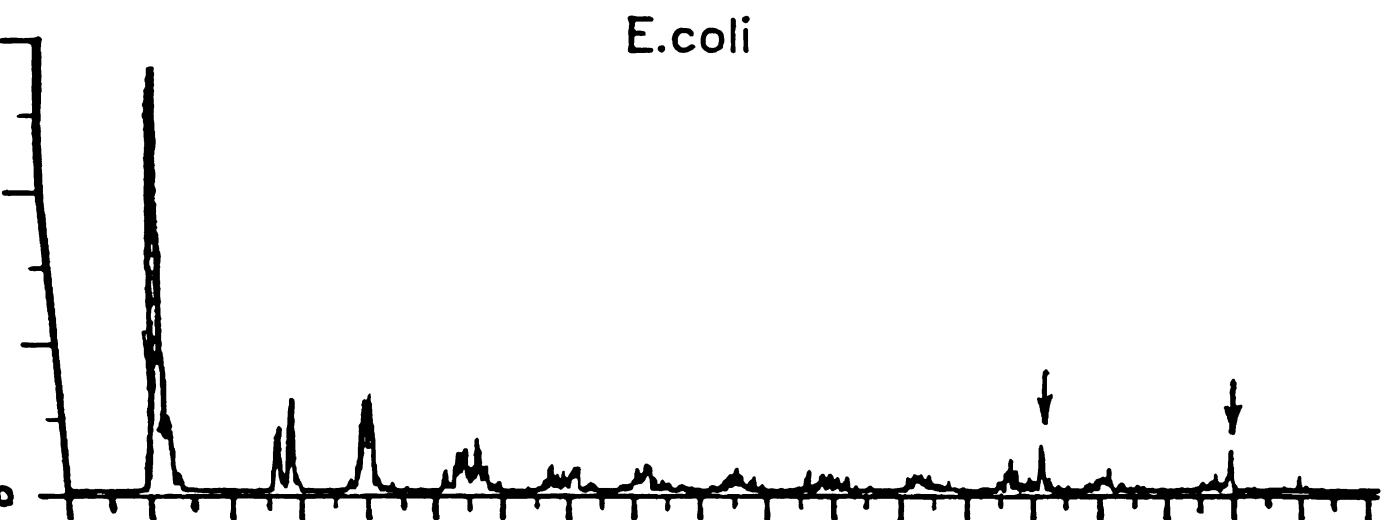


Figure 4.6 Parent ion spectra of  $m/z$  71: PY/MS/MS spectra of *B. cereus*, *B. subtilis* and *E. coli*

two bacteria. Therefore, the ion pair 202-71 and/or 229-71 could be monitored during analysis to detect the presence of *E.coli*. *B.cereus* can be identified by the parent daughter ion pair 127-71 and *B.subtilis* by the ion pair 144-84, as seen in figures 4.7 and 4.8. The identity of these ions, or of the neutrals lost, is not known at this time, and may never be known, for it is immaterial what the neutrals are. The fact that they designate specific bacteria is all that is important for successful analysis.

While it is exciting that parent-daughter pairs were found that are specific for a particular species, it is disappointing that the mixed ion-daughter spectra are apparently not useful in the search for the ion-

The parent scans that were specific for a particular bacterial species are not specific for the species that factor analysis predicted. *B.subtilis* can be identified by a scan listed under *B.subtilis* in table 4.2. The m/z 127 parent scan that is useful for finding *B.cereus* was predicted to find *E.coli*. The best scan for finding *E.coli*, the m/z 71 parent scan, is not even listed in table 4.2. This scan was accidentally omitted into the scan list which was used to collect data.

The best method to determine differences in MS/MS data remains a comparison of the entire MS/MS map. Complete maps of the MS/MS data could be used to identify unique ion-pairs that would be useful for screening purposes, or entire MS/MS maps could be used as detailed fingerprints for the identification of species in the same way that fingerprints are used in normal mass spectrometry today.

Generating a complete map of all the daughters of all the peaks in a primary spectrum will require instrument modifications. The current method of sample introduction, using a short column, provides just

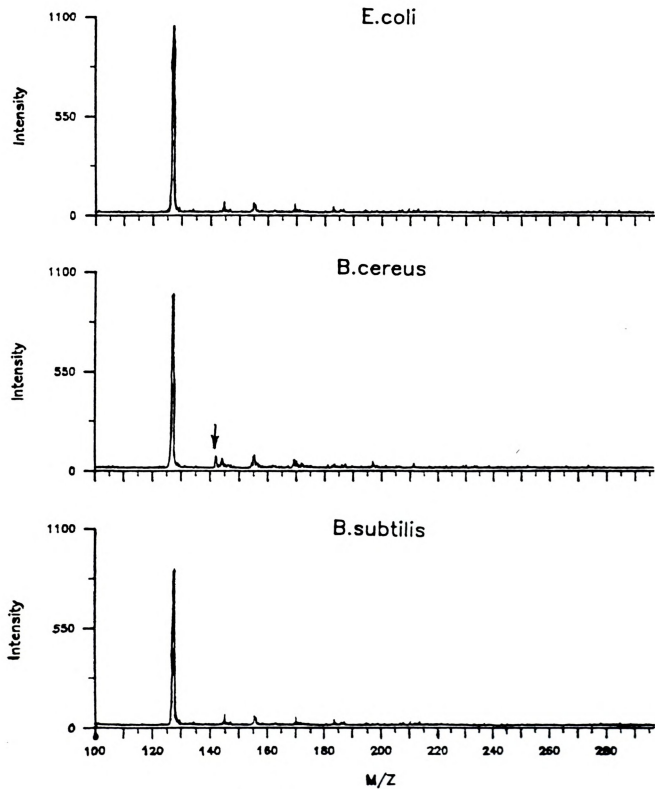


Figure 4.7 Parent ion spectra of m/z 127: PY/MS/MS spectra of *B. cereus*, *B. subtilis* and *E. coli*



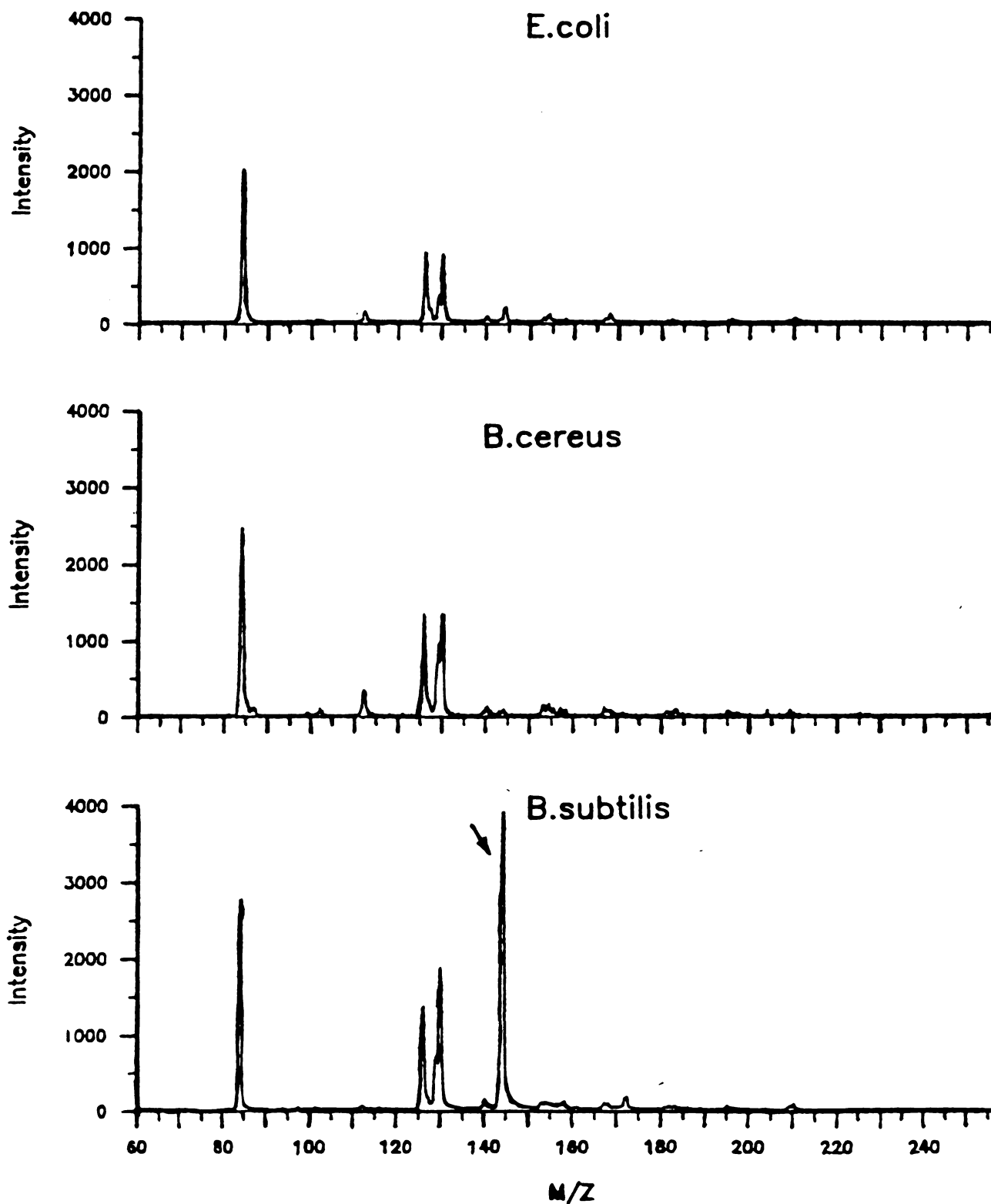


Figure 4.8 Parent ion spectra of m/z 84: PY/MS/MS spectra of *B. cereus*, *B. subtilis* and *E. coli*.

enough ion current to be detected, and the sample lasts for only a few scans. A system that brings a steady flow of a larger quantity of pyrolysate to the ion source will have to be designed before collecting complete MS/MS maps becomes practical.

Mixed daughter spectra not only contain peaks representing daughter ions but they also have peaks from unfragmented parent ions. Therefore, daughter spectra were collected for several of the computer-suggested ions which did not produce useful parent spectra. These spectra were similar to the parent spectra, for they, too, did not have significant species-related peaks.

#### 4. Mixture analysis by pyrolysis tandem mass spectrometry

The next step in developing PY/MS/MS into a viable technique for identifying bacteria in mixtures was to test the ion-pairs identified as characteristic for specific bacteria in a mixture. A mixture of *B.cereus* in a matrix of corn starch was chosen for this experiment because *B.cereus* has been identified as the bacteria responsible in several food poisoning cases involving foods made with corn starch<sup>(1)</sup>.

A set of scans, including the parent scans found to be specific for *B.cereus*, was programmed into the instrument's control system. This set of scans was used to collect data for pyrolyzed *B.cereus*, plain corn starch, and a sample of corn starch spiked with *B.cereus*. The normal mass spectra of the three samples are shown in figure 4.9. The largest peak in all three spectra, at  $m/z$  80, has been removed so that the other smaller peaks would be visible in the normalized spectra. Upon examination, it is apparent that the spectra of the bacteria and the corn starch are different. The spectrum of the bacteria has intense peaks at  $m/z$  106, 123, 124 and 140 which are smaller in the corn starch spectrum

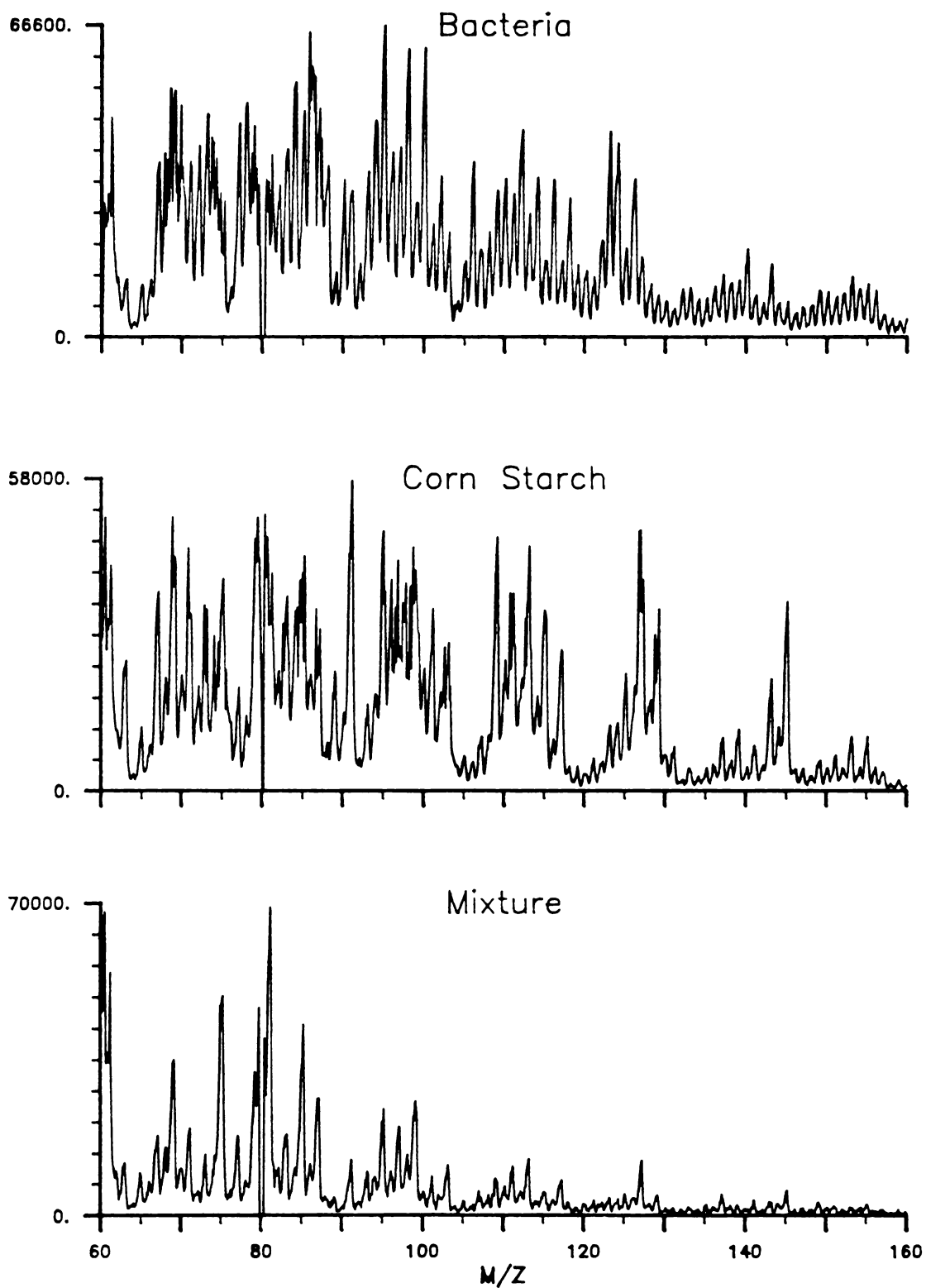


Figure 4.9 Pyrolysis mass spectra of *B.cereus*, plain corn starch and corn starch spiked with *B.cereus*. (m/z 80 has been removed for clarity)

which has more intense peaks at  $m/z$  91, 112, 127 and 145. Even though the spectrum of a pyrolyzed mixture is not necessarily the exact sum of the spectra of the individual components in the mixture because intermolecular reactions may occur<sup>(44)</sup>, pyrolysis spectra of mixtures are generally treated as summed spectra<sup>(45)</sup>. The spectra of the spiked corn starch, however, does not appear to be of a mixture for it closely resembles that of the corn starch. The prominent corn starch peaks are all visible in the spectrum of the mixture, while none of the prominent bacterial peaks are evident. The bacterial peaks are present, but because the pyrolysis spectra contain peaks at every mass, the presence of the bacteria is hidden under the larger peaks from the corn starch ions. Tsao and Voorhees<sup>(43)</sup> and Windig et al.<sup>(12)</sup> have recently developed a computer method to deconvolute the information available in the PY/MS spectra of mixtures. This information, however, cannot be obtained by a visual examination of the spectrum, as evidenced by the spectrum of the spiked corn starch.

The MS/MS data collected did provide a means to visually detect the presence of the bacteria in the mixture. The  $m/z$  84 parent scan of the bacteria has a peak at  $m/z$  126 which is not present in the spectra of the corn starch. This ion can therefore be used as a flag for the bacteria, since corn starch does not have an interfering ion at this mass. The parent spectrum of  $m/z$  84 ion in the mixture does show the  $m/z$  126 peak. This indicates that the bacteria were present in the mixture. The  $m/z$  84 parent scans of the three samples are shown in figure 4.10.

The 126-84 ion-pair seen in the mixture spectrum is not specific for *B.cereus*. This ion-pair was found in the spectra of all the bacteria

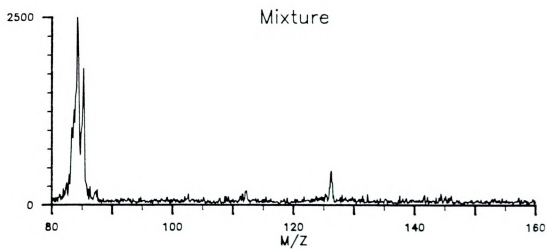
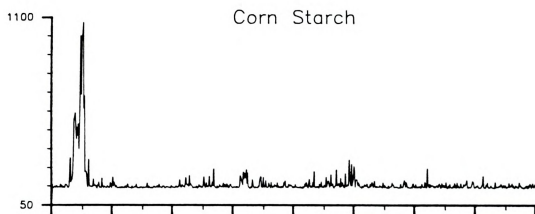
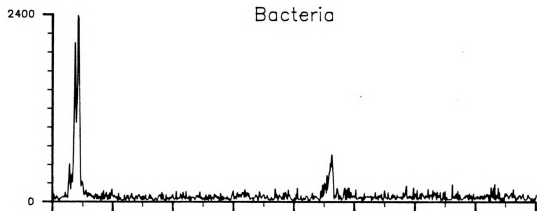


Figure 4.10 Parent ion spectra of m/z 84: PY/MS/MS spectra of *B.cereus*, plain corn starch and corn starch spiked with *B.cereus*.

tested (figure 4.8), therefore, the presence of a peak representing this ion-pair in a spectrum only determines that there are bacteria present. Which bacteria are present cannot be determined by this information. The data collected to determine the specific bacteria present in the sample were inconclusive.

#### D. CONCLUSIONS

Combining pyrolysis with tandem mass spectrometry provides researchers with a very powerful analytical tool that has a tremendous amount of untapped potential. Pyrolysis allows the tandem mass spectral analysis of many new samples that were previously reserved for other analytical techniques. Tandem mass spectrometry opens the PY/MS field, once limited to pure samples, to the analysis of mixtures. The addition of another mass analyzer to a PY/MS instrument can aid researchers in many fields, including those researching the pyrolysis process itself, by providing more information about the nature of the ions represented in pyrolysis mass spectra.

The data presented in this chapter show that PY/MS/MS can identify components in a mixture. Information characteristic of the mixture was obtained that was not available by using only PY/MS. Data presented show that it is possible to find parent/daughter ion-pairs in the pyrolysate of bacteria which are characteristic for particular bacterial species. Peaks representing certain of these ion-pairs were present in the spectra of the mixture, indicating the presence of bacteria. A new technique, using methane as a carrier gas for the pyrolysate and as the chemical ionization reagent gas, offers a viable alternative to low energy electron impact ionization for producing

simplified, minimal fragmentation, mass spectra. CI/PY/MS provides both increased sensitivity and more abundant high mass ions.

The methods presented here were the result of a feasibility study initiated to explore the possibility of interfacing pyrolysis and triple quadrupole mass spectrometry for the detection of microbes. The data discussed in this chapter were obtained under a time limit with borrowed equipment. Therefore, many areas of inquiry had to be left unanswered. The positive results of these initial experiments suggest that this line of research should proceed and that additional experiments should be undertaken to improve upon the methods used here and answer the many remaining questions.

Possible side effects of chemical ionization were never explored, nor were the use of other reagent gases. A satisfactory method to detect and identify useful unique ion-pairs was not established. Questions regarding the reproducibility of the spectra and the effect that different operating conditions have on the spectra were left for others to answer. Optimum instrument parameters were never established. There are also several modifications that could be made to the instrument, including those discussed in earlier sections, in order to improve the quality of the data collected. The possibility of interfacing the pyrolyzer directly to the ion source should be investigated. Instead of using a long narrow gas chromatography column to transport the pyrolysate, an expansion chamber, similar to that described by Meuzelaar and Kistemaker<sup>(46)</sup>, may be a useful alternative.

Solving some of the questions posed above would enable PY/MS/MS technology to become the central component of a fully automated process monitoring system for use with complex mixtures. Currently, automated

pyrolysis techniques are limited by the long computer computation times necessary to differentiate species. Meuzelaar et al. have reported an automated PY/MS instrument which they developed that used primitive robotics to feed bacterial samples into the pyrolyzer<sup>(47)</sup>. Their system can pyrolyze 30 samples per hour, but the thousands of scans collected must then be analyzed off-line on a large, CDC-Cyber 73-28, computer system in order to obtain useful information. PY/MS/MS has the potential to minimize the need for computer analysis of pyrolysis data. Computers only need to be used during method development, to aid in the determination of the areas of the MS/MS data field that are useful for differentiation. After ion-pairs have been found, however, species could be identified visually by the instrument operator or electronically by the instrument control system. Such a system would be truly automated and could be tailored for use in any of the many fields where detection and identification of microorganisms is of interest.



## E. REFERENCES

1. *Manual of Clinical Microbiology* 3<sup>rd</sup> ed.; Lennette, E.H., Ed.; American Society for Microbiology: Washington D.C., 1980, Chapter 7.
2. Gutteridge, C.S., Norris, J.R.; *J.Appl.Bacteriol.*, 1979, 47, 5.
3. Bieman, K.; *Anal.Chem.*, 1986, 58, 1289A
4. Burlingame, A.L., Baillie, T.A., Derrick, P.J.; *Anal.Chem*, 1986, 58, 165R
5. Kaufman, R., Hillenkamp, F., Remy, E.; *Microscopica Acta*, 1972, 73, 1
6. Wechsing, R, et al.; *Mikroskopie*, 1978, 34, 47
7. Evans, C.A.; *Anal.Chem.*, 1972, 44, 67A
8. Windig, W., Haverkamp, J., Kistemaker, P.G.; *Anal. Chem.*, 1983, 55, 88.
9. Meuzelaar, H.L.C., Haverkamp, J., Hileman, F.D.; *Pyrolysis Mass Spectrometry of Recent and Fossil Biomaterials: Compendium and Atlas*; Elsevier Scientific: New York, 1982
10. Weiten, G., Meuzelaar, H.L.C., Haverkamp, J.; in *Gas Chromatography-Mass Spectrometry Applications in Microbiology*; Odham, O., Larsson, L., Mardh, P., Eds.; Plenum: New York, 1984, Chapter 10
11. Meuzelaar, H.L.C., Windig, W., Harper, A.M., Huff, S.M., McClennen, W.H., Richards, J.M.; *Science*, 1984, 226, 268.
12. Espitalie, J., et al.; in *Analytical Pyrolysis* ; Voorhees, K., Ed.; Butterworths: London, 1984, Chapter 9
13. Smith, C.G.; in *Analytical Pyrolysis* ; Voorhees, K., Ed.; Butterworths: London, 1984, Chapter 14
14. Windig, W., McClennen, W.H., Stolk, H., Meuzelaar, H.L.C.; *Optical Eng.*, 1986, 25, 117
15. Madorsky, S.L., Strauss, S.; *Ind.Eng.Chem.*, 1948, 40, 848
16. Zemaný, P.D., *Anal.Chem.*, 1952, 24, 1709
17. Davison, W.H.T., Slaney, S., Wragg, A.L.; *Chem.and Ind.*, 1954, 1356
18. Oyama, V.I., *Nature*, 1963, 200, 1058.
19. Reiner, E., *Nature*, 1965, 206, 1272

20. Reiner, E.; Hicks, J.J.; Ball, M.M.; Martin, W.J., *Anal. Chem.*, 1972, 44, 1058 .
21. Levy, R.L., *Chromatogr. Rev.*, 1966, 8, 48
22. Irwin, W.J.; Slack, J.A., *Analyst*, 1978, 103, 673
23. Genuit, W., Boon, J.J.; *J. Anal. Appl. Pyrol.*, 1985, 8, 25
24. Boon, J.J., et al.,; *Org. Geochem.*, 1984, 6(Adv. Org. Geochem. 1983), 805
25. Gillam, A.H., Wilson, M.A.; *Org. Geochem.*, 1985, 8, 15
26. Eudy, W.L., Walla, M.D., Morgan, S.L.; *Analyst*, 1985, 110, 381
27. Walla, M.D., Lau, P.Y., Morgan, S.L., Fox, A., Brown, A.; *J. Chromatogr.*, 1984, 288, 399
28. Eudy, W.L., Walla, M.D., Hudson, J.R., Morgan, S.L.; *J. Anal. Appl. Pyrol.*, 1985, 7, 231
29. Morgan, S.L., Jacques, C.A.; *Anal. Chem.*, 1982, 54, 741
30. Bayer, F.L., Morgan, S.L., in *The Analysis of Biopolymers by Analytical Pyrolysis Gas Chromatography*; Levy, E.J., Liebman, S., Eds., Dekker: New York, 1985, Chapter 6
31. Fox, A., Morgan, S.L.; in *Rapid Detection and Identification of Microorganisms*, Nelson, W.H., Ed.; VCH: Deerfield Beach, FL, 1985, Chapter 5
32. Coupe, N.B., Jones, C.E., Perry, S.G.; *J. Chromatogr.*, 1970, 47, 291
33. Meuzelaar, H.L.C.; Kistemaker, P.G., *Anal. Chem.*, 1973, 45, 587 .
34. Bozorgzadeh, J.H., Beynon, J.H., Wiebers, J.L.;
35. Levsen, H., Schulten, H.R.; *Biomed. Mass Spec.*, 1976, 3, 137
36. Meuzelaar, H.L.C., Posthumus, M.A., Kistemaker, P.G., Kistemaker, J.; *Anal. Chem.*, 1973, 45, 1546
37. Haverkamp, J., Wieten, G., Boerboom, A.J.H., Dallinga, J.W., Nibbering, N.M.M.; in *Analytical Pyrolysis*; Voorhees, K., Ed.; Butterworths: London, 1984, Chapter 10
38. Giacobbo, H., Simon, W.; *Acta Helv.*, 1964, 39, 162
39. Wells, G., Voorhees, K.J., Futrell, J.H.; *Anal. Chem.*, 1980, 52, 1782
40. Whitehouse et al.; *J. Anal. Appl. Pyrolysis*, 1985, 8, 515
41. Risby, T.H., Yergey, A.L.; *Anal. Chem.*, 1978, 50, 327A

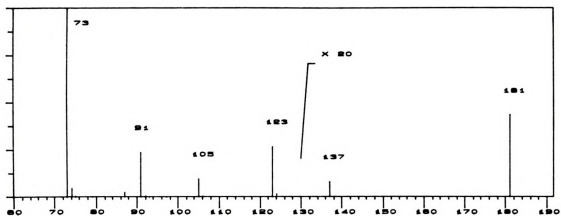
42. Risby, T.H., Yergey, A.L.; *J.Phys.Chem.*, 1976, 80, 2839
43. Tsao,R., Voorhees,K.J.; *Anal.Chem.*, 1984, 56, 1339
44. Van de Meent, D., de Leeuw, J.W., Schenck, P.A., Windig, W.,  
Haverkamp, J.; *J.Anal.Appl.Pyrolysis*, 1982, 4, 133
45. Tsao,R., Voorhees,K.J.; *Anal.Chem.*, 1984, 56, 368
46. Meuzelaar, H.L.C., Kistemaker, P.G., *Anal.Chem.*, 1973, 45, 587
47. Meuzelaar, H.L.C., Kistemaker, P.G., Eshuis, W., Boerboom, H.A.J.,  
*Adv.Mass Spec.*, 1978, 7B, 1452

## APPENDICES

Appendix 2A: Methanol CI mass spectra of test mixture

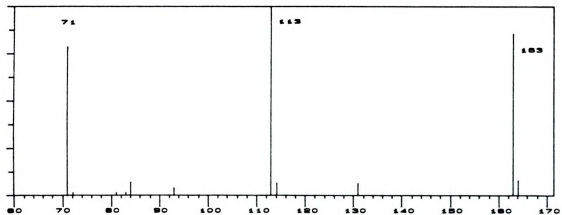
2,3 Butanediol

mw = 90



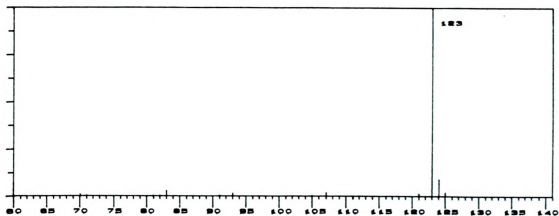
1-Octanol

mw = 130



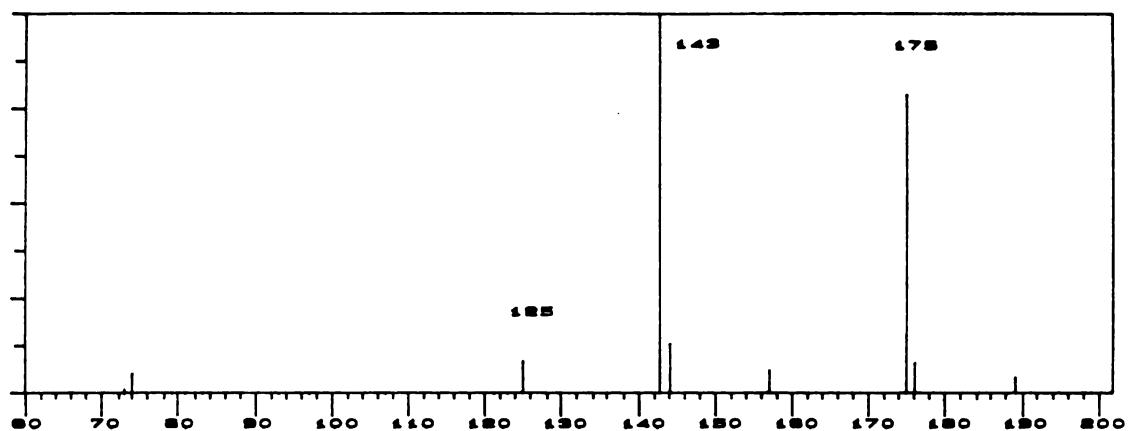
2,6 Dimethylphenol

mw = 122

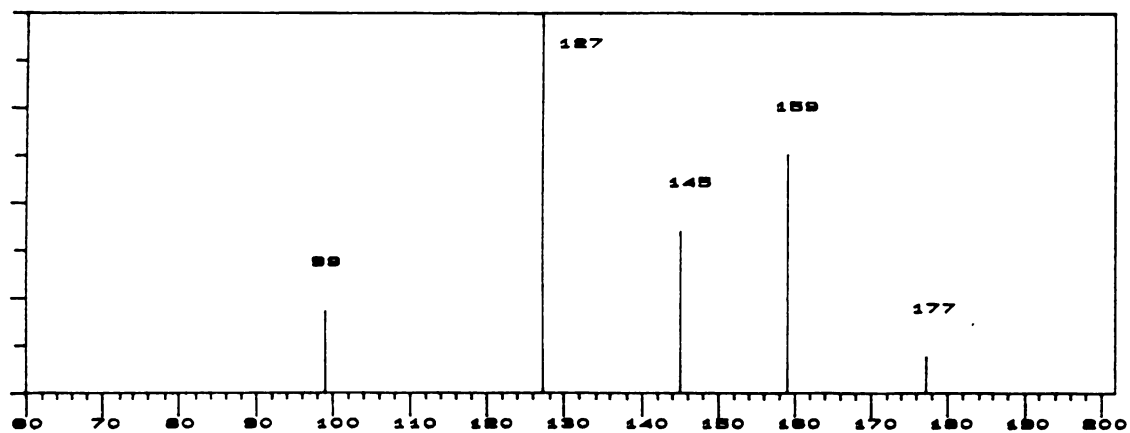




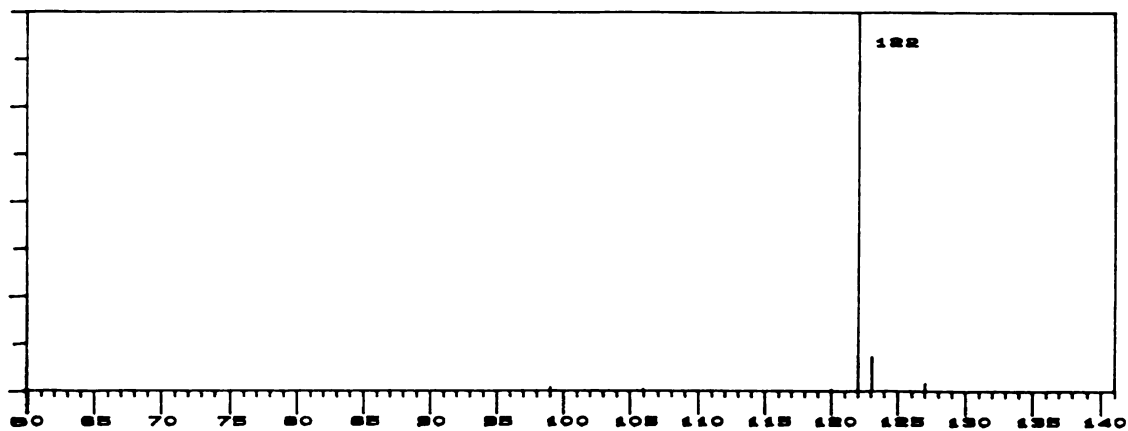
Nonal      mw = 142



2-Ethylhexanoic acid      mw = 144

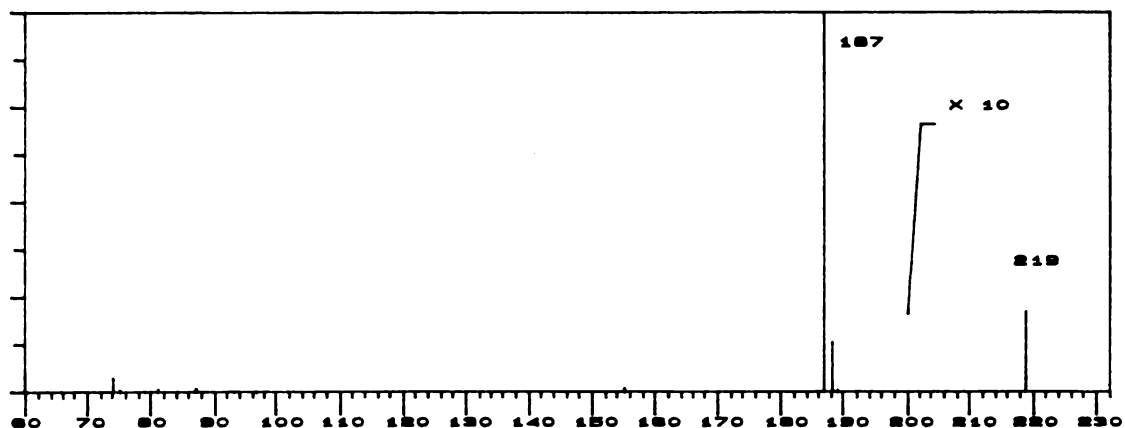


2,6 Dimethylaniline      mw = 121

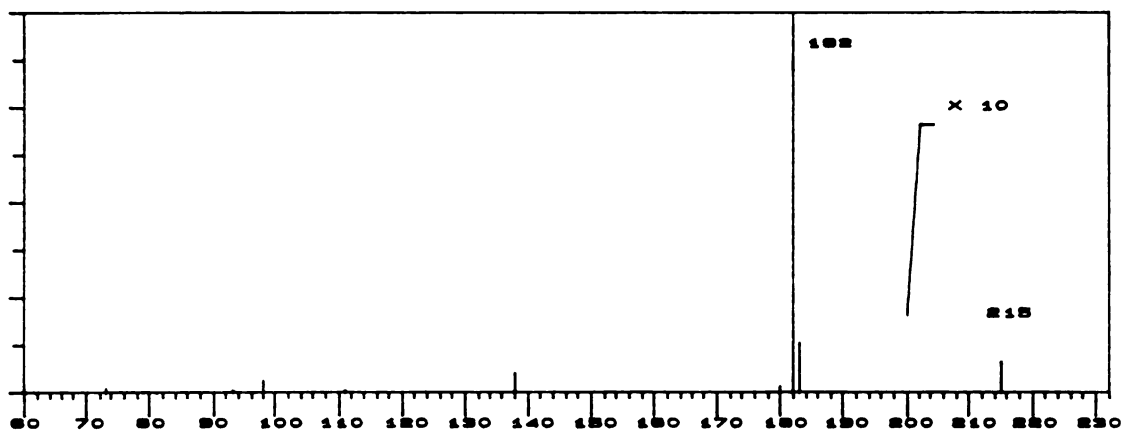




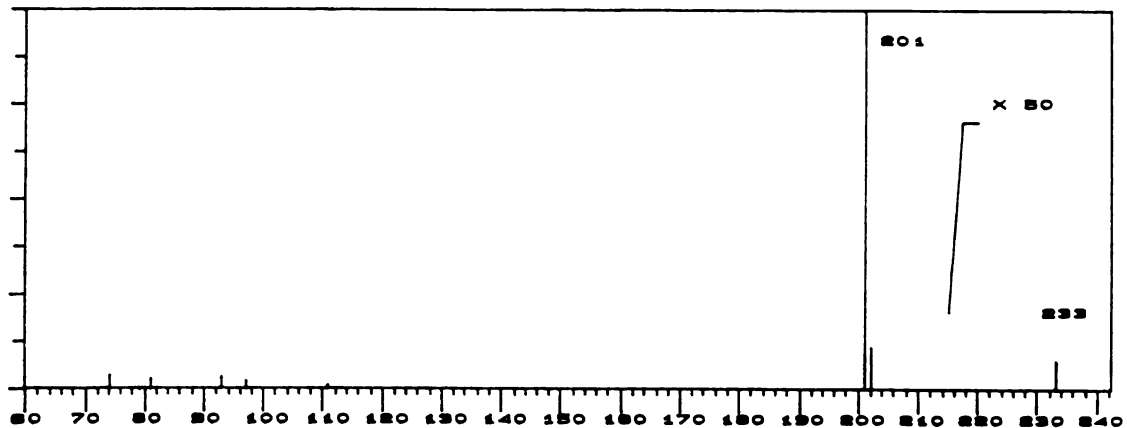
C<sub>10</sub> acid methyl ester      mw = 186



Dicyclohexylamine      mw = 182

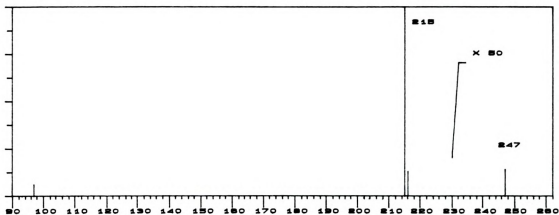


C<sub>11</sub> acid methyl ester      mw = 200



C<sub>12</sub> acid methyl ester

MW = 214

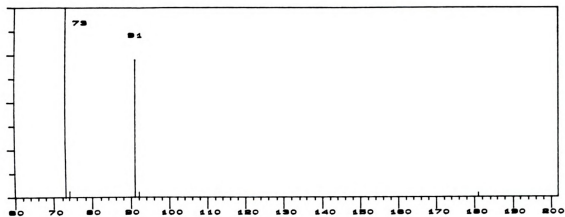


Appendix 2B: Isobutane CI mass spectra of test mixture



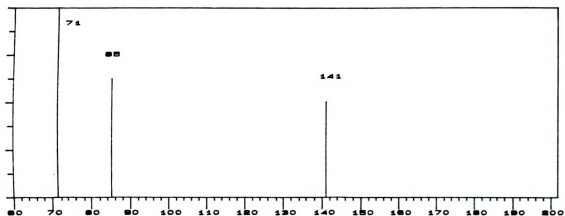
2,3 Butanediol

mw = 90



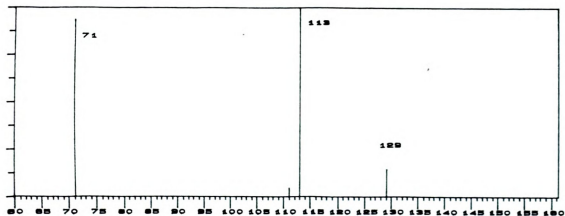
Decane

mw = 142



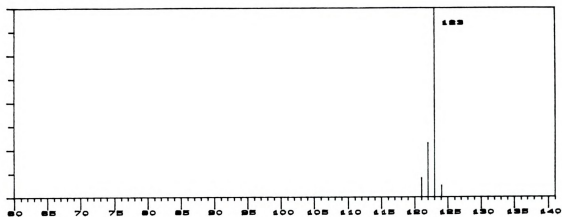
1-Octanol

mw = 130



2,6 Dimethylphenol

MW = 122



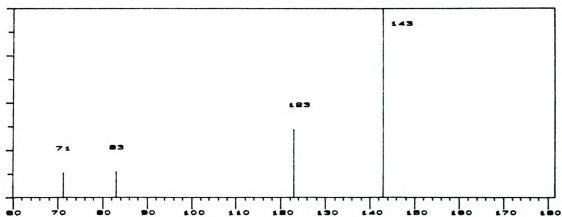
2,6 Dimethylphenol

MW = 122

&

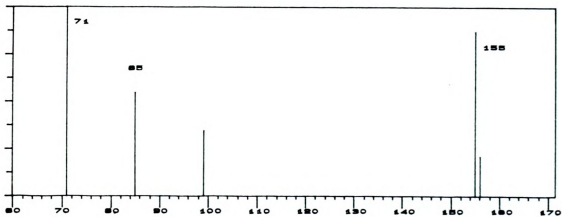
Nonal

MW = 142



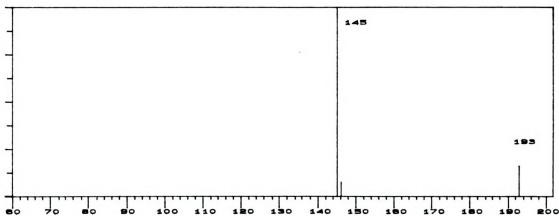
Undecane

MW = 156



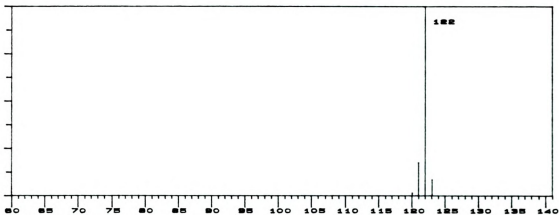
2-Ethylhexanoic acid

mw = 144



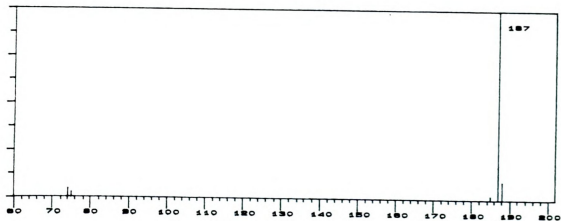
2,6 Dimethylaniline

mw = 121



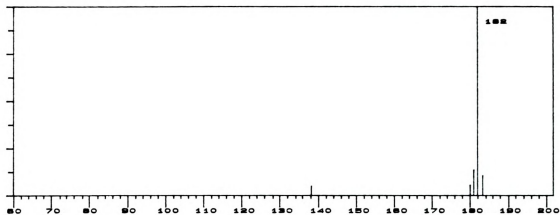
C10 acid methyl ester

mw = 186



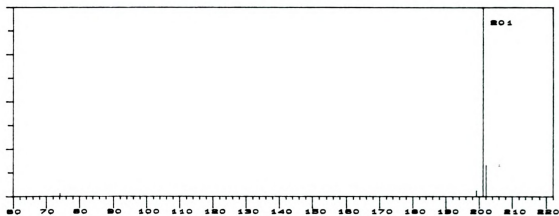
Dicyclohexylamine

mw = 182



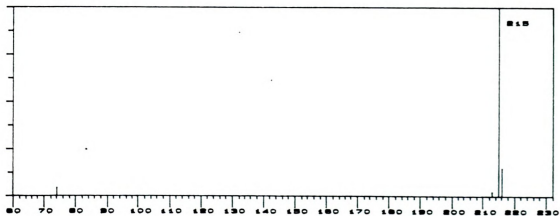
C<sub>11</sub> acid methyl ester

mw = 200



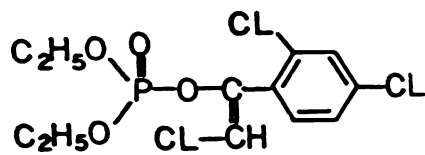
C<sub>12</sub> acid methyl ester

mw = 214

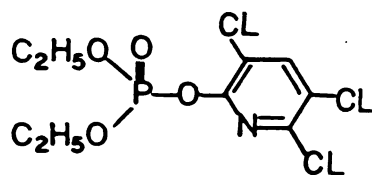
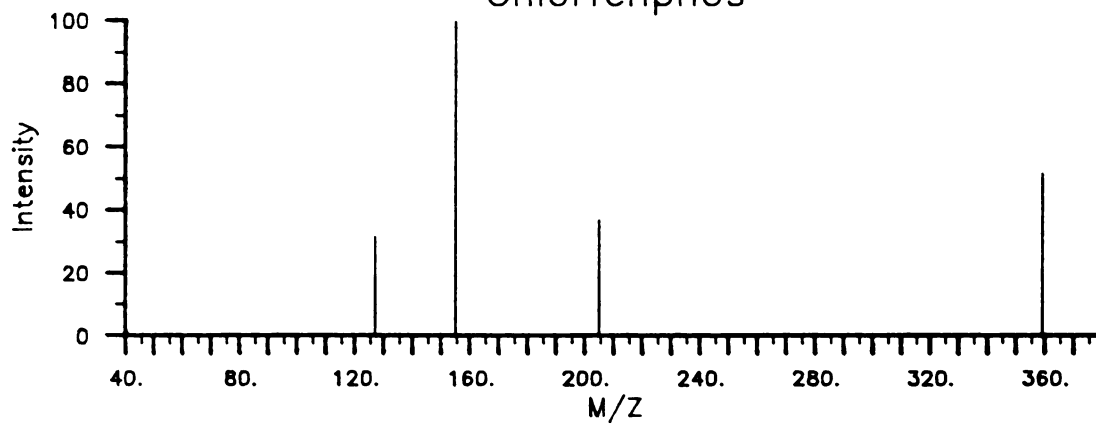




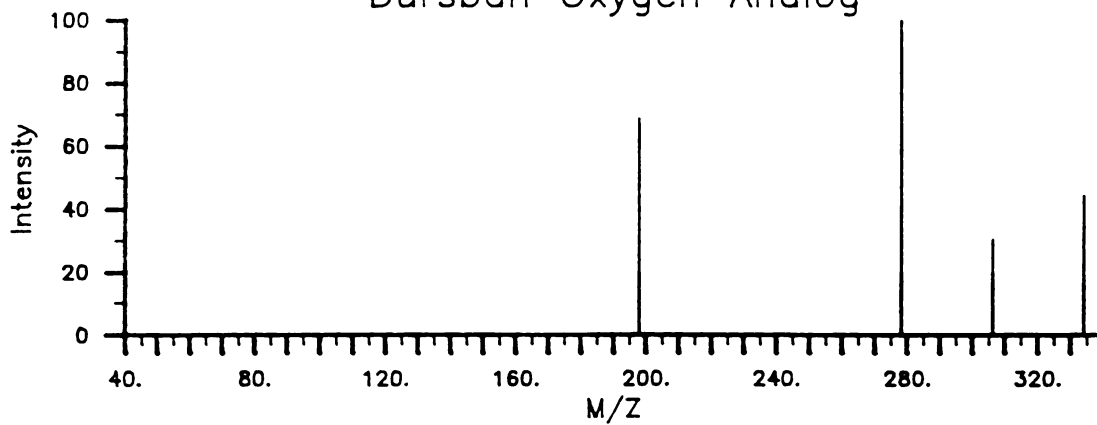
Appendix 3A: CAD spectra of the  $(M+H)^+$  ions of the  
organophosphorus pesticides

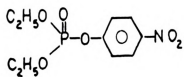


Chlorfenphos

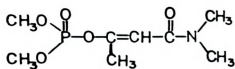
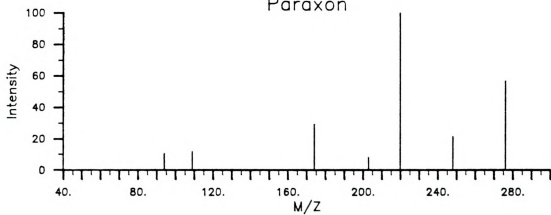


Dursban Oxygen Analog

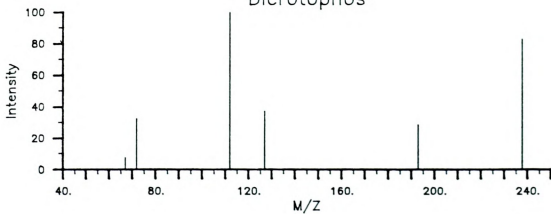


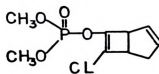


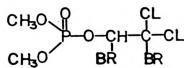
Paraxon



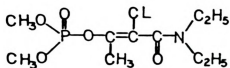
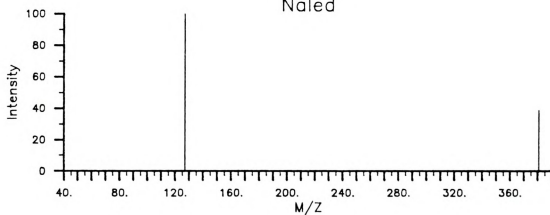
Dicrotophos



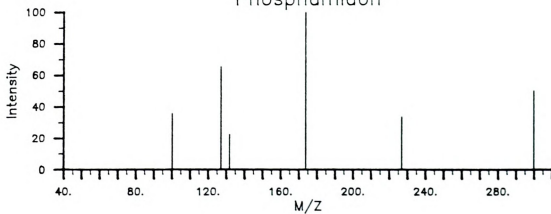


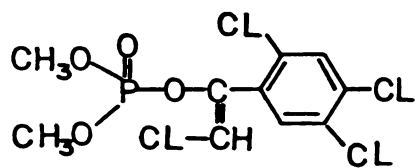


Naled

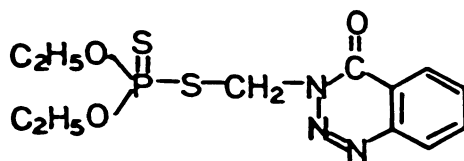
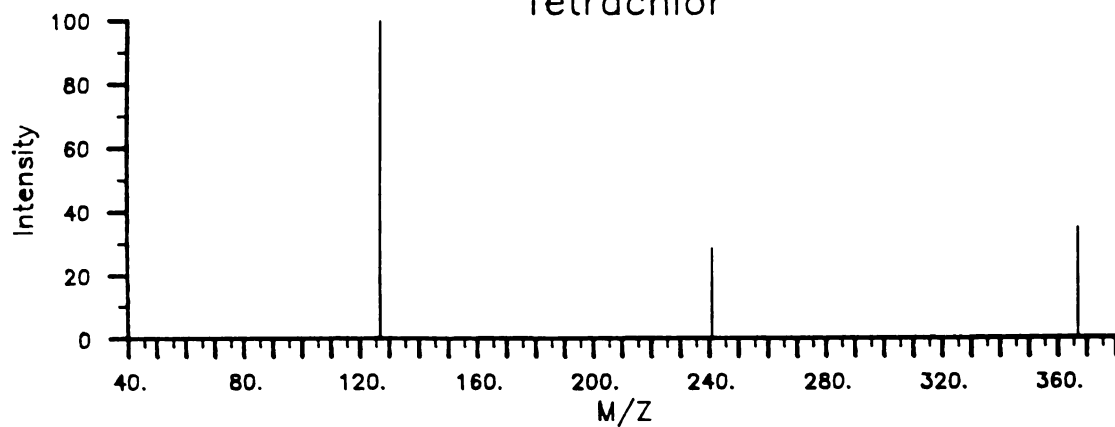


Phosphamidon

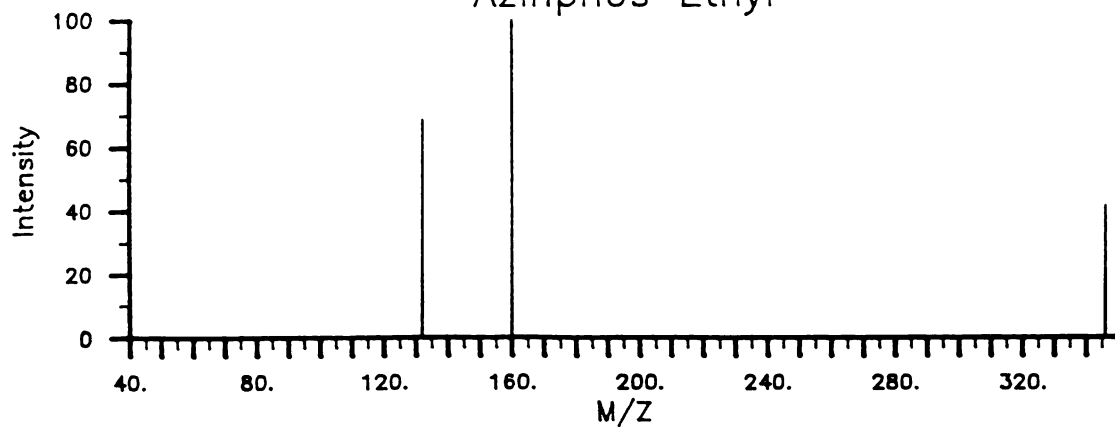


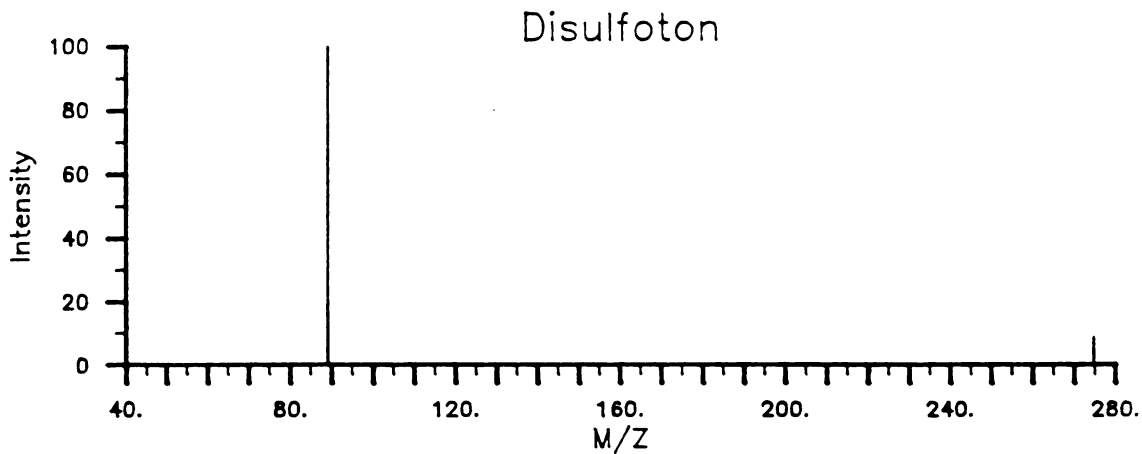
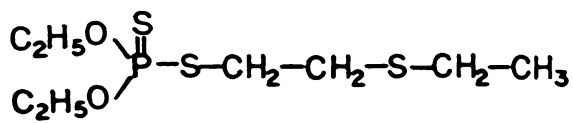
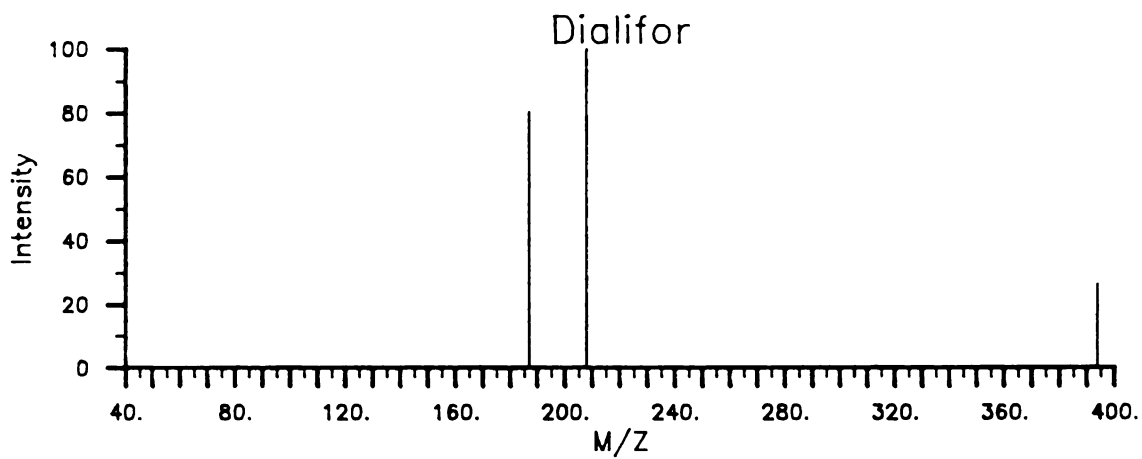
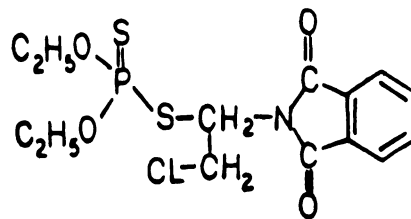


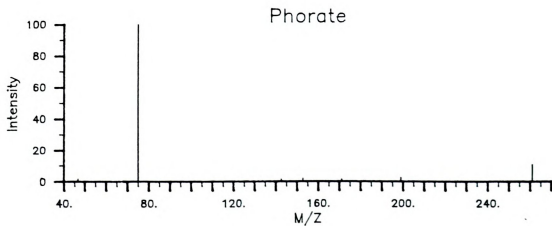
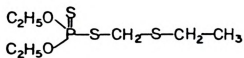
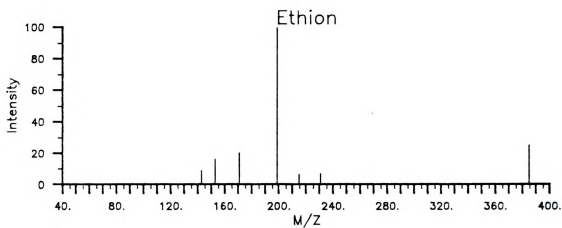
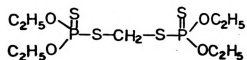
Tetrachlor



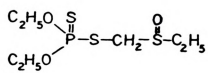
Azinphos Ethyl



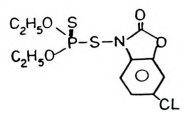
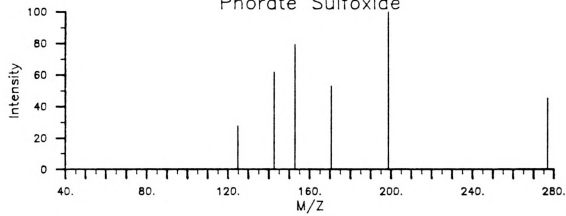




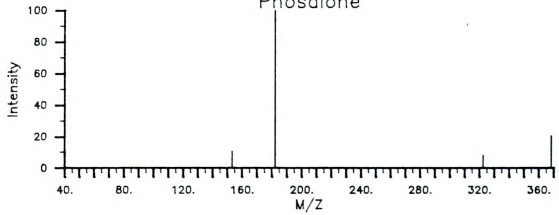


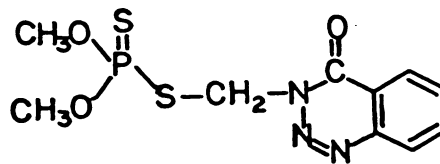


Phorate Sulfoxide

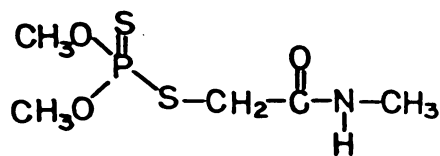
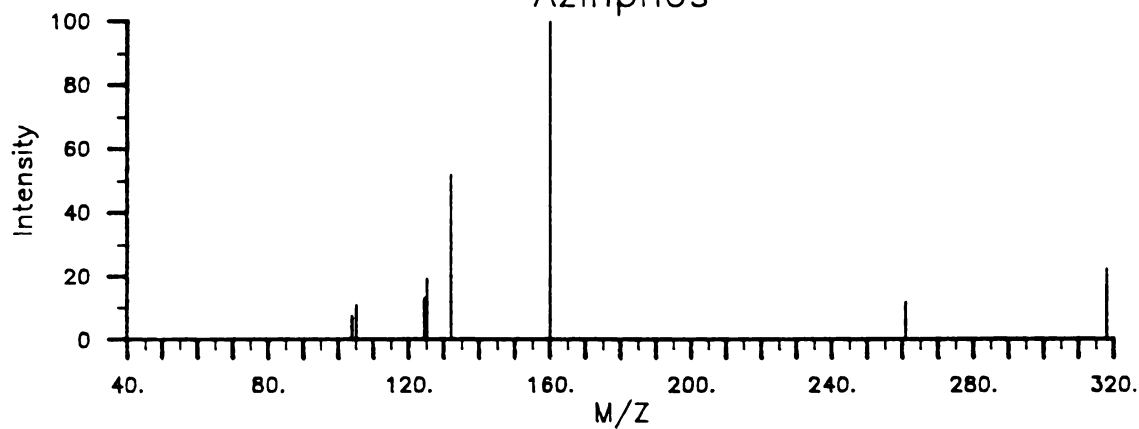


Phosalone

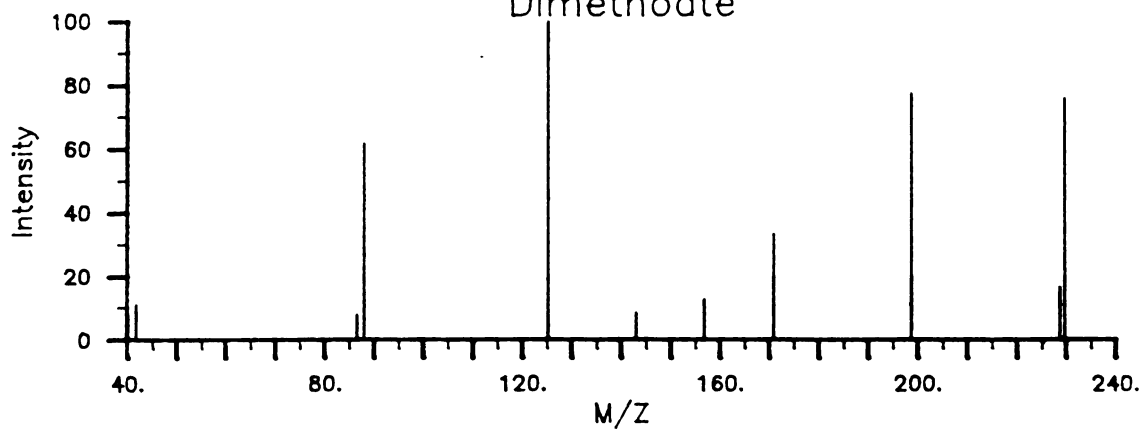


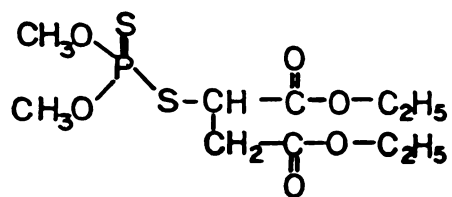


Azinphos

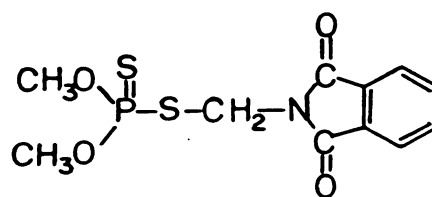
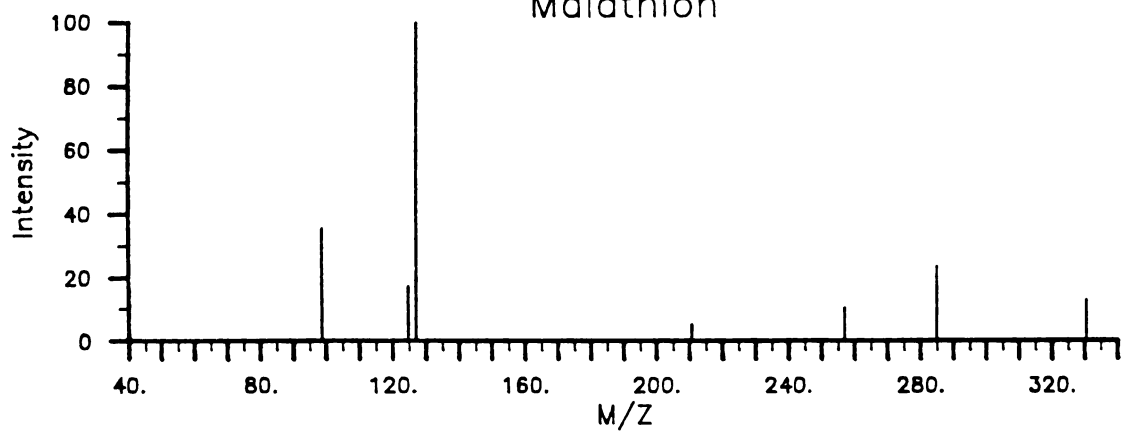


Dimethoate

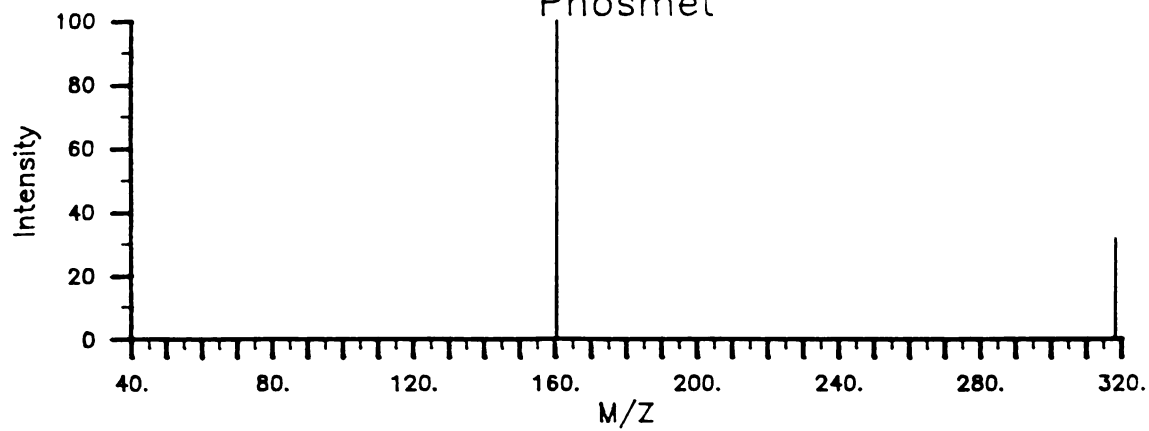


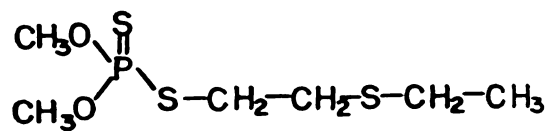


Malathion

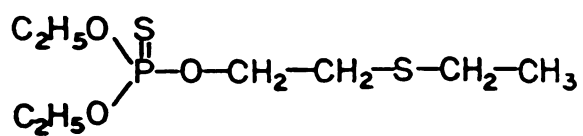
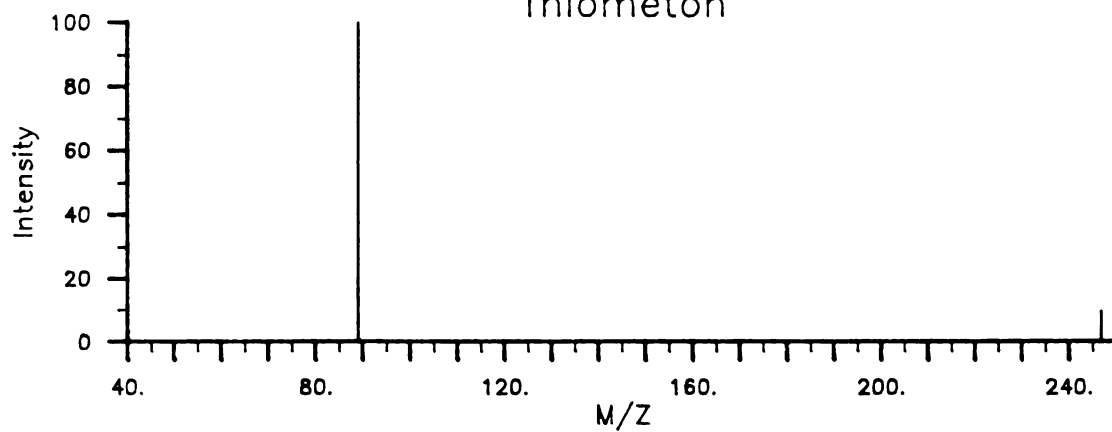


Phosmet

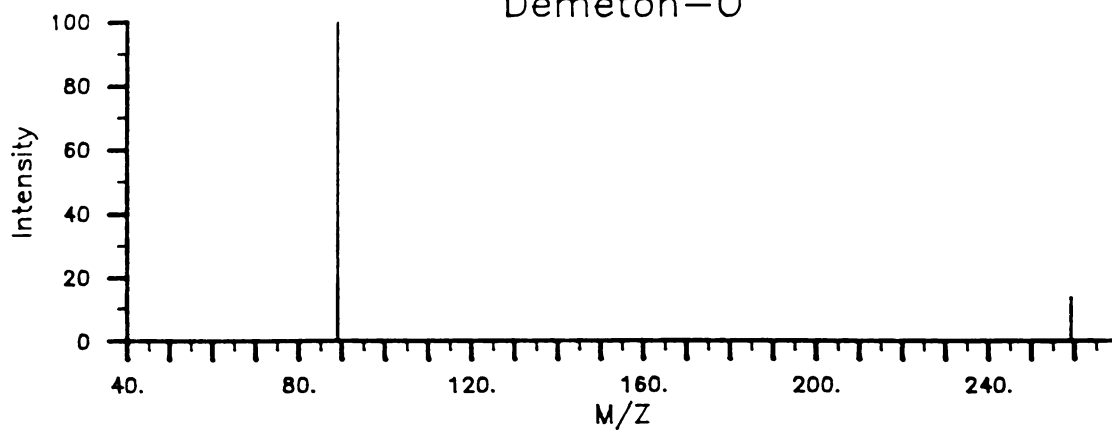


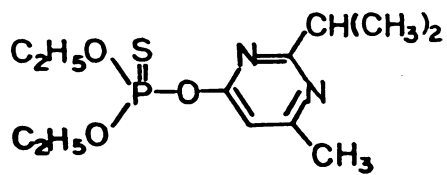


Thiometon

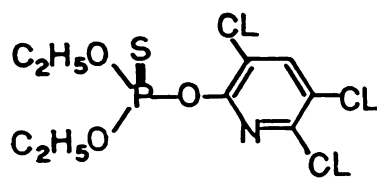
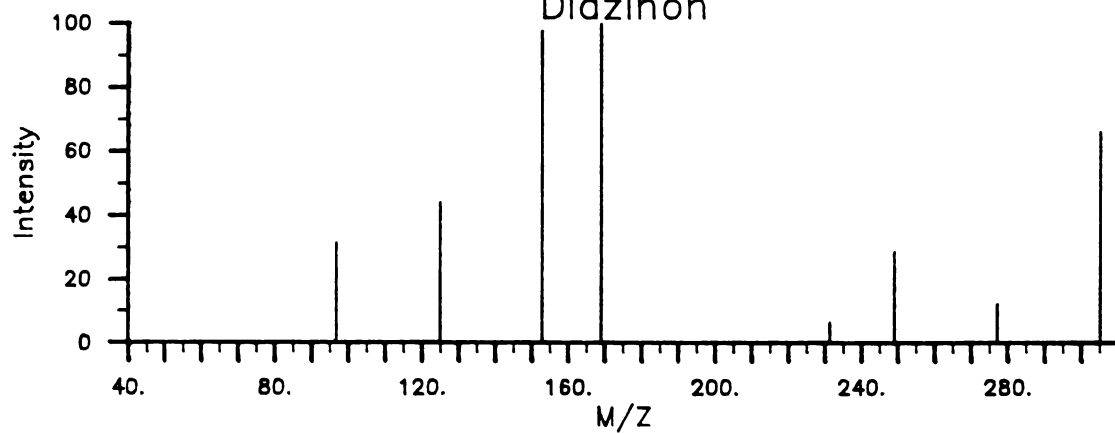


Demeton-O

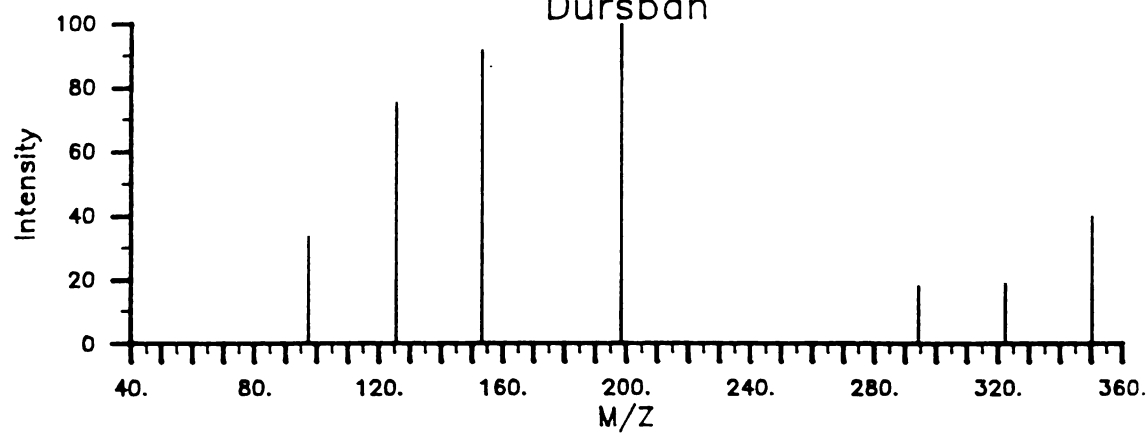


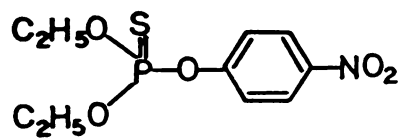


Diazinon

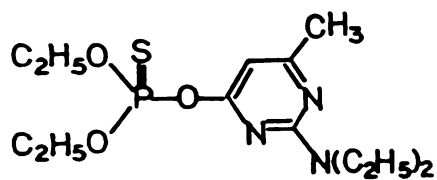
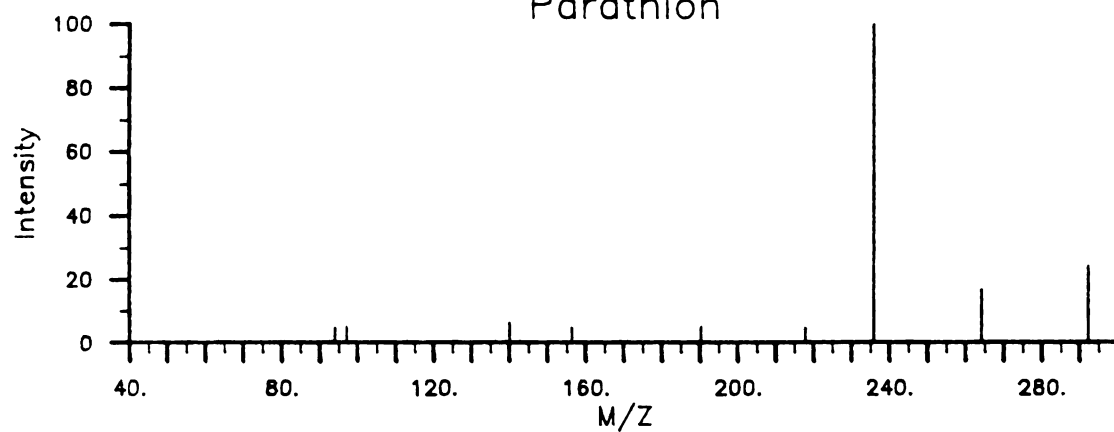


Dursban

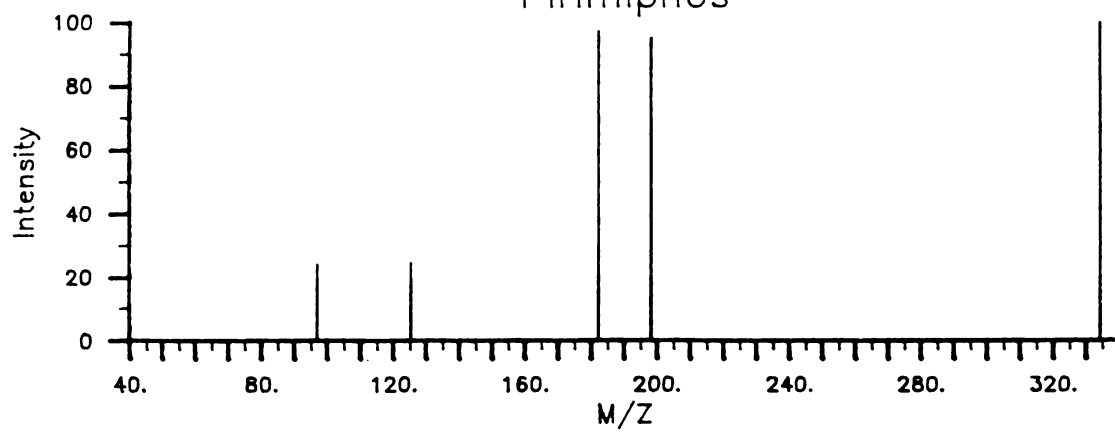


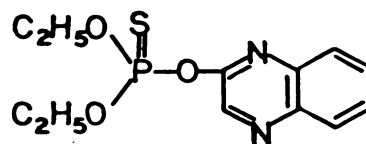


Parathion

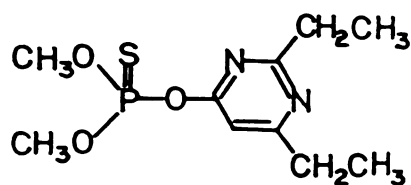
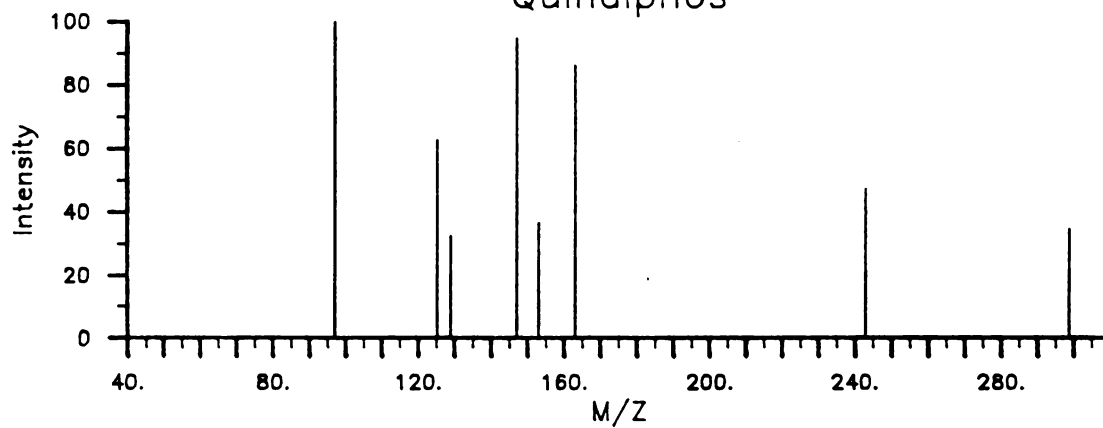


Pirimiphos

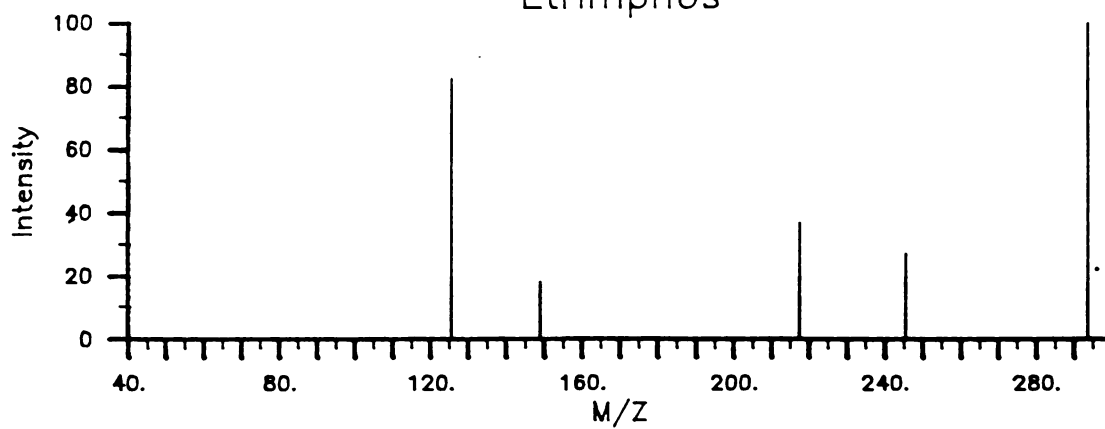


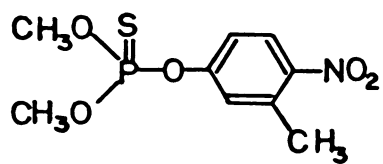


Quinalphos

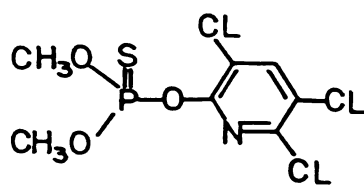
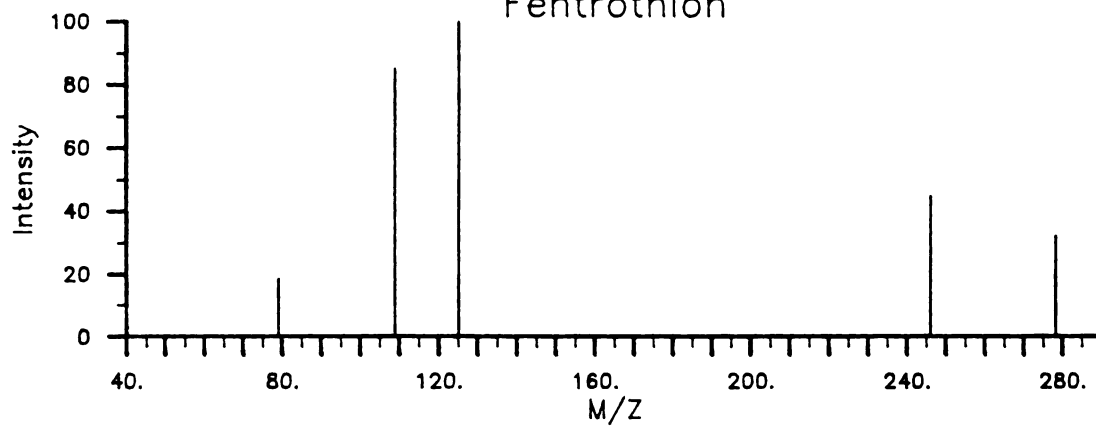


Etrimphos

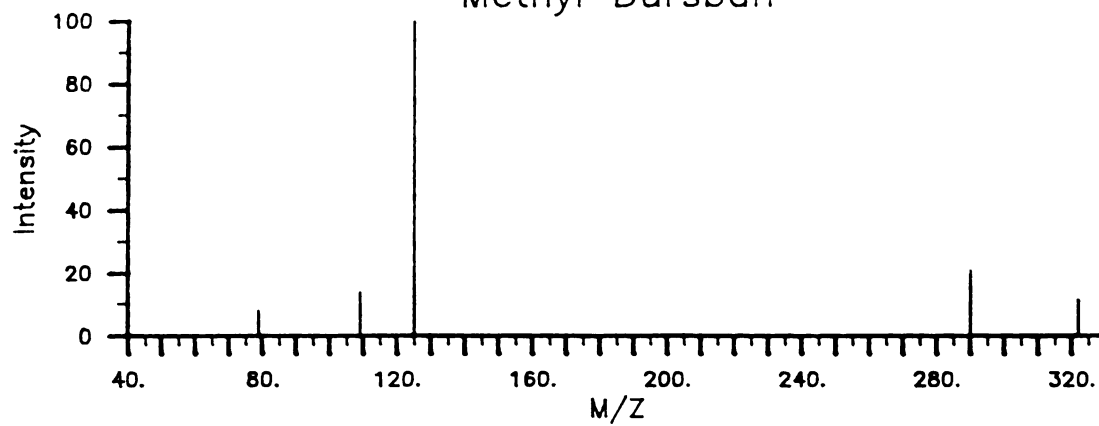




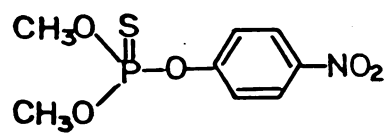
Fentrothion



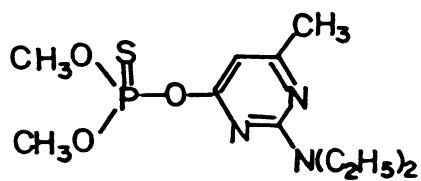
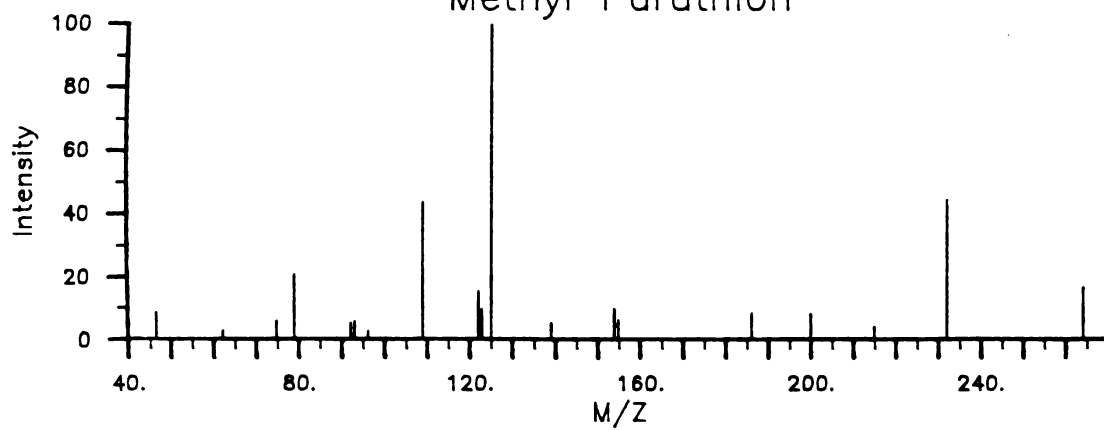
Methyl Dursban



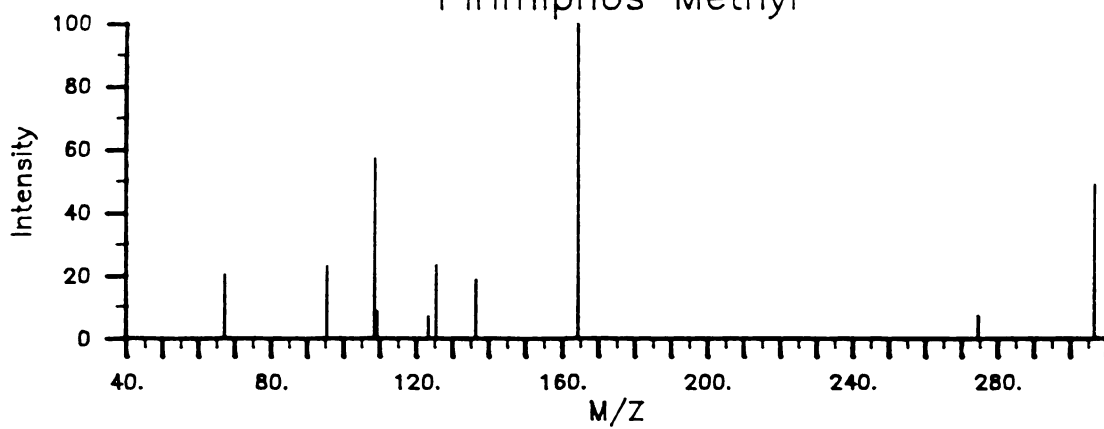


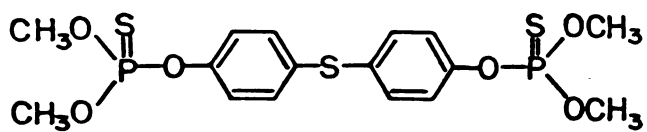


Methyl Parathion

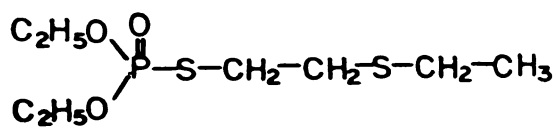
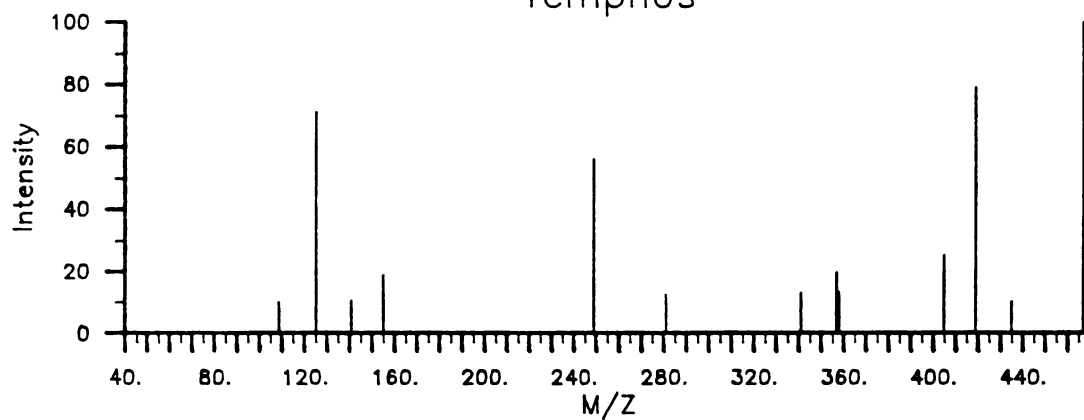


Pirimiphos Methyl

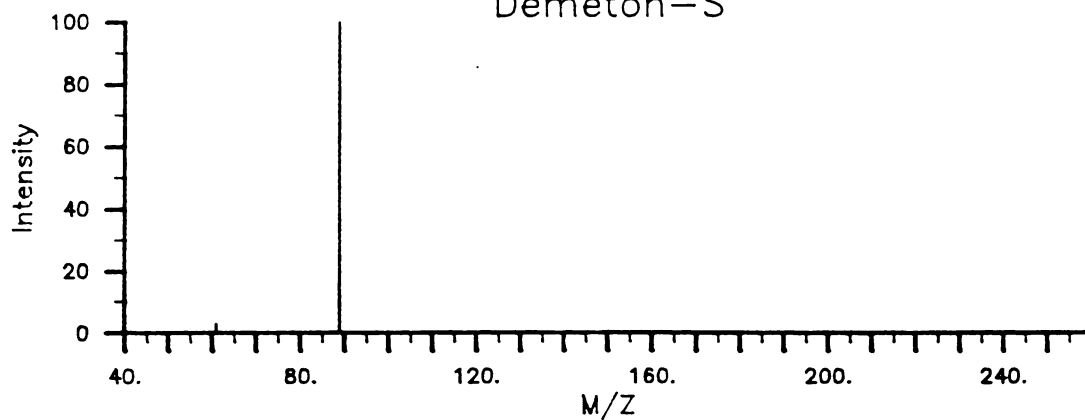


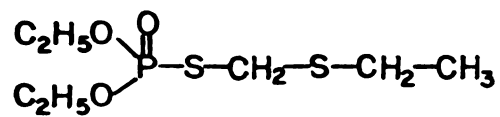


Temphos

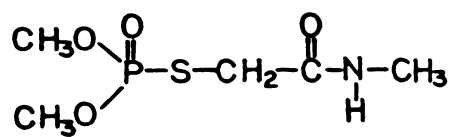
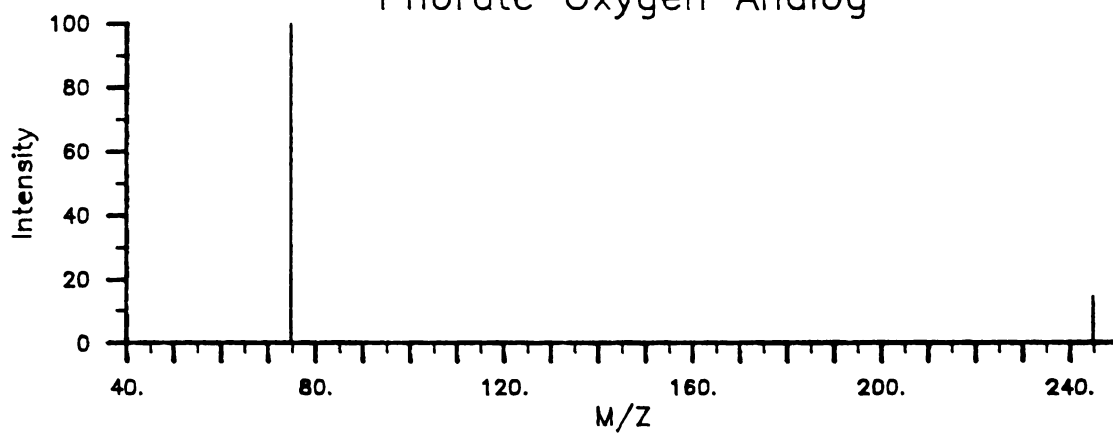


Demeton-S

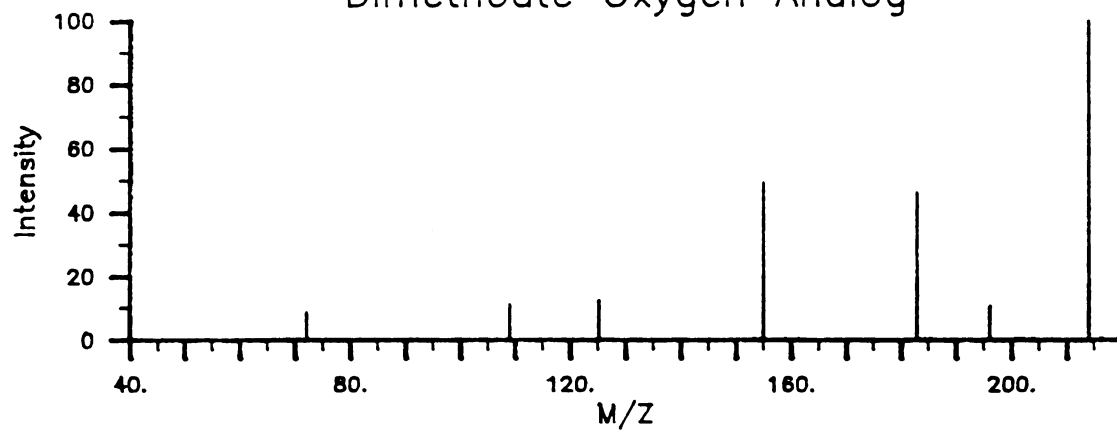


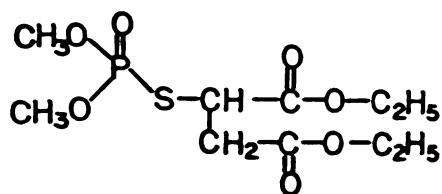


Phorate Oxygen Analog

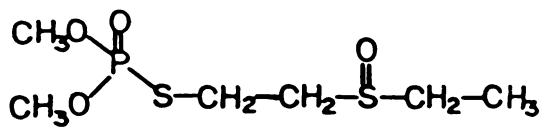
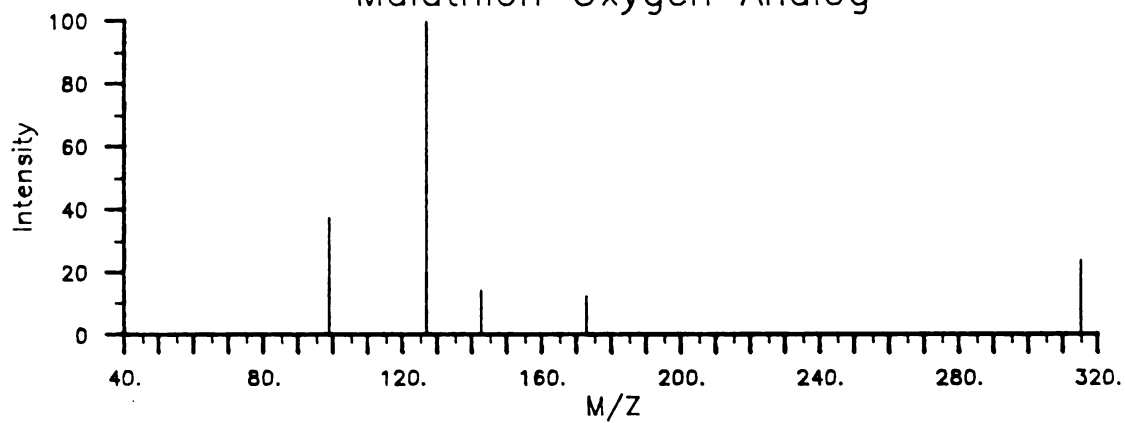


Dimethoate Oxygen Analog

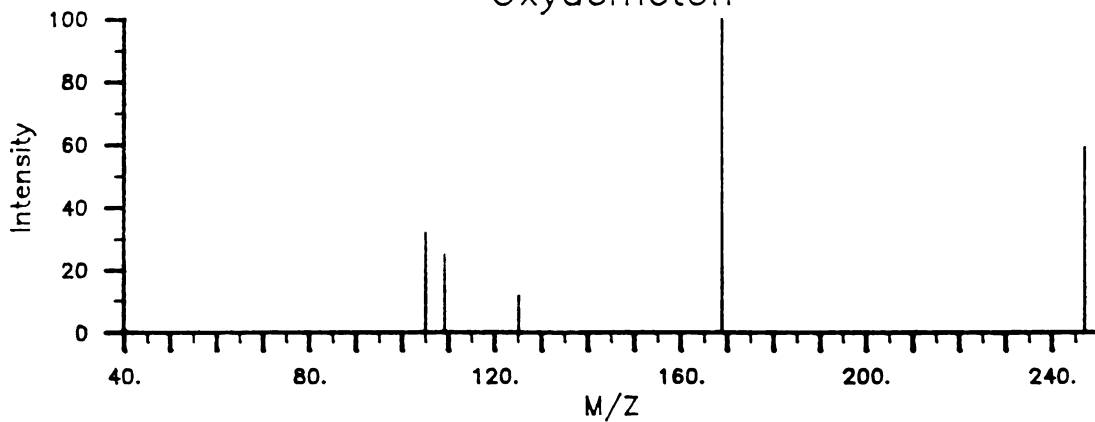




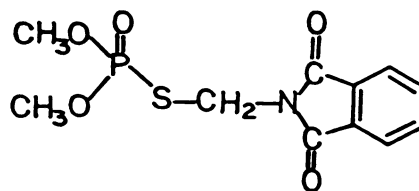
Malathion Oxygen Analog



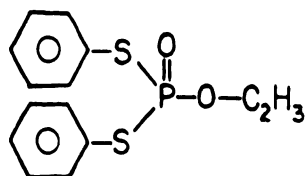
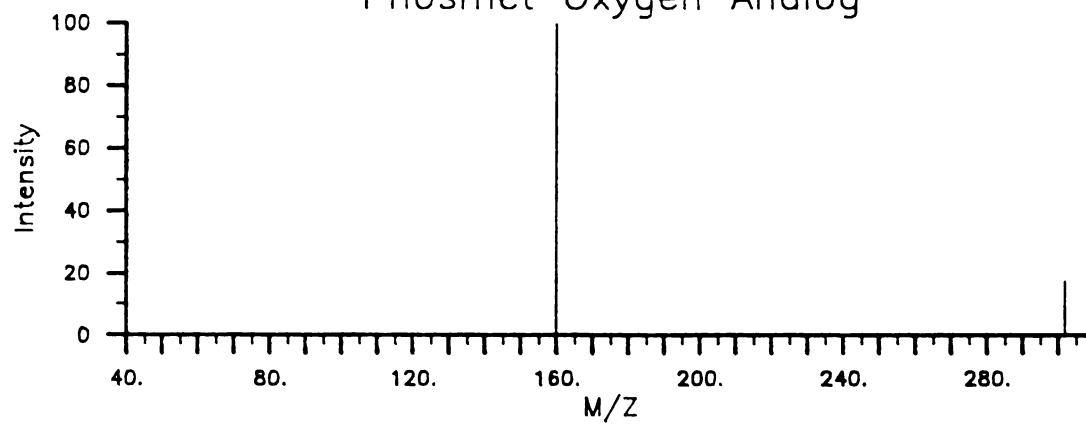
Oxydemeton



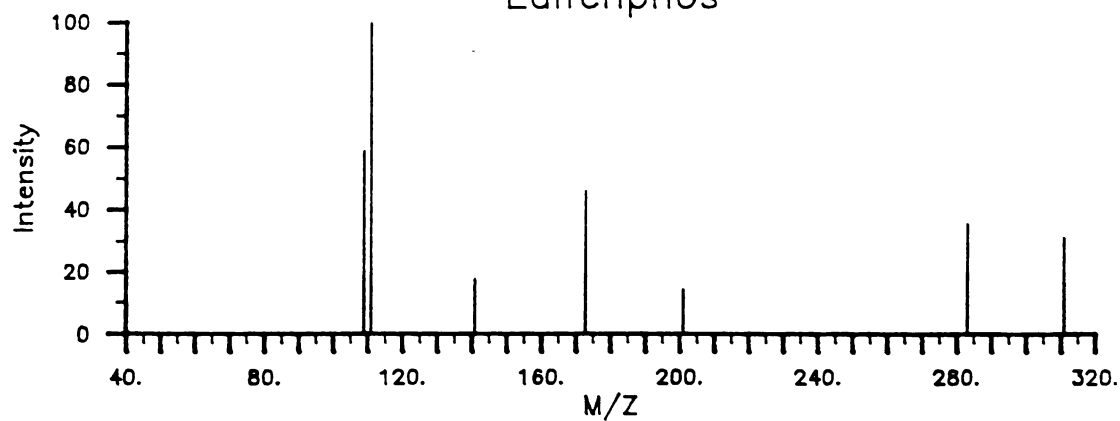


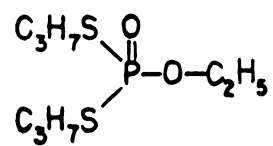


Phosmet Oxygen Analog

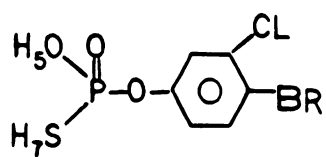
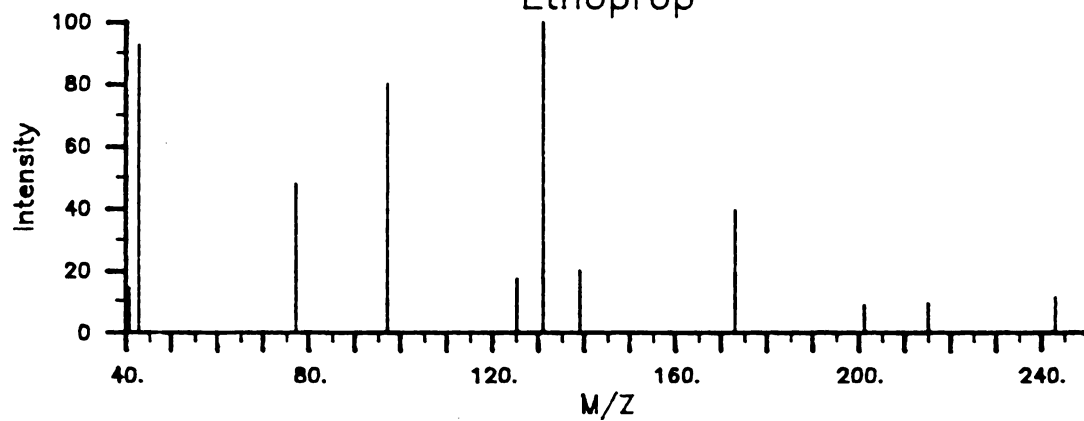


Edifenphos

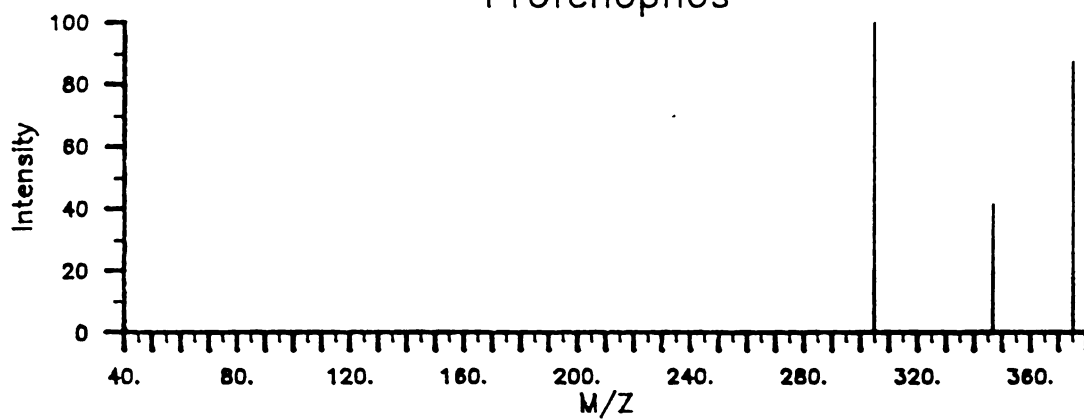


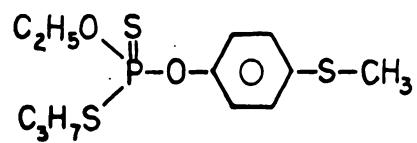


Ethoprop

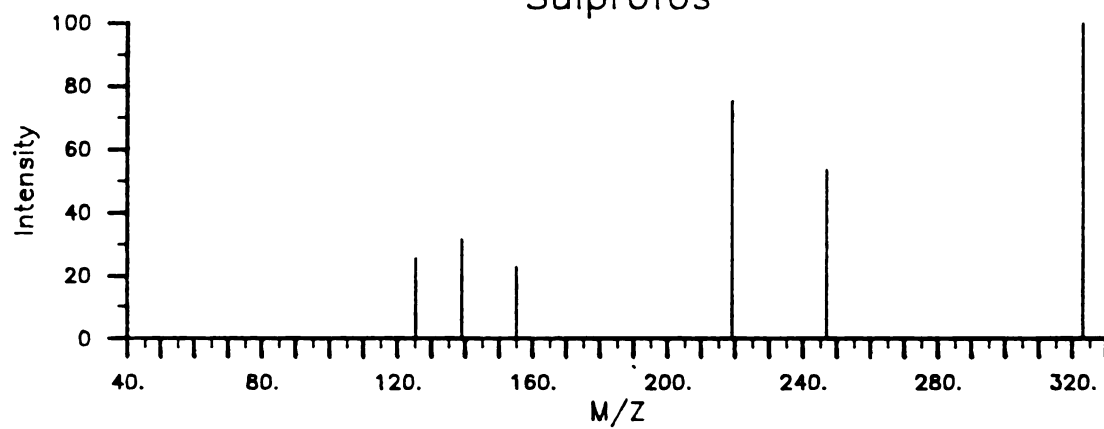


Profenophos





Sulprofos





MICHIGAN STATE UNIVERSITY LIBRARIES



3 1293 03062 8523